Detrital Zircon U-Pb Geochronology and Paleodrainage Reconstruction of the Blackhawk-Castlegate Succession, Wasatch Plateau and Book Cliffs, Utah

By

Bridget Solana Pettit
B.S., The University of Texas at Austin, 2015

Submitted to the graduate degree program in the Department of Geology and the Graduate Faculty of the University of Kansas in partial fulfillment of the requirements for the degree of Master of Science.

_____

Chair: Mike Blum

_____

Andreas Möller

_____

Greg Ludvigson

Date Defended: 6 July 2017

The thesis committee for Bridget Solana Pettit certifies that this is
the approved version of the following thesis:

Detrital Zircon U-Pb Geochronology and Paleodrainage Reconstruction of the Blackhawk-Castlegate Succession, Wasatch Plateau and Book Cliffs, Utah

_____

Chair: Mike Blum

Date Approved: 6 July 2017

Abstract

The Blackhawk Formation and Castlegate Sandstone are Campanian fluvial-deltaic and shoreline deposits within the Sevier foreland-basin fill along the Wasatch Plateau and Book Cliffs in Utah. Long-standing age constraints on the Blackhawk and Castlegate are based on correlation to ammonite zones in downdip mudstones, which are themselves constrained by radiometric dating of volcanic ash beds, and are therefore dependent on correlation methods and models. This study examines the Blackhawk-Castlegate succession with the following objectives: (i) test a hypothesis that very fine sands and coarse silts yield a more robust population of maximum depositional ages (MDAs) from volcanogenic detrital zircons (DZs) that approximate true depositional age than medium to fine sands; (ii) develop an independent geochronological framework of MDAs through U-Pb dating of volcanogenic DZs; and (iii) propose a paleodrainage reconstruction for the Blackhawk-Castlegate succession in light of new data.

MDAs calculated throughout the succession approximate the time of deposition for the upper Blackhawk (77.7 ± 1.7 Ma in Horse Canyon and 79.6 ± 1.7 Ma in Tusher Canyon), Lower Castlegate (75.8 ± 1.8 Ma in Horse Canyon), and potentially the Bluecastle Tongue (75.9 ± 1.9 Ma in Price Canyon). In the case of the upper Blackhawk and Lower Castlegate, the MDAs are both up to 2 Myrs younger than the age constraints determined by ammonite zone correlations, and raise questions concerning the temporal significance of the classic Castlegate Sequence Boundary and relationships with basin-evolution models.

Previous studies indicate that Santonian drainages were dominated by an axial fluvial system with headwaters in the Mogollon Highlands, with lesser contributions from the Sevier fold-and-thrust belt and the various Cordilleran magmatic sources. The DZ U-Pb age data in this

study is analyzed using multidimensional scaling, spatial relationships between clusters, and examination of specific peaks in age distributions. Regional sediment routing patterns appear to be quite similar during the Campanian deposition of the Blackhawk-Castlegate succession: there is evidence for an axial drainage flowing north from the Mogollon Highlands that passed by an area that is now Straight Canyon, intersected by transverse fluvial systems in the area that is now Price Canyon that drain the largely recycled strata exposed in the Sevier fold-and-thrust belt.

The DZ U-Pb age data collected and used for this thesis are uploaded as three supplementary Excel files: KBH Data, BC Data Unbiased, and BC Data Biased. The first two files have the data used for multidimensional scaling and peak analysis of kernel density estimates, but lack some grains used for MDA calculations. The targeted population of n=50 grains for MDAs is included in the BC Data Biased file.

Acknowledgments

I am extremely thankful to my advisor, Dr. Mike Blum, for his direction, support, and patience. I would also like to thank my committee members: Dr. Andreas Moeller for his guidance in the mineral separation stages and expertise in zircon complexities, and Dr. Greg Ludvigson for his advice throughout this project and insightful review of this thesis. Dr. Noah McLean provided invaluable support in modifying the MATLAB code that ultimately enabled identification of the rivers described in this study. Feedback from Dr. Tim Lawton, Dr. Joel Saylor, and Nicolas Bartschi propelled interpretations forward.

My field assistants, Ty Tenpenny and Maggie Duncan, made my time in the Utah desert far more engaging, and I will forever be thankful for their time and thought-provoking discussions. Many thanks to the Arizona LaserChron staff, Deserae Jennings, and Maggie Duncan for their tremendous support in obtaining U-Pb data.

I am thankful for the financial support the Roscoe G. Jackson III and Chevron Graduate Fellowships provided. This project was funded through Mike Blum's professorship funds, the KU Department of Geology, the Geological Society of America Graduate Research Grants program, American Association of Petroleum Geologists' Grants-in-Aid, the Association for Women Geoscientists Osage Chapter, and the Kansas Geological Foundation.

Most of all, I thank my parents for their unwavering support throughout my education, and Hal for his love and encouragement.

Table of Contents

List of Figures

List of Tables

1 Introduction

Interpretation of terrestrial stratigraphic records poses a number of different problems. Among these are the source areas for, and routing of, sediments that comprise the stratigraphic record, and difficulties resolving time in terrestrial strata to resolve rates of deposition, the temporal significance of key surfaces, and relationships between deposits, surfaces, and independently known-forcing mechanisms (tectonic activity, sea-level change, climate cycles). U-Pb dating of detrital zircons in terrigenous clastics is now a proven provenance tool, but also holds promise for developing geochronological frameworks. This study applies detrital zircon U-Pb provenance and geochronological methods to the well-known and widely studied Campanian-age Blackhawk and Castlegate succession of the Wasatch Plateau and Book Cliffs, Utah, to advance our ability to identify and differentiate paleodrainage and sediment routing systems, and to develop more robust geochronological frameworks in terrestrial deposits.

The Blackhawk and Castlegate are generally known to represent fluvial, deltaic, and shoreline strata derived from the Cretaceous Sevier orogenic belt, and thought to generally represent west-to-east fluvial sediment transport, discharging to the western margin of the Western Interior Seaway. Existing age assignments on the Blackhawk and Castlegate are based on correlation to ammonite zones in downdip mudstones, and are therefore dependent on correlation methods and models. This study examines the Blackhawk-Castlegate succession with the following objectives in mind: (a) use a large dataset of detrital-zircon U-Pb ages to present a more detailed reconstruction of paleodrainage and sediment routing throughout the Wasatch Plateau and Book Cliffs, (b) where possible, develop an independent geochronological framework for Blackhawk and Castlegate deposition through U-Pb dating of young volcanogenic detrital zircons (DZs), (c) test a hypothesis that detrital-zircon populations, including the young

volcanogenic DZs that approximate true depositional age, are grain-size and facies dependent, and (d) revisit existing interpretations of the Blackhawk-Castlegate succession in light of new data presented herein.

2 Background

2.1 Geologic Setting

The Campanian Blackhawk Formation and Castlegate Sandstone comprise part of the Mesaverde Group within the Jurassic and Cretaceous Sevier retroarc foreland basin system of the Western Interior Seaway. The Sevier foreland basin developed from the Jurassic to early Eocene during westward migration of the North American plate and subduction of the Farallon plate (Figure 1) (Jordan, 1981; Beaumont, 1981; Burchfiel and Davis, 1975; Kauffman and Caldwell, 1993; Liu and Nummedal, 2004; DeCelles, 2004; Liu et al., 2011). The Mesaverde Group extends north-south through the foreland-basin system from Wyoming to New Mexico, and represents a series of prograding clastic wedges, deposited first in a classical foredeep depozone when flexure from the orogenic load to the west dominated subsidence patterns, then in a broader zone of accommodation that reflected the increased importance of dynamic subsidence (DeCelles and Currie, 1996; White et al., 2002; Liu et al., 2011; Painter and Carrapa, 2013).

Sediment for the Mesaverde Group as a whole, and the Blackhawk and Castlegate in particular, is generally recognized to have been derived from the Sevier fold-and-thrust belt and the Cordilleran magmatic arc farther west (Kauffman and Caldwell, 1993; DeCelles and Coogan, 2006). Much of the Sevier fold-and-thrust belt consists of Proterozoic through early Mesozoic sedimentary and metasedimentary rocks that accumulated in a passive margin setting on the western margin of Laurentia. Detrital zircon studies show that passive margin strata were generally derived from the Neoproterozoic Grenville (ca. 1250-950 Ma populations present in Neoproterozoic and younger rocks) and the Paleozoic Appalachian (ca. 500-300 Ma, present in Devonian and younger rocks) orogens that comprise northeastern, eastern, and southern Laurentia, and sediments were transported to the west prior to development of the Cordilleran

magmatic arc and Sevier orogen (e.g. Gehrels and Pecha, 2014). Initial reversal of drainage patterns is thought to be reflected in the Jurassic Morrison Formation, deposited by river systems flowing west to east in a backbulge setting when the Sevier fold-and-thrust belt and foredeep was located much farther west (e.g. DeCelles, 2004; Fuentes et al., 2009). By Campanian time, the Sevier orogenic front had migrated to the east, and placed the main inferred sediment source, the Canyon Range culmination, some 70 km to the west of the study locations for this thesis (Armstrong, 1968; DeCelles and Coogan, 2006; Flood and Hampson, 2014, Fig. 1B of Hampson et al., 2014) (Figure 2).

Blackhawk and Castlegate strata represent alluvial-deltaic environments of deposition that are well-exposed in the Wasatch Plateau and Book Cliffs of east-central Utah, and have been the subject of numerous research studies and teaching exercises by academics and industry professionals. These units have been subdivided into three clastic wedges that prograded eastward into the north-south trending foreland basin and seaway (e.g. Aschoff and Steel, 2011), at a time when the seaway extended up to 1200 km from west to east and more than 5000 km from north to south (Molenaar and Rice, 1988; Kauffman and Caldwell, 1993). The downdip marine equivalents of the Blackhawk and Castlegate alluvial-deltaic and shorezone facies are referred to as the Mancos shale, and comprise the volumetric majority of the Mesaverde Group.

The oldest unit of interest for this thesis is the shallow-marine Star Point sandstone, which some consider to be the basal Blackhawk (e.g. Aschoff and Steel, 2011), but others treat as a separate formation. As classically defined, the Blackhawk Formation exhibits an overall progradational-aggradational architecture, and is subdivided into six members, which, in ascending order, are the Spring Canyon, Aberdeen, Kenilworth, Sunnyside, Grassy, and Desert. Each member contains heterolithic fluvial and coastal-plain strata updip, and transitions eastward

to progradational deltaic and shoreface facies, then into the Mancos Shale marine succession (Spieker, 1946; Young, 1955; Fisher et al., 1960; Fig. 2 of Yoshida, 2000). The Castlegate Sandstone is divided into (a) the amalgamated, cliff-forming Lower Castlegate Sandstone, which is commonly interpreted to represent braided-stream deposition (Pfaff, 1985; Adams and Bhattacharya, 2005; McLaurin and Steel, 2007), (b) the mudstone-dominated Upper Castlegate, interpreted to be meandering-stream deposits on a coastal plain (Chan and Pfaff, 1991); and (c) the Bluecastle Tongue, which is again amalgamated and similar in architecture to the Lower Castlegate (Pfaff, 1985). Overall, the Castlegate Sandstone is thought to represent a transition from low to high accommodation throughout its deposition (Van Wagoner, 1995; Yoshida et al., 1996; among others). Measurements of Blackhawk and Castlegate sandbodies indicate generally small river systems, with paleo-bankfull flows in the 4-7 m range (McLaurin and Steel, 2000; Hajek and Heller, 2012; Rittersbacher et al., 2014).

To date, there are sparse chronometric ages on the terrestrial part of the Blackhawk-Castlegate succession (Lippert, 2014; Morehouse, 2015). Age estimates and correlation models have therefore relied heavily on ammonite biostratigraphy in the Mancos Shale, which is calibrated to radiometrically-dated volcanic ash beds (Krystinik and DeJarnett, 1995; Fouch et al., 1983; Cobban et al., 2006). Figure 3 is a time-space correlation of Cretaceous strata through Utah from Seymour and Fielding (2013), which illustrates the distribution of ammonite biozones and radiometric ages through the Mesaverde Group: 17 ammonite biozones constrain the Campanian part of the marine Mancos shale, but their ages are only constrained by ashes that correlate to the lower Blackhawk and uppermost Castlegate. Hence, the inferred ages of key stratigraphic units and surfaces in between are based on assumptions about rates of deposition and other factors.

Correlations from the marine Mancos Shale to specific parts of the Blackhawk-Castlegate succession have employed sequence stratigraphic and other models, resulting in a number of different interpretive frameworks over the years (Young, 1955; McLaurin and Steel, 2000; Miall and Arush, 2001; Hampson, 2010; Aschoff and Steel, 2011; Hampson et al., 2012; Seymour and Fielding, 2013; Liu et al., 2014; among many others). A regionally extensive erosion surface separates the mud-prone Blackhawk Formation from the overlying amalgamated Castlegate Sandstone: this surface has played important roles in the development of sequence stratigraphic concepts (e.g. Van Wagoner et al., 1990; Van Wagoner, 1995; Kamola and Van Wagoner, 1995; Olsen et al., 1995; Yoshida et al., 1996; Yoshida, 2000; McLaurin and Steel, 2000, 2007; Howell and Flint, 2003; Hampson and Howell, 2005; Adams and Bhattacharya, 2005), and illustrates the significance of different correlation models. For example, Van Wagoner (1995) illustrated two contrasting stratigraphic models for the significance of this erosion surface (Figure 4): treating this basal erosion surface as an unconformity, a classical sequence boundary that everywhere separates younger from older strata, results in a different interpretation than if this same surface is treated as an autogenic scour that represents Castlegate fluvial deposits cutting across and truncating genetically-related deltaic, shorezone, and shallow-marine facies. As discussed in Bhattacharya (2011), Holbrook and Bhattacharya (2012), and Blum et al. (2013), the first of Van Wagoner's (1995) models became the standard sequence stratigraphic model, but can be falsified in Quaternary analogs and experiments, whereas the alternative model is consistent with those same Quaternary analogs and is verified by experiments. The Wheeler Diagrams (Figs. 17 and 18) of Bhattacharya (2011)) illustrates the implications of these two models for placement of different stratigraphic units in a time-space framework.

Existing chronostratigraphic data and sequence-stratigraphic frameworks have also been used to calculate durations for specific packages of strata, and identify allogenic signals that have controlled fluvial deposition (e.g. Yoshida et al., 1998; McLaurin and Steel, 2000; Flood and Hampson, 2014; Rittersbacher et al., 2014; Liu et al., 2014; Miall, 2014; Gani et al., 2015; among many others). In fact, for two decades or more, most interpretations of the Blackhawk-Castlegate succession featured sequence stratigraphic concepts (see the recent review by Hampson, 2016), which in turn featured stratigraphic architecture controlled by relative sea-level change and corresponding changes in accommodation within a generally dip-oriented (west-east) view of the succession as a whole. More recently, however, alternative interpretations have been published for the Blackhawk (Hampson et al., 2012; Rittersbacher et al., 2014; Flood and Hampson, 2015; Hampson, 2016) especially, which integrate the significance of autogenic processes like avulsion and delta switching to produce the observed alluvial-deltaic architecture in the along-strike (north-south) direction. The significance of avulsion and other autogenic processes in the along-strike direction is discussed later in this thesis.

2.2 Detrital Zircon Provenance and Geochronology

U-Pb dating of detrital zircons (DZs) is a proven provenance tool (see reviews by Fedo et al., 2003; Andersen, 2005; Gehrels, 2012). Zircons are exceedingly durable minerals that are produced in igneous and metamorphic settings (the protoliths), then exhumed and eroded to accumulate in sedimentary rocks as detrital grains. Primary detrital zircon protolith source terrains in North America are reasonably well-understood, as illustrated in Figure 5 and Table 1, and large numbers of analyses of detrital populations in older sedimentary rocks provide the basis to understand recycling of populations through time (Laskowski et al., 2013; Gehrels and

Pecha, 2014). However, a number of factors complicate the use of populations of detrital zircon U-Pb ages for provenance. Among these, Pb-loss, inheritance, and overgrowths present potential challenges during analysis (Gehrels, 2012, among others); concordia diagrams that connect equal $^{206}Pb/^{238}U$ and $^{207}Pb/^{235}U$ ages can be used to identify and filter discordant and reverse discordant ages that result from these factors. Moreover, differential zircon fertilities between protolith source terrains introduce a natural bias into detrital studies (Moecher and Samson, 2006; Malusa et al., 2015), and it can be difficult to distinguish between grains that are eroded directly from bedrock protolith sources vs. grains that are recycled from older sedimentary rocks.

Using detrital zircons to reconstruct paleodrainage in North America began in earnest with Riggs et al. (1996), and has since progressed with studies by Rainbird et al. (2001), Dickinson and Gehrels (2008b), Gehrels et al. (2011), Licht et al. (2015), and many others. Earlier studies often featured smaller grain counts (n=117 or less; Dodson et al., 1988; Vermeesch, 2004; Andersen, 2005) for each sample, whereas current standards commonly target n=300 per sample, to increase the probability of capturing the low-abundance populations that may represent an important fingerprint for specific source terrains, enabling the evaluation of linked routing systems throughout the sample area (according to Dodson et al. (1988) and Fedo et al. (2003), and verified by studies by Andersen (2005), Pullen et al. (2014), and Saylor and Sundell (2016)).

Detrital zircons can also be used to define the maximum depositional age (MDA) of a stratigraphic unit, based on the youngest population of U-Pb ages: described by Gehrels (2014), as the "Law of Detrital Zircons," sedimentary rocks can be no older than the youngest included population of detrital zircons. MDAs can approximate true depositional age (TDA) if there is contemporaneous volcanism that expels zircon-bearing ash, whereas if zircon protoliths are

intrusive, there will be a time gap of perhaps significant duration between crystallization and deposition as detrital grains, due to the time required for exhumation, erosion, and introduction of zircons into the fluvial transport system. A number of factors therefore also complicate the use of detrital zircons for geochronology. Primary among these may be a lack of magmatic activity within the contributing drainage area during deposition, such that syndepositional volcanogenic zircons are not available to the transport system. This is an acute problem in much of the Cretaceous strata of the Sevier foreland-basin system, where there are well-known paucities of volcanogenic zircons during several key time periods: these include the early Cretaceous magmatic lull in the Cordilleran arc (Armstrong and Ward, 1993; Ducea, 2001; DeCelles, 2004; Barth et al., 2013; May et al., 2013), as well as a general reduction in arc magmatism, with eastward migration of volcanic centers, during the late Cretaceous period of concern for this study. Regardless, even if volcanogenic zircons are produced during the time of deposition, the drainage area must be proximal enough to the volcanic ash fallout zone to receive fallout of young volcanogenic zircons in a sufficient concentration to ensure representation in the rocks that are sampled. While Coffey et al. (2014) suggests fine-grained zircons can be transported as far as 400 km, recent studies at the University of Kansas (Hallman, 2016; Turner, 2017; Sitek, 2017) show zircon-bearing ashes from the Yellowstone hotspot track as far as Kansas and Nebraska. According to the <earthchem.org> database, potential source locations of 80-72 Ma volcanogenic grains that might contribute to the Blackhawk-Castlegate succession are the volcanic centers of Arizona, northern Nevada, and central Idaho (Figure 6).

3 Methods

3.1 Field Sampling Methodology and Measured Sections

Canyons that dissect the margins of the Wasatch Plateau and Book Cliffs of east-central Utah provide strike and dip sections, respectively, through the Mesaverde Group. From west to east, Straight Canyon, Price Canyon, Horse Canyon, Tusher Canyon, and Thompson Canyon were chosen as new study locations, or had been previously sampled and analyzed by ExxonMobil (XOM) Upstream Research for DZ provenance and geochronology. In each case, sites were chosen for accessibility, availability of previous work, and sufficient spacing to provide broad geographic coverage of the Blackhawk-Castlegate succession. A map of the canyon locations used for this study is shown in Figure 7, and the coordinates of each sample location are included in Table 2.

Descriptions of the combined sample set are presented in Table 2, the vertical and spatial distributions of which are represented in a correlation panel in Figure 8. The measured sections used to make the correlation panel are included in Appendix A. Samples for DZ provenance and geochronology studies were collected with different purposes in mind during the XOM studies vs. the present work.

1. XOM studies were conducted to evaluate the nature and significance of the Blackhawk-Castlegate unconformity, and test whether the geochronological framework could be improved with maximum deposition ages (MDAs). For this reason, DZ samples were collected from upper Blackhawk and Castlegate channel-belt sandstones at Price, Horse, and Tusher Canyons. XOM samples are designated with the prefix BC.
2. For this project, samples were first collected at Thompson Canyon to test specifically whether DZ populations, especially volcanogenic zircons of late Cretaceous age that can

provide MDAs, are preferentially concentrated in fine-grained facies. DZ samples were collected from Blackhawk channel-belt sandstone, abandoned channel-fill fine sand and coarse silt, and crevasse-splay fine sand and silt, as well as Castlegate channel-belt sandstone, and abandoned channel-fill fine sand and coarse silt (Figure 9). This approach was guided by two assumptions: (a) that fine-grained zircons transport farther in volcanic ash than coarser fractions, and can be introduced to drainage basins that are farther from the source, perhaps as far as 400 km (Coffey et al., 2014), and (b) once present in a drainage basin, coarse silt-sized zircons are hydrodynamically equivalent during fluvial sediment transport to lower fine to very fine sand (Lawrence et al., 2011 and Malusa et al., 2015), and can therefore be transported significant distances in suspension in the upper part of the water column relative to the coarser fractions that transport as bedload. Therefore, sampling fine-grained fluvial facies deposited in channel fills and crevasse splays would increase the likelihood of recovery of young volcanogenic grains that yield MDAs that approximate true depositional ages (TDAs), relative to sampling coarser channel-belt sandstones. Samples collected specifically for this project are designated with the prefix KBH.

3. Also for this project, samples were collected to examine stratigraphic changes in DZ populations. The existing XOM BC samples from Price, Horse, and Tusher Canyons were augmented by systematically sampling (a) vertically from the Star Point Formation through the Blackhawk and Lower Castlegate Sandstone at Straight Canyon, (b) through the Blackhawk at Horse Canyon, and (c) through the upper Blackhawk at Tusher Canyon (Figure 8). This vertical and lateral distribution of samples is designed to develop a more

comprehensive analysis of paleodrainage and sediment routing systems, interpreted through the statistical analysis described below.

Numerous studies have been published of the Blackhawk-Castlegate succession within the study area, which were used to guide sample collection at each location. However, new generalized stratigraphic sections were measured in Straight Canyon and Horse Canyon at 1 m scale using a tripod-mounted laser range finder to constrain new KBH DZ samples within a stratigraphic context. Descriptions of lithology, grain size, sedimentary structures, and trace fossils are reported for each unit, and generally followed nomenclature in Bohacs et al. (2014). Locations of each sample were recorded using GPS, and all sections and sample locations are compiled in an ArcGIS database and reported in Table 2.

Finally, seven samples were collected from Blackhawk channel-belt sandstones in Horse Canyon at accessible locations for analysis of grain size of specific samples, as well as vertical grain-size trends. Samples were crushed using the disc mill at the University of Kansas, taking care to leave the gap sufficiently wide so as to not break individual grains. An ATM Sonic Sifter was then used to measure the relative weight percent distribution of specific grain sizes.

3.2 Detrital Zircon U-Pb Dating and Statistical Analysis

In this study, U-Pb dating of detrital zircons was used as a tool for paleodrainage and geochronology studies. First-generation U-Pb age data (n=100) from the Blackhawk-Castlegate succession in Horse, Tusher, and Thompson Canyon were released to M. Blum and the public domain by ExxonMobil Upstream Research. This XOM-BC sample set was collected before it became commonplace to analyze grains in higher quantities: for the BC samples, U-Pb ages were obtained on an initial random pick of n=100 grains per sample, plus a targeted population of

n=50 grains that exhibited characteristics suggesting young first-cycle volcanogenic grains, and would therefore yield MDAs that approximate true depositional age (TDA). This introduces a bias to the age distributions, hence the biased and unbiased data sets are presented in two separate data sheets, however, provenance analyses were only performed on the unbiased data.

The present study upgraded the original XOM BC random sample of n=100 to target populations of n=300, which improves the chances of recovering low abundance populations (e.g. Dodson et al., 1988; Fedo et al., 2003; Andersen, 2005; Pullen et al., 2014; Saylor and Sundell, 2016); all new KBH samples were processed with the n=300 target in mind. Mineral separation was performed at the University of Kansas and the University of Arizona, whereas all U-Pb analyses were performed at the Arizona LaserChron Center using the Laser Ablation Inductively Coupled Plasma Mass Spectrometer, following the methodology in Appendix B. In this study, 20 μm diameter spots in a 40 μm diameter cleaning pit were placed primarily in the center of each grain, taking care to avoid inclusions. A repository of backscattered electron images and example spot locations of the KBH sample mounts is included in Appendix C. Due to the inherent uncertainties associated with each of the U-Pb decay systems, the "best age" reported here is attained using $^{207}Pb/^{206}Pb$ age for grains older than 0.8-1.0 Ga, and $^{206}Pb/^{238}U$ age for grains younger than 0.8-1.0 Ga (Gehrels, 2000; Gehrels et al., 2008). Ages that are >20% discordant or >5% reverse discordant are excluded from further analyses. All analyses, including raw analytical data, as well as probability-density, histogram, and concordia plots are attached as supplementary files named "KBH Data," "BC Data Unbiased," and "BC Data Biased."

Detrital zircon source terrains in North America are well-understood and illustrated in Figure 5 (Laskowski et al., 2013). The DZ U-Pb age distribution for each BC and KBH sample was first analyzed to characterize the provenance, then samples were compared to each other to

identify similarities and differences, so as to reconstruct the paleo-sediment routing system of the Wasatch Plateau and Book Cliffs. The following established statistical techniques were used to both visualize DZ populations, and identify similarities and differences within and between populations:

a. Kernel Density Estimates (KDEs) are estimates of the true age distribution, produced from the U-Pb age distribution of a sample set (Vermeesch et al., 2016). KDE plots are constructed as a visual tool to compare and differentiate all samples, to compare and contrast samples stratigraphically in each canyon, and to compare and contrast samples at the same stratigraphic position in different canyons.
b. Multidimensional scaling (MDS) produces a graphical plot in which the distance between samples is a function of their Kolmogorov-Smirnov dissimilarities, such that similar samples plot closest to one another and dissimilar samples are farthest apart, and is an intuitive method to identify sample populations with similar age distributions (Borg and Groenen, 2005; Vermeesch, 2013). The 31 samples in this study underwent gap analysis to determine the optimal number of clusters (k=10), and were then analyzed using a modified MATLAB code that identified 10 unique, color-coded clusters of samples based on their Kolmogorov-Smirnov distance. These clusters were the basis for further provenance studies, with the implication that samples within each cluster represent a similar source area or similarly mixed populations.
c. Pie charts are created by dividing the number of grains within each population's age range (outlined in Table 1) by the total number of grains in the sample or group of samples. Analyses whose uncertainty falls within the age range are also included.

Composite age distributions from each cluster were analyzed on the basis of the presence

and absence of specific peaks to reconstruct regional and local paleodrainage patterns, and identify primary vs mixed populations. Age distributions were compared to maps of North American tectonic elements through time from Whitmeyer and Karlstrom (2007), data from the <earthchem.org> community database, and paleodrainage interpretations for older units throughout the Western Interior to identify primary transverse and/or longitudinal fluvial systems responsible for deposition in the study area. Individual clusters were then compared with each other to identify mixed populations, the spatial distribution of signals within the study area, and updip-to-downdip links within the Blackhawk-Castlegate sediment-dispersal system.

Maximum depositional ages (MDAs) are calculated using the mean square weighted deviation (MSWD) of the youngest statistically overlapping U-Pb ages for individual grains, following Dickinson and Gehrels (2009). MDAs were calculated using an excel macro from the Arizona Laserchron Center, which can be found at: <https://drive.google.com/file/d/0B9ezu34P5h8eTl96SzRtXzB5YXM/view>. Potential source locations for young volcanogenic zircons have been identified using the community database <earthchem.org>, a map of which is presented in Figure 6.

4 Results

4.1 Detrital Zircon U-Pb Dating and Statistical Analysis

Detrital zircon U-Pb age populations within the Blackhawk-Castlegate succession represent the aggregate signal of fluvial sediment transport from the Sevier fold-and-thrust belt to the western margins of the Western Interior Seaway. The headwaters for Blackhawk and Castlegate rivers also likely derived sediments from the Mogollon Highlands to the south, and the Cordilleran magmatic arc to the west and southwest, and thus share the primary population groups seen in many stratigraphic units throughout the Cretaceous Western Interior (e.g. Houston et al., 2000; Dickinson and Gehrels, 2009; Laskowski et al., 2013; Gehrels and Pecha, 2014; Lawton et al., 2014). As shown in Figure 10, ~69% of all U-Pb ages within the BC and KBH datasets represent grains that were ultimately derived from Yavapai-Mazatzal (23%), Midcontinent (18%), and Grenville (28%) protolith sources. Grains that were ultimately derived from the Cordilleran magmatic arc, as well as Appalachian, Neoproterozoic and early Paleozoic peri-Gondwanan, Trans-Hudson, and shield signals, each comprise between 4-8% of the aggregate U-Pb age population. This aggregate population indicates that the majority of the DZ U-Pb signal in the Blackhawk-Castlegate succession is recycled from sedimentary rocks of the late Proterozoic and Paleozoic to early Mesozoic Western US passive margin (see Laskowski et al., 2013; Gehrels and Pecha, 2014).

The distributions of U-Pb ages for each BC and KBH sample are presented as normalized KDE plots for purposes of visualization of major population groups, and visual comparison between samples, then statistically compared to each other using MDS, cluster analysis, and comparisons of major abundance peaks. U-Pb ages from samples that fall within the same cluster are grouped into composite age distributions, and analyzed as a function of time and

location to visualize how Campanian sediment-routing systems within this study area evolved through time.

4.1.1 Kernel Density Estimates (KDEs)

BC and KBH samples collected through the Wasatch Plateau and Book Cliffs contain a diverse suite of age populations. Age distributions for all samples are presented as normalized KDEs in Figure 11, whereas a full explanation of primary protolith source regions and potential recycled source terrains is illustrated in Figure 5 and outlined in Table 1.

While there are variations in age population groups across all samples, the larger-scale trends are summarized below from youngest to oldest:

- Zircons with latest Paleozoic to Mesozoic ages (ca. 275-72 Ma) comprise 2.4% of all samples, but vary between samples in proportions that range from 0-11%. These grains comprise the Western Cordillera age population group, with ultimate sources in the Cordilleran magmatic arc and associated Sierra Nevada batholith of Southern California and Nevada, and the various volcanic rocks of Southeast Arizona. As noted by many workers (e.g. Bateman, 1983, 1992; Barton et al., 1988; Armstrong and Ward, 1993; Christiansen et al., 1994; Barton, 1996; Ducea, 2001; Barth et al., 2013; May et al., 2013), peaks in magmatic flux in the Sierra Nevada occurred in the late Jurassic and mid-late Cretaceous, with a magmatic lull in the early Cretaceous: the Western Cordillera population within the Blackhawk-Castlegate succession displays this characteristic bimodal age distribution.
- Zircons with Mesoproterozoic to late Paleozoic U-Pb ages (ca. 1300-300 Ma) constitute an average 39% of all grains in each sample. These Appalachian (average 7% of each sample), Neoproterozoic and early Paleozoic Peri-Gondwanan (4%), and Grenville (28%)

grains are regionally pervasive. Zircons of these age populations were initially deposited in the Paleozoic and early Mesozoic Laurentian passive margin that drained the Appalachian-Ouachita Cordillera of eastern Canada through the southcentral US (e.g. Dickinson and Gehrels, 2009; Gehrels and Pecha, 2014; Lawton et al., 2010; Laskowski et al., 2013), or the ancestral Rocky Mountains in western Colorado (e.g. Lawton et al., 2015). There are no primary protolith sources for these populations to the west of the present study area, hence these populations are recycled from the Laurentian passive margin sedimentary and metasedimentary units that were entrained in the Sevier fold-and-thrust belt, and reintroduced to the paleodrainage systems that contributed to the Blackhawk-Castlegate succession.

- Paleo-Proterozoic and late Meso-Proterozoic grains with U-Pb ages ca. 1800-1300 Ma comprise an average of 41% of all samples. Zircons with ages of ca. 1800-1600 Ma comprise an average of 23% in each sample, and were originally derived from Yavapai-Mazatzal basement rock, which was likely limited during the Cretaceous to primary exposures in the Mogollon Highlands of central Arizona and the granitoid intrusions that coincide with the Yavapai orogenic peak (e.g. Wasserburg and Lanphere, 1965; Hayes, 1970; Thomas et al., 1984; Whitmeyer and Karlstrom, 2007; Spencer and Pecha, 2012). In this and other datasets throughout the Western Interior, Yavapai-Mazatzal grains commonly co-occur with zircons with ages of ca. 1550-1300 Ma, which represent the Midcontinent granite-rhyolite province and granitic intrusions into Yavapai-Mazatzal basement, and which comprise ~18% of all samples (e.g. Dickinson and Gehrels, 2009; Laskowski et al., 2013; Lawton et al., 2015). This population was also likely limited in terms of exposure during the Cretaceous to the same area of central Arizona, but is

common in Laurentian passive margin sediments within the Sevier fold-and-thrust belt (Dickinson and Gehrels, 2009), and much of this signal within the Blackhawk-Castlegate succession may therefore be recycled.

- Zircons with U-Pb ages >1800 Ma include the Penokean/Trans-Hudson population (average 8% of each sample), Archean Peri-Gondwanan (2%), and Archean shield of the Wyoming and/or Superior provinces (6%). Combined, these populations also represent Laurentian passive margin sediments that were entrained in the Sevier fold-and-thrust belt (Dickinson and Gehrels, 2009), and are likely recycled as well.
- Grains of various ages that do not fall within large population groups, labeled "Other" in Figures 10 and 12, and Table 1, are generally <1% of the total; their source is unclear, and they play no role in provenance interpretations.

4.1.2 Multidimensional Scaling (MDS) and Cluster Analysis

As a first step in organizing individual samples into larger groups with similar age distributions, and thus provenance interpretations, samples were objectively compared using multidimensional scaling with a MATLAB code modified to identify statistical clusters (Borg and Groenen, 2005; Vermeesch, 2013; Noah McLean, personal communication, 2017). This analysis differentiated 10 clusters, with each cluster containing between two and eight individual BC and/or KBH samples (Figure 13). Samples within each cluster were then lumped to generate composite, representative normalized KDE plots (Figure 14). Age population differences between each cluster are illustrated using pie diagrams in Figure 12. Within the Discussion section below, these clusters are used to identify potential signals of primary axial fluvial systems vs. mixed populations within the Blackhawk-Castlegate paleodrainage system. Age

populations were compared to paleodrainage interpretations for older units throughout the Western Interior, the Whitmeyer and Karlstrom (2007) maps of significant terranes, orogenic belts, and rifts, and the <earthchem.org> community databases to generate paleodrainage interpretations.

Clusters have been assigned names of color for discussion purposes, and are described below, beginning with those clusters that contain the farthest updip facies (defined here as upper Blackhawk and Castlegate), and the most updip locations (Straight and Price Canyons):

- *Light Green Cluster*. The Light Green cluster contains three samples, including the uppermost Blackhawk (KBH-19) and Lower Castlegate (KBH-01) at Straight Canyon, the farthest updip location sampled, and a Lower Castlegate sample (BC-10) from Horse Canyon. Within the broader distribution of major populations, as described above, these samples are distinguished by the presence of young grains (ca. 80-72 Ma), a distinct Midcontinent peak at ca. 1430 Ma, and distinct Yavapai-Mazatzal peaks at ca. 1700 Ma and ca. 1775 Ma. The absence of a peak at ca. 1640 Ma, which is present in every other cluster, suggests that Blackhawk-Castlegate strata in Straight Canyon were deposited by a river system whose headwaters did not have a source for the 1640 Ma grains. Because these three samples cluster together, the implication would be that they represent the same paleoriver system, with the same source terrain.
- *Yellow Cluster.* The Yellow cluster is the largest (eight samples), and includes the upper Blackhawk (BC-14) and lowermost Castlegate (BC-13) at Price Canyon, the second updip location, as well as six samples from more downdip locations: KBH-18 (middle Blackhawk) and BC-07 (Upper Castlegate/Bluecastle Tongue) from Horse Canyon, BC-01 (upper Blackhawk from Tusher Canyon), and KBH-04 and 05 (upper Blackhawk) and

KBH-07 (Lower Castlegate) at Thompson Canyon. Defining characteristics of the Yellow cluster in Price Canyon include a prominent Yavapai-Mazatzal peak at ca. 1640 Ma, with a corresponding very minor presence of ca. 1430 Ma, 1700 Ma and 1775 Ma ages, and absence of Western Cordilleran grains. Peaks are generally less well-defined and more evenly spread across the age distribution in comparison with the Light Green cluster, which can be explained by multiple sources of recycled material.

- *Brown Cluster.* The Brown cluster is composed of Lower and Upper Castlegate samples from Price Canyon (BC-15 and BC-16), an updip location, as well as KBH-17 (middle Blackhawk) at Horse Canyon, a downdip facies and location. The Brown cluster is strikingly similar to the Yellow cluster discussed above: key differences include a less prominent peak at ca. 1170 Ma (Grenville), higher significance of the ca. 1640 Ma peak, and fewer ca. 1700 Ma and 1775 Ma ages.
- *Black Cluster.* The Black cluster includes BC-17 (Bluecastle Tongue) in Price Canyon, an updip facies and location, and BC-09 (Lower Castlegate) in Horse Canyon, a downdip location. Additionally, these samples have the highest concentration of ca. 1100 Ma, 1170 Ma, and 1775 Ma grains of any cluster, as well as a prominent Midcontinent peak at ca. 1430 Ma, and a minor presence of the first two Yavapai-Mazatzal peaks of ca. 1640 Ma and 1700 Ma ages.
- *Pink Cluster.* The Pink cluster contains BC-08 (Upper Castlegate) in Horse Canyon and BC-06 (lower Sego) in Tusher Canyon. The representative age distribution is an amalgamation of grains belonging to all peaks previously described, but has an anomalously high (11%) amount of zircons belonging to the Western Cordillera population and the highest and most distinct ca. 100 Ma and 160 Ma peaks.

- *Blue Cluster.* The Blue cluster, which includes the downdip facies of KBH-15 (lower Blackhawk) at Straight Canyon, and downdip locations of BC-11 (upper Blackhawk) at Horse Canyon, and KBH-08 (upper Blackhawk) at Tusher Canyon, is similar to the Light Green cluster described above. Differences include a stronger presence of grains in the Western Cordillera and Appalachian populations and distinct peaks at ca. 1170 Ma and 1640 Ma. This cluster has the greatest proportion of young grains ca. 80-72 Ma, suggesting significant input from an area with active volcanic ash deposition.
- *Lavender Cluster.* The Lavender cluster is composed of lower and upper Blackhawk samples (KBH-10 and KBH-16, respectively) in Horse Canyon, a downdip location, and is highly similar to the Brown cluster discussed above. Differences include a minor presence of grains at ca. 100 Ma, 320 Ma, and 2080 Ma. The similarity between the two clusters with respect to the Yavapai-Mazatzal population is rare and notable, as this appears to be the population with the most variations between clusters.
- *Red, Turquoise, and Dark Green Clusters.* The remaining clusters share presence and absence of the same peaks in varying proportions, but encompass updip and downdip facies from all locations except Price Canyon. The Red cluster includes: KBH-02 (Star Point) and KBH-12 (middle Blackhawk) of Straight Canyon, and KBH-11 (lower Blackhawk) of Horse Canyon; the Turquoise cluster includes: BC-03 (upper Blackhawk) and BC-05 (Lower Castlegate) of Tusher Canyon, as well as KBH-03 (upper Blackhawk) of Thompson Canyon; and the Dark Green cluster includes: and KBH-09 (upper Blackhawk) of Tusher Canyon and KBH-06 (Lower Castlegate) of Thompson Canyon. All are defined by minor presence of grains at ca. 100 Ma, 420 Ma and 600 Ma, all three Grenville peaks at ca. 1060 Ma, 1100 Ma, and 1170 Ma, and comparatively even

distribution of grains through the Yavapai-Mazatzal population. They vary only in their Midcontinent peaks: the Red cluster has all three peaks at ca. 1350 Ma, 1430 Ma, and 1500 Ma, the Turquoise cluster has peaks at ca. 1350 Ma and 1430 Ma, and the Dark Green cluster only has the ca. 1430 Ma peak and other various-aged grains distributed throughout the Midcontinent population.

The presence and absence of specific peaks defines a high-resolution fingerprint of primary and distinct source areas, updip to downdip links between samples, and inferred paleorivers and the routes traveled by each. The upper Blackhawk and Lower Castlegate at Straight Canyon are statistically indistinct from each other, but distinct from the upper Blackhawk and Lower Castlegate at Price Canyons: because these stratigraphic intervals represent the farthest updip facies, and the two locations represent the most proximal, updip locations, they are considered to be "parent," or axial, systems. Samples that are statistically indistinct from these parents, but located farther downdip, stratigraphically or geographically, are representative of the downstream extents of the same axial systems, whereas others likely represent a mixture of these parents and are termed "daughters." A more thorough discussion of potential primary and/or recycled sources for age peaks and their respective clusters, as well as overarching paleodrainage interpretations for the study area, is provided in the Discussion section.

4.1.3 Maximum Depositional Ages (MDAs)

Many of the young grains used to calculate MDAs herein were part of the biased n=50 pick within the original ExxonMobil BC sample set, where grains were preferentially picked

because they exhibited characteristics (lightest colors, euhedral shape) that suggest young ages, and/or a lack of recycling over time, as degree of pink coloration generally increases with age and older grains have more opportunities for recycling (Silver and Deutsch, 1963; Gehrels, 2012). By contrast, only a few young grains that approach true depositional age were recovered from the KBH samples, or within the BC samples after the analysis count was increased to an unbiased n=300 target population. The comparatively high proportion of young grains in the BC biased picks suggests this may be a viable method when targeting young volcanogenic grains for purposes of obtaining MDAs. This approach biases the age distribution for each BC sample if they are used for provenance analyses as well, but makes it possible to calculate MDAs for key parts of the Blackhawk-Castlegate succession. U-Pb ages used for MDA calculations are outlined in Table 3, and weighted MDAs are plotted in Figure 15.

To begin, samples in the Star Point and lower Blackhawk Formation contain very few young (<80 Ma) zircons in quantities greater than 1, which makes a statistically robust age difficult. By contrast, samples in the upper Blackhawk contain up to 5% grains derived from the Western Cordilleran magmatic arc in the unbiased age distributions, with ages as young as 76.0 ± 2.8 Ma. Three samples in the upper Blackhawk, collected from Horse and Tusher Canyons, produce enough young zircons from the biased dataset to calculate an MDA. Each sample plots in a different cluster, and they are therefore interpreted to be from different source areas; for this reason, they are calculated as separate MDAs. Samples in Horse Canyon produce MDAs of 77.7 ± 1.7 Ma (n=7) from sample BC-10, and 77.6 ± 2.3 Ma (n=6) from BC-11, and youngest grains of 76.0 ± 2.8 Ma and 76.2 ± 3.0 Ma, respectively. Sample BC-03 from Tusher Canyon has a calculated MDA of 79.6 ± 1.7 Ma (n=8), and a youngest grain of 78.5 ± 3.6 Ma. The older mean MDA for the upper Blackhawk in Tusher Canyon, relative to Horse Canyon, may reflect a lack

of syndepositional volcanogenic zircons in the contributing drainage area, and therefore yields an MDA that does not approximate TDA, or, conversely, the upper Blackhawk in Tusher Canyon may, in fact, be older than the upper Blackhawk at Horse Canyon.

An abundance of young grains throughout the Castlegate Sandstone make it possible to calculate MDAs through its three main subunits, as follows:

- Sample BC-09, collected in the Lower Castlegate Sandstone in Horse Canyon, just above the Castlegate Unconformity, contains 14 young grains with overlapping uncertainties: however, the youngest grain is 72.6 ± 3.9 Ma, which is too young for this stratigraphic context, and was therefore not considered. Remaining grains with overlapping error terms produced an MDA of 75.8 ± 1.8 Ma (n=13). The MDAs calculated for the uppermost Blackhawk and the Lower Castlegate, directly above and below the Castlegate unconformity in Horse Canyon therefore differ by ~1.9 Myrs, which is consistent with an unconformity representing significant missing time.
- BC-06, collected from the lower Sego Sandstone in Tusher Canyon, produces a calculated MDA of 80.2 ± 3.5 Ma (n=3) and youngest grain of 79.2 ± 3.6 Ma; this is older than the Lower Castlegate below, and is therefore not useful from a chronostratigraphic standpoint as it does not approximate TDA.
- Sample BC-17, collected from the Bluecastle Tongue in Price Canyon, has a calculated MDA of 75.9 ± 1.9 (n=6) Ma, with a youngest grain of 74.2 ± 3.0 Ma. This MDA differs by only ~0.1 Myrs from the MDA produced by BC-09 (Lower Castlegate in Horse Canyon), and may suggest very little time is represented by Castlegate-Bluecastle Tongue deposition. On the other hand, BC-17 and BC-09 are the only two samples in the Black cluster. The nearly identical MDAs and youngest grains substantiate the approach in

interpreting samples within a single cluster to have a similar paleodrainage history: the two samples in the Black cluster may represent transport of young zircons produced by the same event, exposed within a single drainage area.

While previous studies have employed DZ U-Pb geochronology for the Mesaverde Group in the Book Cliffs (Lippert, 2014; Morehouse, 2015), the age assignments presented here represent the first U-Pb age-based geochronological framework using statistically robust ($n \geq 3$) MDAs in an assemblage of n=300 grains per sample for a significant part of the Mesaverde Group in the study area. A lack of biostratigraphic control in the upper Blackhawk and Lower Castlegate means that previous age estimates for these units, and the inferred unconformity between them, is constrained only by extrapolation of ages between ash layers in the Mancos shale, then correlations to the more updip Blackhawk-Castlegate fluvial-deltaic and shoreline facies. Previous correlations suggest this unconformity formed in the range ca. 80.56 – 75.84 Ma, but likely around ca. 79 – 77 Ma (Gill and Hail, 1975; see summary in Seymour and Fielding, 2013). The MDAs presented above indicate the upper Blackhawk and Lower Castlegate are both up to 2 Myrs younger than previously thought, and suggest the unconformity between them formed between ca. 79.6 Ma (at Tusher Canyon) or 77.7 Ma (at Horse Canyon) to ca. 75.8 Ma, with the amount of missing time possibly dependent on location. The youngest grains for each of the key stratigraphic intervals are up to 3.2 Myrs younger than the MDA, suggesting an even younger age is possible for each unit.

4.1.4 Grain Size Dependence in Thompson Canyon

As discussed above, due to differences in hydrodynamic transport mechanisms, sampling fine-grained fluvial facies deposited in channel fills and crevasse splays was hypothesized to increase the likelihood of recovery of young volcanogenic zircons that yield maximum depositional ages (MDAs) that approximate true depositional ages (TDAs), relative to sampling coarser channel-belt sandstones. Figure 11E displays the KDE age distributions of the five samples collected from Thompson Canyon for this task. Each sample reflects the overarching age distributions and clusters described in the previous section, as described above, but there were no grains younger than 89.2 ±2.1 Ma, which is ~10 Myrs older than true depositional age.

These results therefore are consistent with a null hypothesis, in which young zircons grains are not preferentially fractionated into finer-grained facies. However, it is important to note that many samples collected from other canyons did not produce young grains, even on the biased n=50 pick (which was not tested in Thompson Canyon), so while these results are consistent with the null hypothesis, it is not possible to know whether the lack of young grains is actually due to a complete absence of young grains in the contributing drainage area. Furthermore, KBH-03 belongs to the Turquoise cluster along with BC-03 (upper Blackhawk) in Tusher Canyon, which has enough young grains to calculate an MDA: by definition, the two samples are statistically indistinct. This co-occurrence of samples that produce young grains belonging to clusters that are made of other samples that lack young grains suitable for MDA calculations occurs in two other clusters (Pink and Blue), and suggests the presence of a long-standing direct source supplying Horse and Tusher Canyons, and later Price Canyon, with young volcanogenic zircons.

Another important observation is that the five samples belong to three separate clusters. KBH-03 represents sandy channel-belt facies that are laterally adjacent to heterolithic abandoned channel-fill deposits from which KBH-05 was collected, yet the two samples belong to the Turquoise and Yellow clusters, respectively. KBH-04, collected from overlying Blackhawk crevasse-splay facies, also belongs to the Yellow cluster. Above the unconformity, KBH-06 from the heterolithic Castlegate channel-fill facies, belongs to the Dark Green cluster, whereas KBH-07, from overlying Castlegate channel-belt sands, belongs to the Yellow cluster. Hence, in addition to the young grains, the signals/clusters are unrelated to certain facies.

4.2 Grain Size of Channel-Belt Sand Bodies

To test the hypothesis of channel-belt grain-size trends varying vertically upsection, channel-belt sand-body thickness and grain size were measured and analyzed in Horse Canyon through the Blackhawk Formation. The results are presented in stratigraphic order in Table 4. Channel-belt sandstones range from 1 to 5 meters in thickness, whereas d50 (median grain size) values range from 1.17 to 2.52 microns, and all samples are poorly to very poorly sorted. The sample size for this analysis was limited, partly due to inaccessibility of exposures on cliff faces, but show no evidence of any vertical trends through the section; a larger sample set may be achieved by expanding this study across multiple canyons.

5 Discussion

The U-Pb ages presented herein provide an opportunity to reevaluate the assigned ages for the upper Blackhawk through Bluecastle Tongue, examine the fractionation of DZ populations by facies or lack thereof, and interpret the sediment routing systems responsible for the deposition of the Blackhawk-Castlegate succession in the study area. DZ U-Pb ages are a proven provenance tool, and the abundance of data throughout the Western Interior allows a high-resolution paleodrainage reconstruction. The paleodrainage discussion will focus on an examination of major age populations, the provenance of specific peaks whose presence or absence contributes to their interpreted headwater source, and an analysis of individual clusters in an attempt to explain regional fluvial systems and smaller-scale mixing of signals. The implication, discussed below, is that Campanian deposits exposed in the Book Cliffs and Wasatch Plateau are the result of complex interactions between multiple fluvial systems with headwaters in different parts of the Western Interior.

5.1 Implications of New Maximum Depositional Ages

The Blackhawk Formation is generally viewed as having been deposited ca. 82-78 Ma (see recent summary in Seymour and Fielding, 2013), based on correlation to ammonite zones in marine strata, the age estimates for which come from extrapolation of rates of accumulation between radiometric ages from volcanic ash beds. A regionally extensive unconformity separates the Blackhawk from the overlying Castlegate Sandstone (Van Wagoner, 1995; Yoshida, 2000; and many others): based on radiometric dates of ash beds that bracket the *Baculites perplexus, Baculites maclearni,* and *Baculites obtusus* ammonite zones, the basal Castlegate unconformity has been interpreted to have formed ca. 78 Ma (Fouch et al., 1983;

Cobban et al., 2006), and, depending on the type and location of the stratigraphic surfaces and set of ages used for correlation, has been thought to represent 3.0-1.6 Myrs (Fouch et al., 1983; Obradovich, 1994; Van Wagoner, 1995; Seymour and Fielding, 2013).

MDAs presented here provide new insight into the chronology of deposition, and are compared to published age estimates in Figure 16. To summarize, in Horse Canyon, the uppermost Blackhawk produced individual U-Pb ages as young as 76.0 ± 2.8 Ma, with a calculated maximum depositional age (MDA) of 77.7 ± 1.7 Ma (n=7), whereas the Lower Castlegate produced U-Pb ages as young as 72.6 ± 3.9 Ma with a calculated MDA of 75.8 ± 1.8 Ma (n=13). The 1.9 Myr time difference between the upper Blackhawk and top of the Lower Castlegate is to some extent an averaging artifact from the MDA calculation, but must account for both the missing time associated with the unconformity, and deposition of a portion of the Lower Castlegate, which suggests there is less missing time than previously thought. Additionally, at Horse Canyon, this unconformity formed ~2 Myrs younger than previous correlations suggest (Gill and Hail, 1975; see summary in Seymour and Fielding, 2013). MDAs from the overlying Bluecastle tongue are calculated to be 75.9 ± 1.9 Ma, with a youngest grain of 74.2 ± 3.0 Ma, some 0.82 to 1.23 Myrs older than previously interpreted (Cobban, 1973; Kirschbaum and Hettinger, 2004; Seymour and Fielding, 2013): these results suggest that previous age assignments have overestimated the depositional age, or the Bluecastle Tongue sample from Price Canyon yielded no syndepositional volcanogenic zircons. The uncertainties associated with each MDA fall within the uncertainties of previous age assignments, illustrating the imperfectness of age-dating using LA-ICPMS; however, the technique of using the youngest grains with overlapping error terms to calculate MDA has been demonstrated by Dickinson and Gehrels (2009) to be a statistically robust method for constraining maximum times of deposition

for strata. Isotope dilution thermal ioniozation mass spectrometry can be utilized in future studies of these units to improve accuracy of the young grains used to calculate MDA.

In addition to providing a revised age model for the Blackhawk-Castlegate succession, MDAs can be used to reinterpret correlation models. Although this task extends beyond the actual scope of, and data availability for, this study, the potential implications of such a reinterpretation are illustrated using a correlation panel in Figure 17 from Liu et al. (2014), wherein the Castlegate Unconformity is reinterpreted to form 2.3 Myrs later than previously thought, and the unconformity underlying the Bluecastle Tongue forms 0.8 Myrs earlier than previously interpreted. In the Liu et al. (2014) correlation panel, the new age assignment for the Castlegate Unconformity moves the correlative surface ~300 m higher than its previously interpreted position in the thickest portion of the associated marine mudstone deposits, and demonstrates the utility in employing detrital zircon U-Pb age dating when correlating key stratigraphic surfaces over long distances.

It is important to note that there are differences between all correlation models for this region with regard to age assignments and the nature of inferred timelines between fluvial-deltaic and shoreline strata, and the more basinal Mancos shale. These differences can be attributed to the inherent difficulty in tracing key surfaces within terrestrial strata, a lack of continuous exposures in the marine-equivalent Mancos Shale, and assumptions made in different genetic models (e.g. Young, 1955; McLaurin and Steel, 2000; Miall and Arush, 2001; Hampson, 2010; Aschoff and Steel, 2011; Hampson et al., 2012; Seymour and Fielding, 2013; Liu et al., 2014; among many others). U-Pb age dating of the terrestrial component illustrates an approach to chronostratigraphic correlation that can link strata in updip and downdip localities that cannot otherwise be physically tied to each other, and is wholly independent of stratigraphic models.

Achieving robust updip to downdip correlation holds the potential for more robust calculations of rates of deposition, such as those attempted in Aschoff and Steel (2011), and enables a better understanding of relationships between deposits, surfaces, and independently known-forcing mechanisms (tectonic activity, sea-level change, climate cycles).

U-Pb ages presented in this paper are clearly not enough to reinterpret Late Cretaceous source-to-sink deposition throughout the Western Interior. However, they contribute to a larger geochronological framework that, when combined with other datasets, such as Szwarc et al. (2014), provide a higher-resolution insight to the depositional history of the region.

5.2 Grain Size Dependence Hypothesis

Detrital zircon U-Pb age data from the upper Blackhawk and Lower Castlegate at Thompson Canyon show that young volcanogenic grains are not observed in the medium to fine sandy channel-belts that are usually sampled, nor the genetically related finer grained crevasse splay and abandoned channel-fill facies that are comprised of fine to very fine sand and silt. There are 3 possibilities that may explain the absence of young grains in these facies. First, coarse silt-sized zircons are hydrodynamically equivalent during fluvial sediment transport to fine lower to very fine upper sand-sized quartz (Lawrence et al., 2011 and Malusa et al., 2015), so the fractionation may not be evident in the fine- to very fine-sandy facies that were sampled. Second, if the young zircons were hydrodynamically equivalent to the lower limits of the coarse-silt sand-sized quartz or finer, they may not have been of adequate size or mass to be recovered from the mineral separation procedures outlined in Appendix B, nor of sufficient size to place a 20 μm diameter spot in a 40 μm diameter cleaning pit. Finally, the drainage area that contributed sediments to Thompson Canyon did not include significant volcanic ash deposition, or

volcanogenic zircons were not transported downstream in a high enough concentration to be recovered in an assemblage of n=300 grains in any of the five samples from this location. Testing this hypothesis at a location that is known to produce young volcanogenic zircons may yield different results. An obvious location would be the upper Blackhawk at Horse Canyon, where young volcanogenic grains were abundant.

One additional unexpected outcome of this test of samples from different facies within the same outcrop was the ability to examine changes in signals, represented by changes in clusters, throughout different facies in a single vertical section. Figure 9 schematically illustrates the facies from which each sample was collected from and their position relative to each other. The 5 samples belong to 3 distinct clusters, suggesting more than one river was involved in deposition. For example, KBH-03 represents the channel-belt facies directly related to the laterally adjacent abandoned channel-fill facies from which KBH-05 was collected, yet the 2 samples belong to the Turquoise and Yellow clusters, respectively. This suggests a distributary from a second system annexed, or contributed to, the topographically low abandoned channel after the formative river had relocated due to avulsion. The Yellow cluster signal then persists through the overlying crevasse splay facies of KBH-04.

Blackhawk fluvial strata at this location are truncated upward by a transgressive surface of marine erosion and flooding, then covered by thick sets of amalgamated hummocky cross beds. The Castlegate Unconformity then overlies these hummocky cross-beds, and represents a significant basinward shift in the fluvial system. The lowermost abandoned channel-fill facies of the Lower Castlegate, represented by KBH-06, belongs to the Dark Green cluster, then sample KBH-07, collected from overlying channel-belt sands, again belongs to the Yellow cluster. These relationships provide support to the notion that the upper Blackhawk had the same

genetically-linked rivers involved in deposition as the Lower Castlegate at the same location, and illustrate the profound influence of avulsion or bifurcation and mixing of populations on the deposits.

5.3 Paleodrainage Reconstruction

5.3.1 Previous Work and Depositional Model

DZ U-Pb data has been utilized in the past to reconstruct large-scale paleodrainage patterns (Dickinson and Gehrels, 2008b; Szwarc et al., 2014; Blum and Pecha, 2014; Blum et al., 2017). The interpretations below use DZ U-Pb data from this study, in conjunction with those of previous studies, to interpret paleodrainage patterns and sediment routing to the Blackhawk-Castlegate fluvial systems: as interpreted here, discrete paleodrainage areas produce statistically distinct parent populations of DZ U-Pb ages. The discussion also addresses the mostly autogenic river dynamics that can explain what are here interpreted to represent daughter, or mixed, populations of U-Pb ages.

In the broadest sense, the western Laurentian passive margin was fed by river systems that drained the Appalachian-Ouachita Cordillera of the eastern and southern US and northern Mexico beginning in the Pennsylvanian (Gehrels and Pecha, 2014). Actual river systems are difficult to identify until late Triassic deposition of the Chinle Formation, which reflects sediment transported to the western margin through a large trunk river from headwaters located in present-day Texas (Riggs et al., 1996; Dickinson and Gehrels, 2009). The Chinle system had tributaries that transported sediment, most likely exposed in the Mogollon Rim in Arizona and the ancestral Rockies in western Colorado (see Lawton et al., 2015), which is distinguished by ca. 1440, 1640 Ma and 1700 Ma peaks. By the time of late Jurassic Morrison Formation

deposition, river systems in the western US had reorganized and were draining the Western Cordillera and flowing east, converging with Appalachian-derived rivers in the Sevier backbulge, and flowing north to the Western Canada sedimentary basin and Boreal Sea (Blum and Pecha, 2014; Blum et al., 2016). Middle Cretaceous flooding of the Western Interior Seaway partitioned the fluvial system (Kauffman, 1977). By the early Santonian, regional paleodrainage included an axial component that was primarily fed by the Mogollon Highlands and Cordilleran Magmatic Arc, with additional input by transverse fans draining the Sevier fold-and-thrust belt (Szwarc et al., 2014; Lawton et al., 2014). Campanian drainages that supplied sediment for the Mesaverde Group are interpreted to have evolved slightly from the drainages of the early Santonian due to withdrawal of the Western Interior Seaway, but the overarching pattern was most likely similar.

From a spatial perspective, locations in the Wasatch Plateau (Straight and Price Canyon) were closer to the Sevier fold-and-thrust belt, and therefore record the most proximal, updip facies within a given interval of time, relative to locations farther east in the Book Cliffs (Horse, Tusher, and Thompson Canyon). The succession in Straight Canyon is also interpreted to be slightly more proximal than Price, as evidenced by the lack of Blackhawk shoreline facies in Straight Canyon. Hovius (1996) calculated a spacing ratio for rivers emerging from linear mountain belts, where the distance between outlets is roughly half of the straight-line distance from the main drainage divide to the base of the mountain front. Straight and Price Canyons are within 25 km of the Sevier fold-and-thrust belt, hence it is reasonable to expect multiple fluvial systems would have emerged from the orogenic belt over the spatial scale of this study.

The Blackhawk-Castlegate succession is interpreted to be the product of overall eastward-prograding fluvial-deltaic and shoreline systems within the Sevier foreland basin

system, with accommodation created by flexural and dynamic subsidence (DeCelles, 2004; Painter and Carrapa, 2013). As is the case for most fluvial systems, Blackhawk-Castlegate rivers would have transitioned from highly migratory systems updip, which produced amalgamated channel-belt sands as seen in the Lower Castlegate, to avulsive, distributive systems farther downdip as channels approach a contemporaneous shoreline, which form narrow channel-belt sand bodies encased in flood-plain mudrocks as seen in the Blackhawk Formation (Adams and Bhattacharya, 2005; Hampson et al., 2012; Rittersbacher et al., 2014). A depositional model illustrating these surface processes and the stratigraphic patterns they build is shown in Figure 18. Recently, a number of authors use the term "Distributive Fluvial System (DFS)" to specifically describe non-marine attached systems with deposition that "radiates outward from an apex located where the river enters the sedimentary basin" (Weissmann et al., 2010; Davidson et al., 2013; Davidson and Hartley, 2014). Here, the term "distributive" is used as an adjective that also describes the pattern that marine-attached coastal-plain fluvial to fluvial-deltaic systems acquire due to avulsion in their downdip reaches. As noted in Sambrook-Smith et al. (2010), diagnostic criteria for the DFS of Weissmann et al. (2010) and others are not unique and can be applied to rivers in other settings.

In a distributive coastal-plain system, then, a small number of larger trunk channels branch downstream into several smaller channels in an overall radial pattern. Therefore, locations in the Wasatch Plateau are interpreted to record trunk channel deposition. As the distance to the shoreline decreases, and rivers enter their backwater reach, fluvial systems experience an increase in avulsive behavior and more variable sinuosity due to bifurcation upon reaching the backwater length (Slingerland and Smith, 2004; Jerolmack and Swenson, 2007; Weissmann et al., 2010; Davidson et al., 2013). Channels avulse due to increased sediment flux

and superelevation of the channel belt, and occur when erodible substrate composition, gradient advantages, and/or floodplain channels are present and triggered by an event, such as a flood (Slingerland and Smith, 1998; Mohrig et al., 2000; Aslan et al., 2005); this is the dominant process by which sediment is spread across the alluvial-deltaic plain (Aslan et al., 2005).

At any single location, progradational patterns are reflected temporally by a vertical increase in channel size and decrease in frequency (Weissmann et al., 2010; Rittersbacher et al., 2014). The vertical decrease in sandbody frequency, increase in maximum and average sandbody size, and decrease in floodplain area to channel area ratio provide evidence for a progradational distributive system (Weissmann et al., 2010; Rittersbacher et al., 2014). Measured grain sizes of dominantly medium and finer sand in the Blackhawk of Horse Canyon, in conjunction with measured channel heights of 4-7 m, place the abandoned channels of the Book Cliffs in a relatively downdip, meandering parameter space (Table 4). In the lower Blackhawk, the presence of tidal signatures and an absence of vertical trends are attributed to deposition within the backwater length of the coastal plain (Rittersbacher et al., 2014). Bifurcation dominates in the lower Blackhawk and through the succession at locations closest to the corresponding shoreline; this surface process increases the probability of mixing channels and their associated signals. Evidence for mixed daughter products, described below, include an increasingly complex signal within the aggregate age distributions, as grains from increasingly multiple sources merge. At increased distances from the shoreline, channel sandbodies are larger and occur at lower frequency than those present in the lowermost intervals and downdip locations, as evidenced by the stratigraphic architecture portion of the block diagram in Figure 18 and the graph in Figure 19 (Rittersbacher et al., 2014). These trends reflect deposition by larger and fewer trunk channels (Davidson et al., 2013).

5.3.2 U-Pb Age Population Analyses

Three dominant signals are present within the DZ U-Pb populations of the Blackhawk-Castlegate succession: the greater Western Cordillera, Sevier fold-and-thrust belt, and Mogollon Highlands. Different proportions of these aggregate signals, and differences in individual peaks, define the different clusters identified in the Results section, and form the basis for paleodrainage reconstruction described below.

5.3.2.1 Population 1: Western Cordillera

Late Paleozoic to Mesozoic to grains (ca. 275-72 Ma) are present in proportions ranging from 0-11%. Two prominent peaks emerge at ca. 100 Ma and 160 Ma, corresponding to well-known magmatic pulses in the Sierra Nevada Batholith, which extends from southern California to northwest Nevada (Bateman, 1983, 1992; Barton et al., 1988; Armstrong and Ward, 1993; Barton, 1996; Ducea, 2001). Presence of this Jurassic and mid-Cretaceous population indicates that exhumed and exposed plutons of the Sierra Nevada may have been part of the paleodrainage area. However, it must be noted that these abundance peaks are seen in DZ samples throughout in the Western Interior, so recycling is a possibility as well. Younger grains, especially those with U-Pb ages ca. 80-72 Ma used in MDA calculations, do not form a visible peak on KDEs, but must be derived from ashfalls linked to their original volcanic source or layers of ash eroded almost immediately following deposition. The <earthchem.org> database shows potential sources for felsic to intermediate composition volcanic rocks of this age in Idaho, Montana, central Nevada, and Arizona (Figure 6). The clusters described in Figure 13 that contain these grains, in order of decreasing occurrence, are: Blue, Light Green, Pink, Black, and Turquoise.

The young grains used for MDAs co-occur with the ca. 100 Ma peak in all samples, which suggests the ash from which young grains were derived was generally sourced from the same area as the rest of the Western Cordilleran population.

5.3.2.2 Population 2: Sevier Fold-and-Thrust Belt

Grains of the Appalachian, Neoproterozoic and early Paleozoic Peri-Gondwanan, and Grenville populations comprise an average of 39% of all samples. This population is ubiquitous throughout the Western Interior, where it occurs within the Laurentian passive margin succession, was ultimately derived from drainage of the Appalachian-Ouachita Cordillera (Link et al., 1993), and reflects large-scale east to west transfer of material during the Neoproterozoic through early to middle Mesozoic (Dickinson and Gehrels, 2003, 2010; Gehrels and Pecha, 2014). Beginning in the late Jurassic, with deposition of the Morrison Formation (Dickinson and Gehrels, 2008a; Fuentes et al., 2009, 2011), older passive margin sediments were entrained in the Sevier fold-and-thrust belt, and transported back to the east (Dickinson and Gehrels, 2008a, 2008b, 2009; Lawton et al., 2010; Lawton and Bradford, 2011). Specific sediment sources for Blackhawk-Castlegate rivers within the Sevier fold-and-thrust belt included the Midas and Sheeprock thrust sheets, which provided Precambrian-Mesozoic clasts to the Blackhawk (Mitra, 1997; Horton et al., 2004), the Oquirrh Group, which is exposed in the thrust sheet of the Santaquin culmination (Horton et al., 2004), and the Precambrian and Paleozoic basement rocks in the Canyon Range Thrust, which share many U-Pb age peaks with the Mesaverde Group (DeCelles and Coogan, 2006, Lawton et al., 2015).

The most important abundance peaks within the thrust-belt derived Paleozoic through Mesoproterozoic DZ populations are the ca. 1060 Ma, 1100 Ma, and 1170 Ma peaks of the

Grenville. The ca. 1060 Ma and 1170 Ma peaks, known to be from the Ottawan and Shawaningan Orogenies, respectively, are common throughout the Western Interior as products of Laurentian passive margin sedimentation, or deposited via eolian transport, as is seen in the Diamond Creek Sandstone of the White River Erg in north-central Utah (Rivers, 1997; Gray and Zeitler, 1997; Becker et al., 2005; Heumann et al., 2006; Lawton et al., 2015). Conversely, the ca. 1100 Ma peak may be from the Llano Uplift of Texas (Mosher, 1998; Reese et al., 2000) or the rocks exposed in the Midcontinent rift (Swanson-Hysell et al., 2014), and transported to the study area by the NW-flowing rivers of the Chinle Fm. for later reworking (Dickinson and Gehrels, 2008b).

5.3.2.3 Population 3: Mogollon Highlands

The Mogollon Highlands were, and still are, a topographic high that exposes 1.9-1.3 Ga Trans-Hudson and Yavapai-Mazatzal orogens, with numerous intrusions linked to the 1.3-1.55 Ga Midcontinent granite-rhyolite province, and persisted through the late Cretaceous (Wasserburg and Lanphere, 1965; Hayes, 1970; Peterson and Kirk, 1977; Ferguson et al., 2004; Spencer and Pecha, 2012). Peaks from the Midcontinent population include ca. 1350 Ma, 1430 Ma, and 1500 Ma, whereas Yavapai-Mazatzal-aged peaks include ca. 1640 Ma, 1700 Ma, and 1775 Ma. Specific details on source regions are as follows:

- The ca. 1350 Ma and 1500 Ma peaks are common in the granite-rhyolite province in the eastern US midcontinent (Dickin and Higgins, 1992; Dickin, 2000), whereas the original protolith source for the 1430 Ma peak are likely the plutonic intrusions into the Yavapai-Mazatzal provinces (Whitmeyer and Karlstrom, 2007).

- The ca. 1430 Ma peak is also common in Paleozoic and Mesozoic strata of the Western Interior, including the Chinle, Dakota, Morrison, Lytle, Oxyoke, and Vinini Formations, and the Jurassic Eolianites (e.g. Dickinson and Gehrels, 2008a, 2008b, 2009; Gehrels and Pecha, 2014), and could have been be recycled from older units.
- The ca. 1640 Ma peak is present throughout many samples in the Western Interior that have a southern source (including the Chinle, Dakota, Morrison, and Lytle), but has 2 possible primary sources: (1) the Mazatzal-aged plutons of the Cochise Block of eastern Arizona (Whitmeyer and Karlstrom, 2007; Dickinson and Gehrels, 2008b; Laskowski et al., 2013), and (2) the ~1.65 Ga quartzite successions in the southwestern US (Whitmeyer and Karlstrom, 2007; Jones et al., 2009).
- The ca. 1700 peak has 2 possible original protolith sources: (1) Yavapai granitoids with an age of 1.72-1.68 Ga, which intruded much of Arizona and Southern California, and (2) the ~1.70 Ga quartzite deposits in southern Colorado, northern New Mexico, central Arizona, and southern California (Whitmeyer and Karlstrom, 2007; Jones et al., 2009). While existing data cannot differentiate between the two, the source regions generally overlap.
- The ca. 1775 Ma peak is likely derived from juvenile crust within the Yavapai province (Whitmeyer and Karlstrom, 2007).

5.3.3 Identification of Blackhawk-Castlegate DZ Parent Populations

As discussed in the Results, U-Pb ages from the 31 DZ samples in this study have been placed into 10 distinct clusters using modified multidimensional scaling, with each cluster named after a distinct color (Figure 13). The proportions of different source signals, as well as the

presence or absence of individual peaks in KDE plots, plays a large role in the determination of source terrains.

The upper Blackhawk and Lower Castlegate samples from Straight Canyon and Price Canyon represent the farthest updip, in terms of modern geographic location, and in terms of their original position within the Campanian sediment dispersal system. In each case, samples above and below the Castlegate Unconformity are statistically indistinct; that is, their K-S dissimilarity P-value is high enough to plot within the same MDS cluster. For clarity, I will hereafter refer to the "Light Green" and "Yellow" clusters as the parent, or primary, signals present in Straight Canyon and Price Canyon, respectively. Their regional paleogeographic interpretations are indicated in Figure 20. Stratigraphically lower samples of the Blackhawk Fm. in Straight Canyon, and all samples in Horse, Tusher, and Thompson Canyons, represent more distal facies and/or downdip locations, and are interpreted here to represent mixtures of the Light Green and Yellow clusters, or daughter populations.

5.3.3.1 Light Green Cluster

The Light Green cluster includes the upper Blackhawk (KBH-19) and Lower Castlegate (KBH-01) samples in Straight Canyon that define a parent river, as well as a Lower Castlegate sample (BC-10) from Horse Canyon, which is interpreted to represent the downstream extension of the same parent river. The most important and diagnostic signals consist of the ca. 1430 Ma Midcontinent peak, and the ca. 1700 Ma and 1775 Ma Yavapai-Mazatzal peaks: these peaks have been identified in other southern-sourced fluvial deposits throughout the Western Interior (Szwarc et al., 2014; Dickinson and Gehrels, 2008b). The specific, and well-defined nature of these peaks in the Light Green cluster is interpreted to reflect derivation from a primary source,

and to provide evidence for an axial, or longitudinal (in the foredeep parallel to the orogenic front), river system with headwaters in southern and central Arizona, most specifically the plutons and juvenile crust exposed in the Mogollon Highlands, as shown in Figure 20 (Whitmeyer and Karlstrom, 2007).

It is also possible that some or all of the Light Green cluster could be derived from recycling of the Cordilleran passive margin of Nevada and Utah, described in Gehrels and Pecha (2014). For example, the Ordovician Vinini Formation and Devonian Oxyoke Canyon Sandstone of central Nevada are potential sources that, when combined, could produce the specific peaks in the Light Green cluster (Gehrels et al., 2000). However, drainage area calculations for the Blackhawk-Castlegate using a mass-balance approach, the presence of the late Cretaceous Nevadaplano topographic high, and other studies that interpret a southern source for the clastic wedge that includes the samples in the Light Green cluster, make this source less likely (Aschoff and Steel, 2011; Hampson et al., 2014; Snell et al., 2014; N. Bartschi and J. Saylor, personal communication). Hence, while some grains in the Light Green cluster are likely reworked from passive margin strata, prominence of the ca. 1430 Ma, 1700 Ma, and 1775 Ma peaks suggest a primary southern source as described above.

5.3.3.2 Yellow Cluster

The Yellow cluster is the largest, and composed of eight samples: the upper Blackhawk (BC-14) and lowermost Castlegate (BC-13) at Price Canyon, KBH-18 (middle Blackhawk) and BC-07 (Upper Castlegate/Bluecastle Tongue) from Horse Canyon, BC-01 (upper Blackhawk from Tusher Canyon), and KBH-04 and 05 (upper Blackhawk) and KBH-07 (Lower Castlegate) at Thompson Canyon. The inclusion of the upper Blackhawk and Lower Castlegate samples in

Price Canyon defines a parent river system, with other samples farther downdip representing downstream extensions of this parent river. The Yellow cluster is differentiated from the Light Green cluster by the presence of a strong 1640 Ma peak, very subtle 1700 Ma and 1775 Ma peaks, a broader spectrum of Midcontinent ages, and a paucity of Western Cordilleran grains. U-Pb ages are more evenly spread between major population groups, with less prominent peaks, which may indicate dominantly recycled material.

From a paleogeographic view, a recycled origin for the Yellow cluster is perhaps the most reasonable explanation, especially given the geographic location: Triassic Chinle, Jurassic eolianites, the Jurassic Morrison Formation, and older Cretaceous rocks of the Sevier foreland contain the necessary Population 2 signals, and were likely part of the advancing Sevier fold-and-thrust belt where they would have served as source material to the transverse rivers draining the orogeny: this area, which contains the Castlegate type area, has been referred to as the Castlegate Fan by a number of authors (e.g. Lawton et al., 2014). There are 2 possibilities that may explain the presence, in low abundance, of the ca. 1700 Ma and 1775 Ma peaks. First, the peaks may represent a convergence of the drainage extending from Straight Canyon, with those peaks diluted by an abundance of other signals present as numerous grains of varying ages are mixed. Conversely, the peaks may represent a fluvial system that predates the river feeding deposits in Straight Canyon, also with a southern source that carried grains of the same ages, and exposed within the drainage area in the Sevier fold-and-thrust belt that acted as a source for deposits in what is now Price Canyon.

A possible source for the prominent ca. 1640 Ma peak may be the Mazatzal-aged plutons of the Cochise Block in eastern Arizona. This interpretation requires an axial river that flowed to the east of the fluvial system responsible for the Light Green cluster, passed by the area that is

now Straight Canyon, and to the area that is now Price Canyon. While this geometry is improbable from a paleogeographic sense, if such a tributary existed, it is likely to have been secondary to the input by transverse fans that drained the Sevier fold-and-thrust belt.

The Yellow cluster is therefore interpreted to represent deposition by fluvial systems that primarily drained the Sevier fold-and-thrust belt, and potentially served as a downdip continuation of the fluvial system responsible for the Blackhawk-Castlegate deposition in what is now Straight Canyon. An interpretation for the spatial distributions of the fluvial systems is depicted in Figure 20.

5.3.4 Blackhawk-Castlegate DZ Daughter Populations

The concept of parent and daughter populations in the Blackhawk-Castlegate succession rests on two premises. First, in addition to the primary parent systems interpreted above for the Light Green and Yellow clusters, it is likely there were smaller transverse systems that drained, and emerged from, the Sevier fold-and-thrust belt. Second, surface dynamics, especially contributive vs. distributive behavior, almost certainly played an important role. For example, as transverse systems flowed to the east, they merged with parent axial systems, which created mixed U-Pb age populations. Then, as the combined streams approached the Western Interior Seaway, they began to avulse and distribute sediments across the north-south oriented coastal plain, with a distributary from one master stream sometimes joining a distributary from another, again creating a mixed population.

It is likely there are more parent systems than the two discussed above from Straight and Price Canyon. However, based on how river systems are organized and behave, it is also likely that there are multiple mixed “daughter” populations in downdip facies of the lower and middle

Blackhawk within Straight and Price Canyon, and within the entire Blackhawk-Castlegate succession at downdip locations like Horse, Tusher, and Thompson Canyons. The following provides an attempt to unravel these daughter populations.

5.3.4.1 Brown Cluster

The Brown cluster includes Lower (BC-15) and Upper (BC-16) Castlegate samples in Price Canyon, as well as a middle Blackhawk sample (KBH-17) in Horse Canyon, and differs from the Yellow cluster only by a higher ca. 1640 Ma peak and more subdued ca. 1700 Ma and 1775 Ma peaks. This suggests contributive and distributive processes may have played a role upstream from Price Canyon. For example, the Brown cluster may represent deposits that were derived from a different river system that also drained the Sevier fold-and-thrust belt, which provided similar but not exactly the same source material, and joined the Light Green river as it flowed to the east through what is now Price Canyon.

5.3.4.2 Black Cluster

The Black cluster is composed of samples BC-17 (Bluecastle Tongue) and BC-09 (Lower Castlegate) in Price Canyon and Horse Canyon, respectively, and has the highest concentration of grains in the ca. 1100 Ma and 1775 Ma peaks. The river feeding these deposits potentially tapped into a major Grenville source, specifically grains of 1100 Ma that likely had an original primary source in the Llano Uplift within the Laurentian Grenville Province of central Texas (Mosher, 1998). Direct transport from the protolith source region via fluvial drainage systems during the Late Cretaceous is implausible due to the presence of the Western Interior Seaway, hence grains of 1100 Ma are part of the recycled population, most likely from late Triassic

Chinle Fm. fluvial deposits that are now included within the fold-and-thrust belt (Dickinson and Gehrels, 2008b).

5.3.4.3 Pink Cluster

The Pink cluster is comprised of BC-08 (Upper Castlegate) in Horse Canyon and BC-06 (lower Sego) in Tusher Canyon, and is most notable for an anomalously high number of zircons belonging to the Western Cordillera population, including those with U-Pb ages of ca. 80-72 Ma. The presence of these grains suggests the Pink cluster represents a river that had both parent signals, and was subsequently joined by a tributary with a drainage area that included active volcanic terrain in Idaho, Nevada, or southwest Arizona, or ash beds from those volcanic sources. Samples within the Pink cluster have been argued to represent a time of rapid progradation, and the potential introduction of multiple sources, including some from the north (Aschoff and Steel, 2011; N. Bartschi and J. Saylor, personal communication).

5.3.4.4 Blue Cluster

The Blue cluster is comprised of 3 samples, KBH-15 (lower Blackhawk in Straight Canyon), BC-11 (upper Blackhawk in Horse Canyon), and KBH-08 (upper Blackhawk in Tusher Canyon). It is interpreted to be the daughter of the Light Green cluster and another unknown parent, because of the larger proportions of grains from Population 2. This is less-so the case with KBH-15 of Straight Canyon, although it has sufficient statistical similarities with the other samples to be included in this cluster.

5.3.4.5 Lavender Cluster

The Lavender cluster has similar characteristics to the Yellow and Brown clusters, the main difference being a moderate peak at ca. 100 Ma. It is composed of only two Blackhawk samples in Horse Canyon: KBH-10 (lower Blackhawk, Kenilworth shoreface sandstone) and KBH-16 (upper-middle Blackhawk). Shoreface sandstones are affected by longshore currents coming from the north, a product of the counterclockwise hydrodynamic circulation in the Western Interior Seaway (Ericksen and Slingerland, 1990; Slingerland and Keen, 1999), and assigning a provenance is therefore more difficult. However, sample KBH-16 from the upper-middle Blackhawk in Horse Canyon was likely within the avulsing coastal-plain part of the system, and thus had a high chance of mixing with avulsing channels from other parents that may have carried the 100 Ma signal that has a high presence in the Pink cluster, but is only a minor signal in half of all other clusters.

5.3.4.6 Red, Turquoise, and Dark Green Clusters.

The Red cluster includes: KBH-02 (Star Point) and KBH-12 (middle Blackhawk) of Straight Canyon, and KBH-11 (lower Blackhawk) of Horse Canyon; the Turquoise cluster includes: BC-03 (upper Blackhawk) and BC-05 (Lower Castlegate) of Tusher Canyon, as well as KBH-03 (upper Blackhawk) of Thompson Canyon; and the Dark Green cluster includes: and KBH-09 (upper Blackhawk) of Tusher Canyon and KBH-06 (Lower Castlegate) of Thompson Canyon. The same peaks are present and absent in all three clusters, however those that are present are made of varying amounts of grains that likely contributed to their statistical dissimilarity. The exception to these similarities are variations in the Midcontinent peaks between the three clusters: the Red cluster has all three peaks at ca. 1350 Ma, 1430 Ma, and 1500

Ma, the Turquoise cluster has peaks at ca. 1350 Ma and 1430 Ma, and the Dark Green cluster only has the ca. 1430 Ma peak. Other key peaks shared by all include: minor peaks at ca. 100 Ma, 420 Ma and 600 Ma, plus all three Grenville peaks at ca. 1060 Ma, 1100 Ma, and 1170 Ma. The resemblance of these age distributions to one another is here interpreted to indicate the spatial and temporal complexity that avulsion introduces into the DZ populations, and the downstream convergence of age distributions as signals become increasingly mixed.

6 Conclusions and Future Work

This thesis presents a comprehensive DZ U-Pb record of 31 samples through the Blackhawk-Castlegate succession exposed in the Wasatch Plateau and Book Cliffs of east-central Utah. MDAs were used to approximate the time of deposition for the upper Blackhawk, Lower Castlegate, and Bluecastle Tongue. Multidimensional scaling, cluster analysis, parent-daughter relationships, and comparison to DZ U-Pb data from other studies were used to reconstruct the paleodrainage system as rivers evolved from updip to their terminus in the Western Interior Seaway.

The data and key interpretations from this study are summarized as follows:

- DZ samples collected from different facies in Thompson Canyon do not support the view that young volcanogenic zircons preferentially fractionate into finer grained deposits, but do not necessarily refute this view either, as none of the samples contained young grains that approximate depositional age. Testing this hypothesis at a location where young volcanogenic grains are known to be abundant, such as the upper Blackhawk at Horse Canyon, may yield different results.
- MDAs calculated throughout the succession approximate, or are up to 2 Myrs younger than, the previously inferred time of deposition for the upper Blackhawk and Lower Castlegate, and potentially the Bluecastle Tongue as well. There is approximately 1.9 Myrs of missing time between the upper Blackhawk and Lower Castlegate in Horse Canyon, which includes time associated with development of the Castlegate unconformity as well as deposition of a portion of the Lower Castlegate. This suggests the Castlegate Unconformity represents less time than previously thought.

- The Light Green and Yellow clusters in the DZ U-Pb record represent "Parent" rivers in Straight and Price Canyon respectively, but are statistically distinct from each other. This indicates that the main sources for each locality were different. Additionally, spacing ratios calculated by Hovius (1996) suggest far more parent rivers were likely involved in deposition of the Blackhawk-Castlegate succession than the two identified in this study, which is more than previously thought by some workers.
- Additionally, the upper Blackhawk and Lower Castlegate samples are statistically indistinct from one another at each location. This provides evidence that the upper Blackhawk represents deposition by the same rivers responsible for the Lower Castlegate deposition at each location, in spite of the unconformity that separates the two units.
- Campanian drainages responsible for deposition of the Mesaverde Group are interpreted to have evolved slightly from the drainages of the early Santonian, as described in Szwarc et al. (2014), but the regional drainage patterns are here interpreted to have been similar. DZ U-Pb data presented here can be explained by an axial (longitudinal) river system flowing north from the Mogollon Highlands, which is represented by the Light Green cluster in Straight Canyon. This axial drainage was joined by transverse fluvial systems that drained and recycled strata exposed in the Sevier fold-and-thrust belt, represented by the Yellow cluster in Price Canyon.
- "Daughter" clusters are proposed as the product of mixed detrital populations to account for input by small transverse fans that drained the proximal Sevier fold-and-thrust belt, then joined the parent rivers, as well as avulsion processes, which likely resulted in parent rivers joining farther downdip in the Book Cliffs part of the study area.

In addition to the above, U-Pb zircon ages and MDA calculations provide a statistically robust way to develop a geochronological framework in some terrestrial strata, which is key for correctly correlating deposits in a source-to-sink framework. Expanding this DZ study across more canyons in the Wasatch Plateau will help in the identification of along-strike variations and better constrain the spacing of the fluvial systems draining the Sevier fold-and-thrust belt. More samples for DZ U-Pb analysis will need to be collected throughout the Book Cliffs, and expanded to units above and below the Blackhawk-Castlegate succession, to achieve robust updip to downdip correlation. This larger geochronological framework can be used to test and revise existing correlation models and suggest alternatives, and to calculate rates of deposition and links with forcing mechanisms.

The large dataset presented in this study illustrates complex interactions between fluvial drainages of varying provenance. This study demonstrates that the stratigraphic record within a single outcrop can be the depositional product of multiple rivers that evolve through time, with surface processes such as avulsion and bifurcation playing key roles in the spreading of sediment across the alluvial-deltaic plain. When combined with multidimensional scaling, cluster identification, and parent-daughter analysis, detrital zircon U-Pb dating can provide powerful insight into regional paleo-depositional systems and local river channel dynamics.

7 References

Adams, M.M., and Bhattacharya, J.P., 2005, No change in fluvial style across a sequence boundary, Cretaceous Blackhawk and Castlegate Formations of central Utah, USA: Journal of Sedimentary Research, v. 75, p. 1038-1051.

Andersen, T., 2005, Detrital zircons as tracers of sedimentary provenance: limiting conditions from statistics and numerical simulation: Chemical Geology, v. 216, i. 3-4, p. 249-270.

Armstrong, R.L., 1968, Sevier orogenic belt in Nevada and Utah: Geological Society of America, Bulletin, v. 79, p. 429-458.

Armstrong, R.L., and Ward, P.L., 1993, Late Triassic to earliest Eocene magmatism in the North American Cordillera: implications for the Western Interior Basin, *in* Caldwell, W.G.E., and Kauffman, E.G., eds, Evolution of the Western Interior Basin, Geological Association of Canada Special Paper 39, p. 49-72.

Aschoff, J.L., and Steel, R.J., 2011, Anatomy and development of a low-accommodation clastic wedge, upper Cretaceous, Cordilleran Foreland Basin, USA: Sedimentary Geology, v. 236, p. 1-24.

Aslan, A., Autin, W.J., and Blum, M.D., 2005, Causes of river avulsion: insights from the late Holocene avulsion history of the Mississippi River, USA: Journal of Sedimentary Research, v. 75, p. 650-664.

Barth, A.P., Wooden, J.L., Jacobson, C.E., and Economos, R.C., 2013, Detrital zircon as a proxy for tracking the magmatic arc system: The California arc example: Geology, v. 41, p. 223-226.

Barton, M.D., 1996, Granitic magmatism and metallogeny of southwestern North America: Transactions of the Royal Society of Edinburgh: Earth Sciences, v. 87, p. 261–280.

Barton, M.D., Battles, D.A., Debout, G.E., Capo, R.C., Christensen, J.N., Davis, S.R., Hanson, R.B., Michelsen, C.J., and Trim, H.E., 1988, Mesozoic contact metamorphism in the western United States, *in* Ernst, W.G., ed., Metamorphism and Crustal Evolution of the Western United States, Englewood Cliffs, New Jersey, Prentice-Hall, Rubey Volume 7, p. 110–178.

Bateman, P.C., 1983, A summary of the critical relationships in the central part of the Sierra Nevada Batholith, California, U.S.A., *in* Roddick, J.A., ed., Circum-Pacific Plutonic Terranes, Geological Society of America, Memoir 159, p. 241–254.

Bateman, P.C., 1992, Plutonism in the central part of the Sierra Nevada batholith, California: U.S. Geological Survey, Professional Paper 1483, 186 p.

Beaumont, C., 1981, Foreland basins: Royal Astronomical Society Geophysical Journal, v. 55, p.

543–548.

Becker, T.P., Thomas, W.A., Samson, S.D., and Gehrels, G.E., 2005, Detrital zircon evidence of Laurentian crustal dominance in the lower Pennsylvanian deposits of the Alleghanian clastic wedge in eastern North America: Sedimentary Geology, v. 182, p. 59–86.

Bhattacharya, J.P., 2011, Practical problems in the application of the sequence stratigraphic method and key surfaces: integrating observations from ancient fluvial-deltaic wedges with Quaternary and modelling studies: Sedimentology, v. 58, p. 120-169.

Blum, M.D., and Pecha, M.A., 2014, Mid-Cretaceous to Paleocene North American drainage reorganization from detrital zircons: Geology, v. 42, p. 607–610.

Blum, M., Martin, J., Milliken, K., and Garvin, M., 2013, Paleovalley systems: Insights from Quaternary analogs and experiments: Earth-Science Reviews, v. 116, p. 128-169.

Blum, M.D., Milliken, K.T., and Snedden, J.W., 2016, Cenomanian Gulf of Mexico paleodrainage from detrital zircons: Source-to-sink sediment dispersal and prediction of basin-floor fans, *in* Mesozoic of the Gulf Rim and Beyond: New Progress in Science and Exploration of the Gulf of Mexico Basin, 35th Annual GCSSEPM Perkins-Rosen Research Conference.

Blum, M., Milliken, K.T, Pecha, M., Snedden, J., and Galloway, W., 2017, Detrital-zircon records of Cenomanian, Paleocene, and Oligocene Gulf of Mexico drainage integration and sediment routing: Implications for scales of basin-floor fans: Geosphere, v. 13, no. 4, p. 1-37.

Borg, I., and Groenen, P.J., 2005, Modern Multidimensional Scaling: Theory and Applications. Springer.

Burchfield, B.C., and Davis, G.A., 1975, Nature and controls on Cordilleran orogenesis, western U.S.: extensions of an earlier synthesis: American Journal of Science, v. 275A, p. 363–396.

Chan, M.A., and Pfaff, B.J., 1991, Fluvial sedimentology of the upper Cretaceous Castlegate Sandstone, Book Cliffs, Utah, *in* Chidsey Jr., T.C., ed., Geology of East-Central Utah, Utah Geological Association, Publication 19, p. 95-109.

Christiansen, E.H., Kowallis, B.J., and Barton, M.D., 1994, Temporal and spatial distribution of volcanic ash in Mesozoic sedimentary rocks of the western interior: An alternative record of Mesozoic magmatism, *in* Caputo, M.V., Peterson, J.A., and Franczyk, K.J., eds., Mesozoic Systems of the Rocky Mountain Region, USA, Denver, Colorado, Rocky Mountain Section, SEPM, p. 73-94.

Cobban, W.A., 1973, Significant ammonite finds in uppermost Mancos Shale and overlying formations between Barker Dome, New Mexico, and Grand Junction, Colorado, *in*

Fassett, J.E., ed., Cretaceous and Tertiary Rocks of the Southern Colorado Plateau, Four Corners Geological Society, A Memoir, p. 148-153.

Cobban, W.A., McKinney, K.C., Obradovich, J.D., and Walasczyk, I., 2006, A USGS zonal table for the Upper Cretaceous Middle Cenomanian-Maastrichtian of the Western Interior of the United States based on Ammonites, Inoceramids, and radiometric ages, USGS Open-File Report 2006-1250, p. 1-46.

Coffey, K.T., Schmitt, A.K., Ford, A., Spera, F.J., Christensen, C., Garrison, J., 2014, Volcanic ash provenance from zircon dust with an application to Maya pottery: Geology, v. 42, no. 7, p. 595-598.

Davidson, S.K., and Hartley, S.K., 2014, A quantitative approach to linking drainage area and distributive-fluvial-system area in modern and ancient endorheic basins: Journal of Sedimentary Geology, v. 84, p. 1005-1020.

Davidson, S.K., Hartley, A.J., Weissmann, G.S., Nichols, G.J., and Scuderi, L.A., 2013, Geomorphic elements on modern distributive fluvial systems: Geomorphology, v. 180-181, p. 82-95.

DeCelles, P.G., 2004, Late Jurassic to Eocene evolution of the Cordilleran thrust belt and foreland basin system, Western USA: American Journal of Science, v. 304, p. 105-168.

DeCelles, P.G., and Coogan, J.C., 2006, Regional structure and kinematic history of the Sevier fold-and-thrust belt, central Utah: GSA Bulletin, v. 118, no. 7/8, p. 841-864.

DeCelles, P.G., and Currie, B.S., 1996, Long-term sediment accumulation in the Middle Jurassic-early Eocene Cordilleran retroarc foreland basin system: Geology, v. 24, p. 591-594.

Dickin, A.P., 2000, Crustal formation in the Grenville province: Nd-isotope evidence: Canadian Journal of Earth Sciences, v. 37, p. 165–181.

Dickin, A.P., and Higgins, M.D., 1992, Sm/Nd evidence for a major 1.5 Ga crust-forming event in the central Grenville Province: Geology, v. 20, p. 137–140.

Dickinson, W.R., and Gehrels, G.E., 2003, U-Pb ages of detrital zircons from Permian and Jurassic eolian sandstones of the Colorado Plateau, USA: Paleogeographic implications: Sedimentary Geology, v. 163, p. 29-66.

Dickinson, W.R., and Gehrels, G.E., 2008a, Sediment delivery to the Cordilleran foreland basin: Insights from U-Pb ages of detrital zircons in Upper Jurassic and Cretaceous strata of the Colorado Plateau: American Journal of Science, v. 308, p. 1041–1082.

Dickinson, W.R., and Gehrels, G.E., 2008b, U-Pb ages of DZs in relation to paleogeography: Triassic paleodrainage networks and sediment dispersal across southwest Laurentia: Journal of Sedimentary Research, v. 78, p. 745-764.

Dickinson, W.R., and Gehrels, G.E., 2009, Use of U–Pb ages of detrital zircons to infer maximum depositional ages of strata: a test against a Colorado Plateau Mesozoic database: Earth and Planetary Science Letters, v. 288, p. 115–125.

Dickinson, W.R., and Gehrels, G.E., 2010, Insights into North American Paleogeography and Paleotectonics from U-Pb ages of detrital zircons in Mesozoic strata of the Colorado Plateau, USA: International Journal of Earth Science, v. 99, p. 1247-1265.

Dodson, M.H., Compston, W., Williams, I.S., and Wilson, J.F., 1988, A search for ancient detrital zircons in Zimbabwean sediments: Journal of the Geological Society, London, v. 145, p. 977-983.

Ducea, M., 2001, The California arc: thick granitic batholiths, eclogitic residues, lithospheric-scale thrusting and magmatic flare-ups: GSA Today, v. 11, no. 11, p. 4–10.

Ericksen, M.C., and Slingerland, R., 1990, Numerical simulations of tidal and wind-driven circulation in the Cretaceous Interior Seaway of North America: Geological Society of America, Bulletin, v. 102, p. 1499–1516.

Fedo, C.M., Sircombe, K.N., and Rainbird, R.H., 2003, Detrital zircon analysis of the sedimentary record: Reviews in Mineralogy and Geochemistry, v. 53, no. 1, p. 277-303.

Ferguson, C.B., Duebendorfer, E.M., and Chamberlain, K.R., 2004, Synkinematic intrusion of the 1.4-Ga Boriana Canyon pluton, northwestern Arizona: Implications for ca. 1.4-Ga regional strain in the western United States: The Journal of Geology, v. 112, p. 165–183, doi:10.1086/381656.

Fisher, D.J., Erdman, C.E., and Reesie, J.B., 1960, Cretaceous and Tertiary formations of the Book Cliffs, Carbon, Emery, and Grand Counties, Utah and Garfield and Mesa Counties, Colorado: U.S. Geological Survey, Professional Paper 332, 80 p.

Flood, Y.S., and Hampson, G.J., 2014, Facies architectural analysis to interpret avulsion style and variability: upper Cretaceous Blackhawk Formation, Wasatch Plateau, Central Utah, USA: Journal of Sedimentary Research, v. 84, p. 743-762.

Flood, Y.S., and Hampson, G.J., 2015, Quantitative analysis of the dimensions and distribution of channelized fluvial sandbodies within a large outcrop dataset: upper Cretaceous Blackhawk Formation, Wasatch Plateau, central Utah, USA: Journal of Sedimentary Research, v. 85, p. 315-336.

Fouch, T.D., Lawton, T.F., Nichols, D.J., Cashion, W.B., and Cobban, W.A., 1983, Patterns and timing of synorogenic sedimentation in Upper Cretaceous rocks of central and northeast

Utah, *in* Reynolds M., and Dolly, E., eds., Mesozoic Paleogeography of West-Central US, SEPM Rocky Mountain Section, Symposium 2, p. 304-334.

Fuentes, F., DeCelles, G., Constenius, K.N., and Gehrels, G.E., 2011, Evolution of the Cordilleran foreland basin system in northwestern Montana, USA: Geological Society of America, Bulletin, v. 123, p. 507-533.

Fuentes, F., DeCelles, G., and Gehrels, G.E., 2009, Jurassic onset of foreland basin deposition in northwestern Montana, USA: Implications for along-strike synchroneity of Cordilleran orogenic activity: Geology, v. 37, p. 379-382.

Gani, M.R., Ranson, A., Cross, D.B., Hampson, G.J., Gani, N.D., and Sahoo, H., 2015, Along-strike sequence stratigraphy across the Cretaceous shallow marine to coastal-plain transition, Wasatch Plateau, Utah, USA: Sedimentary Geology, v. 325, p. 59-70.

Gehrels, G.E., 2000, Introduction to detrital zircon studies of Paleozoic and Triassic strata in western Nevada and northern California, *in* Soreghan, M.J., and Gehrels, G.E., eds., Paleozoic and Triassic Paleogeography and Tectonics of Western Nevada and Northern California: Geological Society of America, Special Paper 347, p. 1-18.

Gehrels, G.E., 2012, Detrital zircon U-Pb geochronology: current methods and new opportunities, *in* Busby, C., and Azor, A.A., eds., Tectonics of Sedimentary Basins, Recent Advances, p. 47-62.

Gehrels, G.E., 2014, Detrital zircon U-Pb geochronology applied to tectonics: Annual Review of Earth and Planetary Sciences. v. 42, p. 127–149.

Gehrels, G.E., and Pecha, M., 2014, Detrital zircon U-Pb geochronology and Hf isotope geochemistry of Paleozoic and Triassic passive margin strata of western North America: Geosphere, v. 10, no. 1, p. 49-65.

Gehrels, G.E., Blakey, R., Karlstrom, K.E., Timmons, J.M., Dickenson, W.R., and Pecha, M., 2011, Detrital zircon U-Pb geochronology of Paleozoic strata in the Grand Canyon, Arizona: Lithosphere, v. 3, p. 183–200.

Gehrels, G.E., Dickinson, W.R., Riley, B.C.D., Finney, S.C., and Smith, M.T., 2000, Detrital zircon geochronology of the Roberts Mountains allochthon, Nevada, *in* Gehrels, G.E., and Soreghan, M.J., eds., Paleozoic and Triassic Paleogeography and Tectonics of Western Nevada and Northern California, Geological Society of America, Special Paper 347, p. 19–42, doi:10.1130/0-8137-2347-7.19.

Gehrels, G.E., Valencia, V., and Pullen, A., 2006, Detrital zircon geochronology by Laser-Ablation Multicollector ICPMS at the Arizona LaserChron Center, *in* Loszewski, T., and Huff, W., eds., Geochronology: Emerging Opportunities, Paleontology Society Short Course, Paleontology Society Papers, v. 11, 10 p.

Gehrels, G.E., Valencia, V., and Ruiz, J., 2008, Enhanced precision, accuracy, efficiency, and spatial resolution of U-Pb ages by laser ablation–multicollector–inductively coupled plasma–mass spectrometry: Geochemistry, Geophysics, Geosystems. v. 9, Q03017, doi:10.1029/2007GC001805.

Gill, J.R., and Hail Jr., W.J., 1975, Stratigraphic sections across Upper Cretaceous Mancos Shale – Mesaverde Group boundary, eastern Utah and western Colorado: U.S. Geological Survey, Oil and Gas Investigation Chart OC-68.

Gray, M., and Zeitler, P., 1997, Comparison of clastic wedge provenance in the Appalachian foreland using U-Pb ages of detrital zircons: Tectonics, v. 16, p. 151–160.

Hajek, E.A., and Heller, P.L., 2012, Flow-depth scaling in alluvial architecture and nonmarine sequence stratigraphy: Example from the Castlegate Sandstone, central Utah, U.S.A.: Journal of Sedimentary Research, v. 82, p. 121-130.

Hallman, J.A., 2016, Spatial and temporal patterns of Ogallala Formation deposition revealed by U-Pb zircon geochronology: M.S. Thesis, University of Kansas.

Hampson, G.J., 2010, Sediment dispersal and quantitative stratigraphic architecture across an ancient shelf: Sedimentology, v. 57, p. 96-141.

Hampson, G.J., 2016, Towards a sequence stratigraphic solution set for autogenic processes and allogenic controls: Upper Cretaceous strata, Book Cliffs, Utah, USA: Journal of the Geological Society, v. 173, p. 817-836.

Hampson, G.J., and Howell, J.A., 2005, Sedimentologic and geomorphic characterization of ancient wave-dominated deltaic shorelines: upper Cretaceous Blackhawk Formation, Book Cliffs, Utah, USA, *in* Bhattacharya, J.P., and Giosan, L., eds., River Deltas – Concepts, Models, and Examples, SEPM, Special Publication No. 83, p. 133-154.

Hampson, G.J., Duller, G.J., Petter, A.L., Robinson, R.A.J., and Allen, P.A., 2014, Mass-balance constraints on stratigraphic interpretation of linked alluvial coastal-shelfal deposits form source to sink: Example from Cretaceous Western Interior Basin, Utah and Colorado, USA: Journal of Sedimentary Research, v. 84, p. 934-960.

Hampson, G.J., Gani, M.R., Sahoo, H., Rittersbacher, A., Irfan, N., Ranson, A., Jewell, T.O., Gani, N.D.S., Howell, J.A., Buckley, S.J., and Bracken, B., 2012, Controls on large-scale patterns of fluvial sandbody distribution in alluvial to coastal plain strata: Upper Cretaceous Blackhawk Formation, Wasatch Plateau, Central Utah, USA: Sedimentology, v. 9, p. 2226-2258.

Hayes, P.T., 1970, Cretaceous paleogeography of south-eastern Arizona and adjacent areas. U.S. Geological Survey, Professional Paper 658-B, 42 p.

Heumann, M.J., Bickford, M.E., Hill, B.M., McLelland, J.M., Selleck, B.W., and Jercinovic,

M.J., 2006, Timing of anatexis in metapelites from the Adirondack lowlands and southern highlands: a manifestation of the Shawinigan orogeny and subsequent anorthosite-mangerite-charnockite-granite magmatism: Geological Society of America, Bulletin, v. 118, p. 1283–1298.

Holbrook, J.M., and Bhattacharya, J., 2012, What happened to my marine reservoir? Implication of falling stage and lowstand fluvial sediment storage during "sequence boundary" scour for sand starvation of coastal marine reservoirs (abstract): American Association of Petroleum Geologists, Annual Meeting.

Horton, B.K., Constenius, K.N., and DeCelles, P.G., 2004, Tectonic control on coarse-grained foreland-basin sequences: an example from the Cordilleran foreland basin, Utah: Geology, v. 32, p. 637-640.

Houston, W.S., Huntoon, J.E., and Kamola, D.L., 2000, Modeling of Cretaceous foreland-basin parasequences, Utah, with implications for timing of Sevier thrusting: Geology, v. 28, p. 267-270.

Hovius, N., 1996, Regular spacing of drainage outlets from linear mountain belts: Basin Research, v. 8, p. 29-44.

Howell, J.A., and Flint, S.S., 2003, Siliciclastic case study: The Book Cliffs, *in* Coe, A.E., ed., The Sedimentary Record of Sea Level Change, Cambridge, UK, Cambridge University Press, p. 135–208.

Jerolmack, D.J., and Swenson, J.B., 2007, Scaling relationships and evolution of distributary networks on wave-influenced deltas: Geophysical Research Letters, v. 34, L23402.

Jones, J.V., III, Connelly, J.N., Karlstrom, K.E., Williams, M.L., and Doe, M.F., 2009, Age, provenance, and tectonic setting of Paleoproterozoic quartzite successions in the southwestern United States: Geological Society of America, Bulletin, v. 121, p. 247-264, doi:10.1130/B26351.1.

Jordan, T.E., 1981, Thrust loads and foreland basin evolution, Cretaceous, western United States: American Association of Petroleum Geologists, Bulletin, v. 65, p. 2506–2520.

Kamola, D.L., and Van Wagoner, J.C., 1995, Stratigraphy and facies architecture of parasequences with examples from the Spring Canyon member, Blackhawk Formation, Utah, *in* Van Wagoner, J.C., and Bertman, G.T., eds., Sequence Stratigraphy of Foreland Basin Deposits–Outcrop and Subsurface Examples from the Cretaceous of North America, American Association of Petroleum Geologists, Memoir, v. 64, p. 27-54.

Kauffmann, E.G., 1977, Evolutionary rates and biostratigraphy, *in* Kauffman, E.G., and Hazel, J. E., eds., Concepts and Methods of Biostratigraphy, Dowden, Hutchinson and Ross Inc., Stroudsburg, PA, p. 109–142.

Kauffman, E.G., and Caldwell, W.G.E., 1993, The Western Interior Basin in space and time, *in* Caldwell, W.G.E., and Kauffman, E.G., eds., Evolution of the Western Interior Basin, Geological Association Canada, Special Paper 39, p. 1-30.

Kirschbaum, M.A., and Hettinger, R.D., 2004, Facies analysis and sequence stratigraphic framework of Upper Campanian strata (Neslen and Mount Garfield Formations, Bluecastle Tongue of the Castlegate Sandstone, and Mancos Shale), eastern Book cliffs, Colorado and Utah: U.S. Geological Survey, Digital Data Series DDS-69-G.

Krystinik, L.F., and DeJarnett, B.B., 1995, Lateral variability of sequence stratigraphic framework in the Campanian and Lower Maastrichtian of the Western Interior Seaway, *in*, Van Wagoner, J.C., and Bertram, G.T., eds., Sequence Stratigraphy of Foreland Basin Deposits: Outcrop and Subsurface Examples from the Cretaceous of North America, American Association of Petroleum Geologists, Memoir 64, p. 11-26.

Laskowski, A.K., DeCelles, P.G., and Gehrels, G.E., 2013, Detrital zircon geochronology of Cordilleran retroarc foreland basin strata, western North America: Tectonics, v. 32, p. 1-22.

Lawrence, R.L., Cox, R., Mapes, R.W., and Coleman, D.S., 2011, Hydrodynamic fractionation of zircon age populations: Geological Society of America, Bulletin, v. 123, no. 1-2, p. 295-305.

Lawton, T.F., and Bradford, B.A., 2011, Correlation and provenance of Upper Cretaceous (Campanian) fluvial strata, Utah, USA, from zircon U-Pb geochronology and petrography: Journal of Sedimentary Research, v. 81, p. 495–512, doi:10.2110/jsr.2011.45.

Lawton, T.F., Buller, C.D., and Parr, T.R., 2015, Provenance of a Permian erg on the western margin of Pangea: Depositional system of the Kungurian (late Leonardian) Castle Valley and White Rim sandstones and subadjacent Cutler Group, Paradox Basin, Utah, USA: Geosphere, v. 11, no. 5, p. 1475-1506.

Lawton, T.F., Eaton, J.G., Godfrey, K.N., and Schellenbach, W.L., 2014, Compositional, paleontological, and detrital-zircon data from Cretaceous strata of the Henry Mountains Basin and implications for connections with dispersal systems of Wahweap and Kaiparowits Formations in southern Utah, U.S.A., *in* Maclean, J.S., Biek, R.F., and Huntoon, J.E., eds., Geology of Southern Utah, Utah Geological Association, Publication 43, p. 373-395.

Lawton, T.F., Hunt, G.J., and Gehrels, G.E., 2010, Detrital zircon record of thrust belt unroofing in Lower Cretaceous synorogenic conglomerates, central Utah: Geology, v. 38, p. 463-466.

Licht, A., Reisberg, L., France-Lanord, C., Soe, A.N., and Jaeger, J.J., 2015, Cenozoic evolution of the central Myanmar drainage system: insights from sediment provenance in the

Minbu sub-basin: Basin Research, p. 1-15.

Link, P.K., Christie-Blick, N., Devlin, W.J., Elston, D.P., Horodyski, R.J., Levy, M., Miller, J.M.G., Pearson, R.C., Prave, A., Stewart, J.H., Winston, D., Wright, L.A., and Wrucke, C.T., 1993, Middle and late Proterozoic stratified rocks of the western US Cordillera, Colorado Plateau, and Basin and Range Province, *in* Reed, J.C., et al., eds., Precambrian; Conterminous U.S., Boulder, Colorado, Geological Society of America, The Geology of North America, v. C-2, p. 463-595.

Lippert, P.G., 2014, Detrital U-Pb geochronology provenance analyses: case studies in the Greater Green River Basin, Wyoming, and the Book Cliffs, Utah: M.S. Thesis, University of Kansas.

Liu, S.F., and Nummedal, D., 2004, Late Cretaceous subsidence in Wyoming: Quantifying the dynamic component: Geology, v. 32, p. 397–400.

Liu, S.F., Nummedal, D., and Gurnis, M., 2014, Dynamic versus flexural controls of Late Cretaceous Western Interior Basin, USA: Earth and Planetary Science Letters, v. 389, p. 221-229.

Liu, S.F., Nummedal, D., and Liu, L., 2011, Migration of dynamic subsidence across the Late Cretaceous United States Western Interior Basin in response to Farallon plate subduction: Geology, v. 39, p. 555-558.

Malusa, M.G., Resentini, A., and Garzanti, E., 2015, Hydraulic sorting and mineral fertility bias in detrital geochronology: Gondwana Research, v. 31, p. 1-19.

May, S.R., Gray, G.G., Summa, L.L., Stewart, N.R., Gehrels, G.E., and Pecha, M.E., 2013, Detrital zircon geochronology from the Bighorn Basin, Wyoming, USA: Implications for tectonostratigraphic evolution and paleogeography: Geological Society of America, Bulletin, v. 123, p. 1403-1422.

McLaurin, B.T., and Steel, R.J., 2000, Fourth-order nonmarine to marine sequences, middle Castlegate Formation, Book Cliffs, Utah: Geology, v. 28, no. 4, p. 359-362.

McLaurin, B.T., and Steel, R.J., 2007, Architecture and origin of an amalgamated fluvial sheet sand, lower Castlegate Formation, Book Cliffs, Utah: Sedimentary Geology, v. 197, p. 291-311.

Miall, A., 2014, The emptiness of the stratigraphic record: a preliminary evaluation of missing time in the Mesaverde Group, Book Cliffs, Utah, USA: Journal of Sedimentary Research, v. 84, p. 457-469.

Miall, A., and Arush, M., 2001, The Castlegate Sandstone of the Book Cliffs, Utah: sequence stratigraphy, paleogeography, and tectonic controls: Journal of Sedimentary Research, v. 71, p. 537–548.

Mitra, G., 1997, Evolution of salient in a fold-and-thrust belt: The effects of sedimentary basin geometry, strain distribution and critical taper, *in* Sengupta, S., ed., Evolution of Geological Structures in Micro- to Macro-scales, London, Chapman and Hall, p. 59-90.

Moecher, D.P., and Samson, S.D., 2006, Differential zircon fertility of source terranes and natural bias in the detrital zircon record: implications for sedimentary provenance analysis: Earth and Planetary Science Letters, v. 257, i. 3-4, p. 252-266.

Mohrig, D., Heller P.L., Paola C., and Lyons, W.J., 2000, Interpreting avulsion process from ancient alluvial sequences: Guadalope-Matarranya system (Northern Spain) and Wasatch Formation (Western Colorado): Geological Society of America, Bulletin, v. 112, p. 1787–1803.

Molenaar, C.M., and Rice, D.D., 1988, Cretaceous rocks of the Western Interior Basin, *in* Sloss, L.L., eds., Sedimentary Cover – North American Craton, US, Geological Society of America, The Geology of North America, v. D-2, p. 77-82.

Morehouse, E.R., 2015, A chemostratigraphic and detrital zircon geochronologic analysis of upper Cretaceous strata: applications for dating and correlating strata: M.S. Thesis, University of Kansas.

Mosher, S., 1998, Tectonic evolution of the southern Laurentian Grenville orogenic belt: Geological Society of America, Bulletin, v. 110, p. 1357–1375.

Obradovich, J.D., 1994, A Cretaceous time scale, *in* Caldwell, W.G.E., and Kauffman, E.G., eds., Evolution of the Western Interior Basin, Geological Association of Canada, Special Paper 39, p. 379-396.

Olsen, T., Steel, R.J., Hogseth, K., Skar, T., and Roe, S.L., 1995, Sequential architecture in a fluvial succession: sequence stratigraphy in the Upper Cretaceous Mesaverde Group, Price Canyon, Utah: Journal of Sedimentary Research, v. B65, p. 265-280.

Painter, C.S., and Carrapa, B., 2013, Flexural versus dynamic processes of subsidence in the North American Cordillera foreland basin: Geophysical Research Letters, v. 40, p. 4249-4253.

Peterson, F., and Kirk, A.R., 1977, Correlation of the Cretaceous rocks in the San Juan, Black Mesa, Kaiparowits, and Henry Basins, southern Colorado Plateau: New Mexico Geological Society, Field Guide 28, p. 167–178.

Pfaff, B.J., 1985, Facies sequences and the evolution of fluvial sedimentation in the Castlegate Sandstone, Price Canyon, Utah, *in* Midyear Meeting Field Guide, Rocky Mountain Section SEPM, p. 10-32.

Pullen, A., Ibanez-Mejia, M., Gehrels, G.E., Ibanez-Mejia, J.C., and Pecha, M., 2014, What

happens when n=1000? Creating large-n geochronological datasets with LA-ICP-MS for geologic investigations: Journal of Analytical Atomic Spectrometry, v. 29, p. 971-980.

Rainbird, R.H., Hamilton, M.A., and Young, G.M., 2001, Detrital zircon geochronology and provenance of the Torridonian, NW Scotland: Journal of the Geological Society, London, v. 158, p. 15-27.

Reese, J.F., Mosher, S., Connelly, J., and Roback, R., 2000, Mesoproterozoic chronostratigraphy of the southeastern Llano uplift, central Texas: Geological Society of America, Bulletin, v. 112, p. 278–291.

Riggs, N. R., Lehman, T.M., Gehrels, G.E., and Dickinson, W.R., 1996, DZ link between headwaters and terminus of the Upper Triassic Chinle-Dockum Paleoriver system: Science, v. 273, p 97-100.

Rittersbacher, A., Howell, J.A., and Buckley, S.J., 2014, Analysis of fluvial architecture in the Blackhawk Formation, Wasatch Plateau, Utah, USA, using large 3D photorealistic models: Journal of Sedimentary Research, v. 84, p. 72-87.

Rivers, T., 1997, Lithotectonic elements of the Grenville province: Precambrian Research, v. 86, p. 117–154.

Sambrook-Smith, G.H., Best, J.L., Ashworth, P.J., Fielding, C.R., Goodbred, S.L., and Prokocki, E.W., 2010, Fluvial form in modern continental sedimentary basins: Distributive fluvial systems: COMMENT: GSA Geology Forum.

Saylor, J.E., and Sundell, K.E., 2016, Quantifying comparison of large detrital geochronology data sets: Geosphere, v. 12, 1, p. 1-18.

Seymour, D.L., and Fielding, C.R., 2013, High resolution correlation of the Upper Cretaceous stratigraphy between the Book Cliffs and the Western Henry Mountains Syncline, Utah, USA: Journal of Sedimentary Research, v. 83, p. 475-494.

Silver, L.T., and Deutsch, S., 1963, Uranium-lead isotopic variations in zircon: a case study: Journal of Geology, v. 71, p. 721-758.

Sitek, B.C., 2017, Analyzing the Cenozoic depositional history of western Kansas: A new approach using paleosol zircon geochronology: M.S. Thesis, University of Kansas.

Slingerland, R., and Keen, T.R., 1999, Sediment transport in the Western interior Seaway of North America: predictions from a climate–ocean–sediment model, *in* Bergman, K.M., and Snedden, J.W., eds., Isolated Shallow Marine Sand Bodies: Sequence Stratigraphic Analysis and Sedimentologic Interpretation, SEPM, Special Publication 64, p. 179–190.

Slingerland, R., and Smith, N.D., 1998, Necessary conditions for a meandering-river avulsion: Geology, v. 26, no. 5, p. 435-438.

Slingerland, R., and Smith, N.D., 2004, River avulsions and their deposits: Annual Review of Earth Planetary Sciences, v. 32, p. 257-285.

Snell, K.E., Koch, L., Druschke, P., Foreman, B.Z., and Eiler, J.M., 2014, High elevation of the 'Nevadaplano' during the Late Cretaceous: Earth and Planetary Science Letters, v. 386, p. 52-63.

Spencer, J.E., and Pecha, M., 2012, U-Pb zircon geochronologic investigation of granitoids and sandstones in the Jerome Canyon and Chino Valley North 7 1⁄2′ Quadrangles, Prescott Area, Central Arizona: Arizona Geological Survey, Open-File Report 12-02, 8 p.

Spieker, E.M., 1946, Late Mesozoic and early Cenozoic history of central Utah: U.S. Geological Survey, Professional Paper 205-D, p. 117-161.

Stacey, J.S., and Kramers, J.D., 1975, Approximation of terrestrial lead isotope evolution by a two-stage model: Earth and Planetary Science Letters, v. 26, p. 207-221.

Swanson-Hysell, N.L., Burgess, S.D., Maloof, A.C., and Bowring, S.A., 2014, Magmatic activity and plate motion during the latent stage of Midcontinent Rift development: Geology, v. 42, i. 6, p. 475-478.

Szwarc, T.S., Johnson, C.L., Stright, L.E., and McFarlane, C.M., 2014, Interactions between axial and transverse drainage systems in the Late Cretaceous Cordilleran foreland basin: Evidence from detrital zircons in the Straight Cliffs Formation, southern Utah, USA: Geological Society of America, Bulletin, v. 127, no. 3/4, p. 372-392.

Thomas, J.J., Shuster, R.D., and Bickford, M.E., 1984, A terrane of 1350- to 1400-my old silicic volcanic and plutonic rocks in the buried Proterozoic of the mid-continent and in the Wet Mountains, Colorado: Geological Society of America, Bulletin, v. 85, i. 10, p. 1150-1157.

Turner, E., 2017, High plains geochronology: U-Pb zircon ages for the ashfall fossil beds and grove lake ash in northeastern Nebraska: Senior Honors Thesis, University of Kansas.

Van Wagoner, J.C., 1995, Sequence stratigraphy and marine to nonmarine facies architecture of foreland basin strata, Book Cliffs, Utah, USA, *in* Van Wagoner, J.C., and Bertram, G.T., eds., Sequence Stratigraphy of Foreland Basin Deposits; Outcrop and Subsurface Examples from the Cretaceous of North America, American Association of Petroleum Geologists, Memoir 64, p. 137-223.

Van Wagoner, J.C., Mitchum, R.M., Campion, K.M., and Rahmanian, V.D., 1990, Siliciclastic sequence stratigraphy in well logs, cores, and outcrops: concepts for high-resolution correlation of time and facies: American Association of Petroleum Geologists, Methods in Exploration Series 7, 55 p.

Vermeesch, P., 2004, How many grains are needed for a provenance study?: Earth and Planetary Science Letters, v. 224, p. 441-451.

Vermeesch, P., 2013, Multi-sample comparison of detrital age distributions: Chemical Geology, v. 341, p. 140-146.

Vermeesch, P., Resentini, A., and Garzanti, E., 2016, An R package for statistical provenance analysis: Sedimentary Geology, v. 336, p. 14-25.

Wasserburg, G.J., and Lanphere, M.A., 1965, Age determinations in the Precambrian of Arizona and Nevada: Geological Society of America, Bulletin, v. 76, p. 735–758.

Weissmann, G.S., Hartley, A.J., Nichols, G.J., Scuderi, L.A., Olson, M., Buehler, H., and Ranteah, R., 2010, Fluvial form in modern continental sedimentary basins: Distributive fluvial systems: Geology, v. 38, no. 1, p. 39-42.

White, T., Furlong, K., and Arthur, M., 2002, Forebulge migration in the Cretaceous Western Interior basin of the central United States: Basin Research, v. 14, p. 43-54.

Whitmeyer, S.J., and Karlstrom, K.E., 2007, Tectonic model for the Proterozoic growth of North America: Geosphere, v. 3, no. 4, p. 220-259.

Willis, A.J., 1997, Non-marine sequence stratigraphy of the Sego Sandstone and Upper Castlegate Sandstone (upper Cretaceous), Book Cliffs, Utah, USA: Ph.D. Dissertation, University of Toronto.

Yoshida, S., 2000, Sequence and facies architecture of the upper Blackhawk Fm. and the Lower Castlegate Sandstone (Upper Cret.), Book Cliffs, Utah, USA: Sedimentary Geology, v. 136, p. 239-276.

Yoshida, S., Miall, A.D., and Willis, A., 1998, Sequence stratigraphic and marine to nonmarine facies architecture of foreland basin strata, Book Cliffs, Utah, USA: Discussion: American Association of Petroleum Geologists, Bulletin, v. 82, no. 8, p. 1596-1606.

Yoshida, S., Willis, A., and Miall, A.D., 1996, Tectonic control of nested sequence architecture in the Castlegate Sandstone (upper Cretaceous), Book Cliffs, Utah: Journal of Sedimentary Research, v. 66, no. 4, p. 737-748

Young, R.G., 1955, Sedimentary facies and intertonguing in the Upper Cretaceous of the Book Cliffs, Utah-Colorado: Geological Society of America, Bulletin, v. 66, p. 177-201.

8 Figures

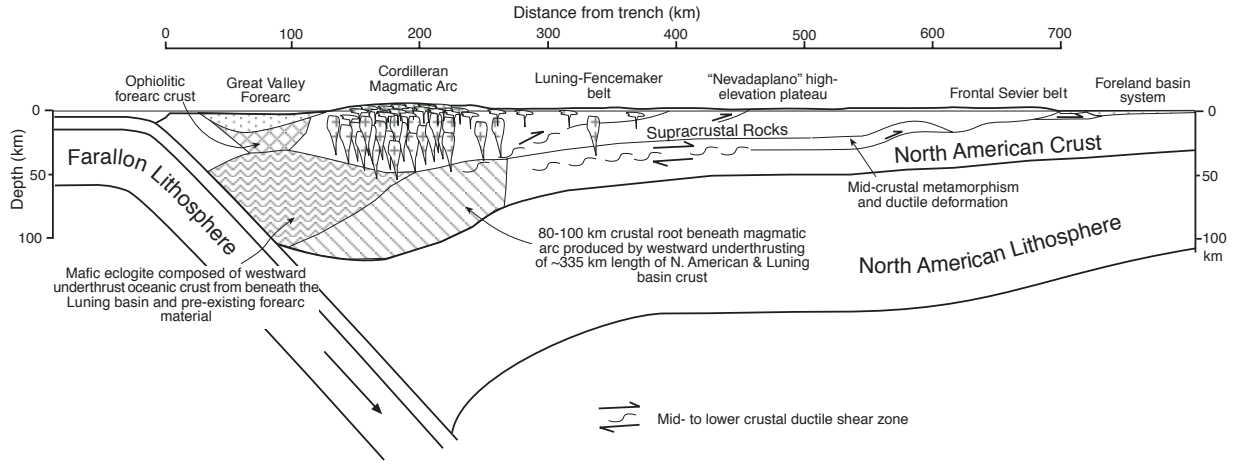

Figure 1: Cross section of the Cordilleran Orogenic Belt through central Utah during the Cretaceous. From DeCelles and Coogan (2006).

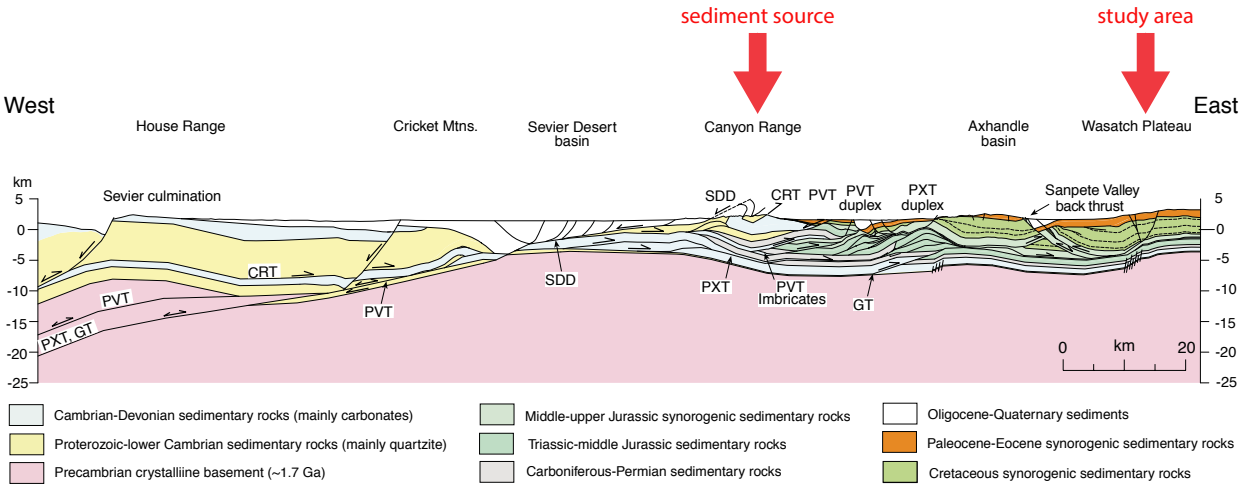

Figure 2: Cross-section of the Sevier fold-and-thrust belt through central Utah. The Canyon Range Culmination, the main sediment source for the Mesaverde Group, is approximately 70 km west of the study area. CRT – Canyon Range Thrust; PVT – Pavant thrust; PXT – Paxton thrust; GT – Gunnison thrust; SDD – Sevier Desert Detachment. Modified from DeCelles and Coogan (2006).

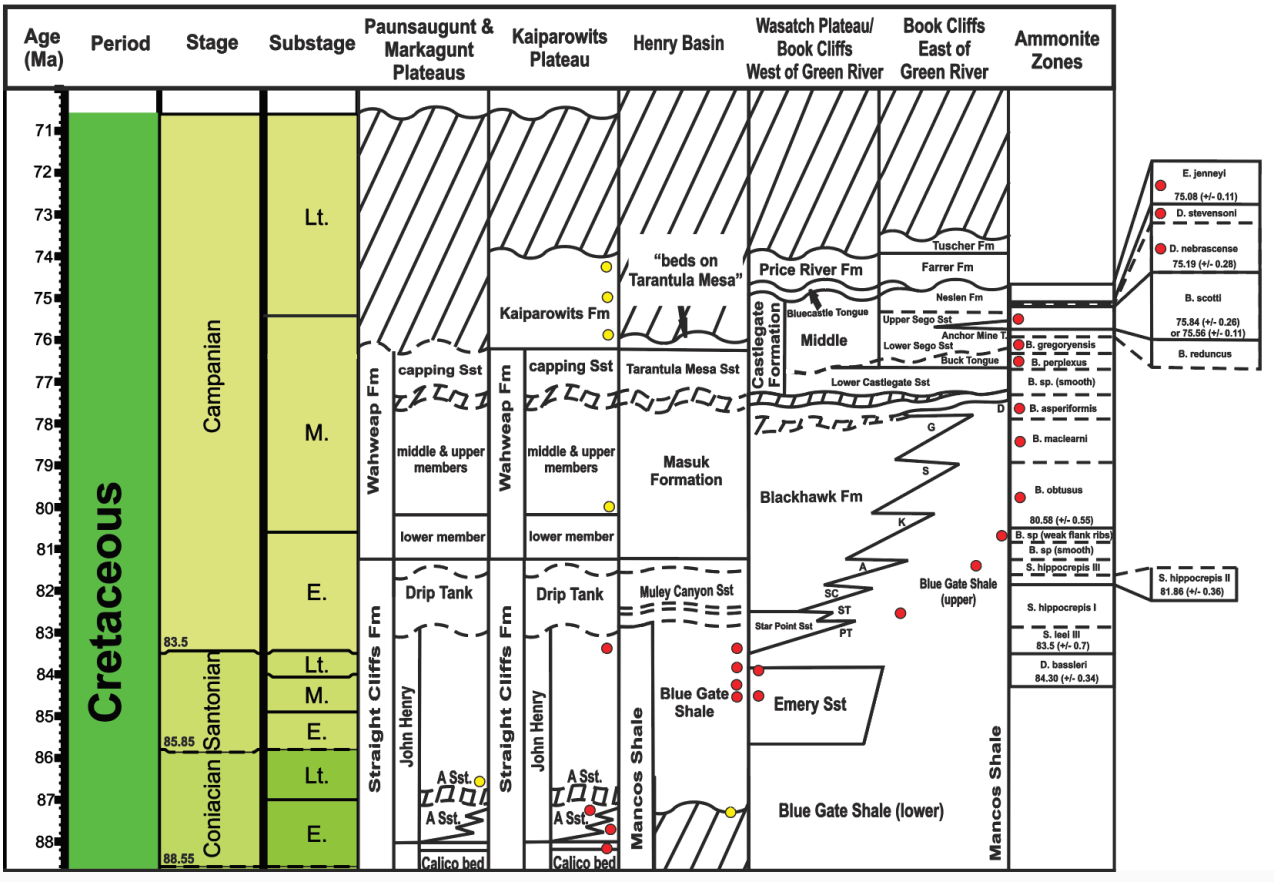

Figure 3: Time-space correlation of upper Cretaceous strata through Utah. Red dots reflect biostratigraphic ammonite and inoceramid positions, and yellow dots represent bentonite locations. Modified from Seymour and Fielding (2013).

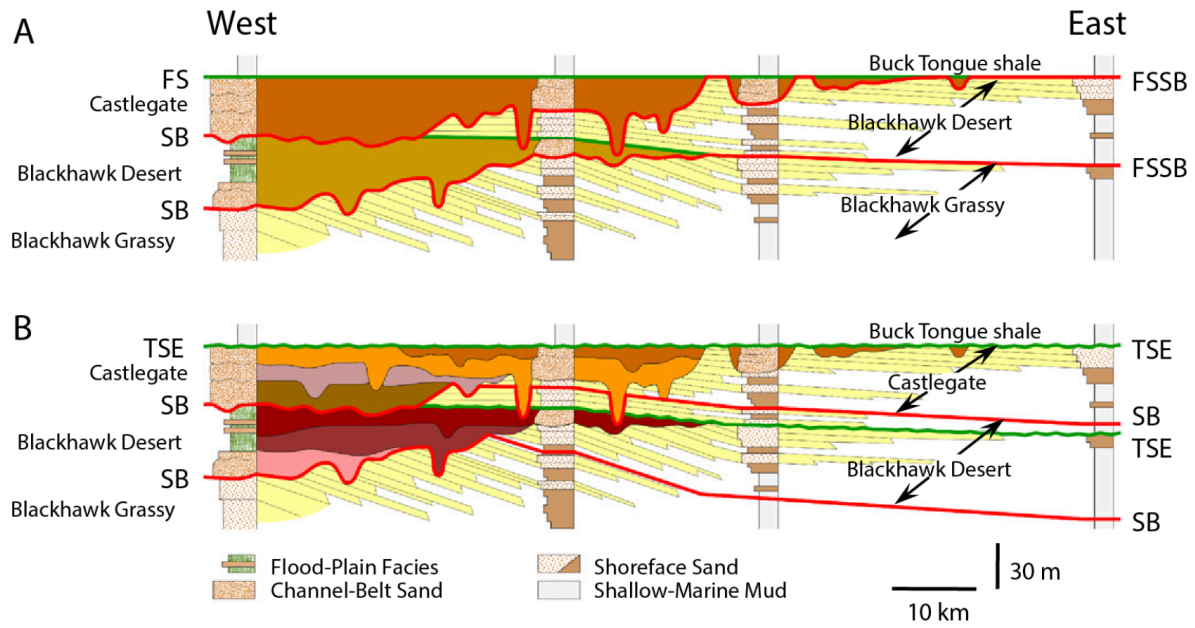

Figure 4: Alternative sequence stratigraphic models for the same deposits, in which A) the sequence boundary is below fluvial packages, separating older and younger strata; and B) the sequence boundary is below fluvial deposits and genetically-related shorezone clinothems. From Blum et al. (2013), originally from Van Wagoner (1995).

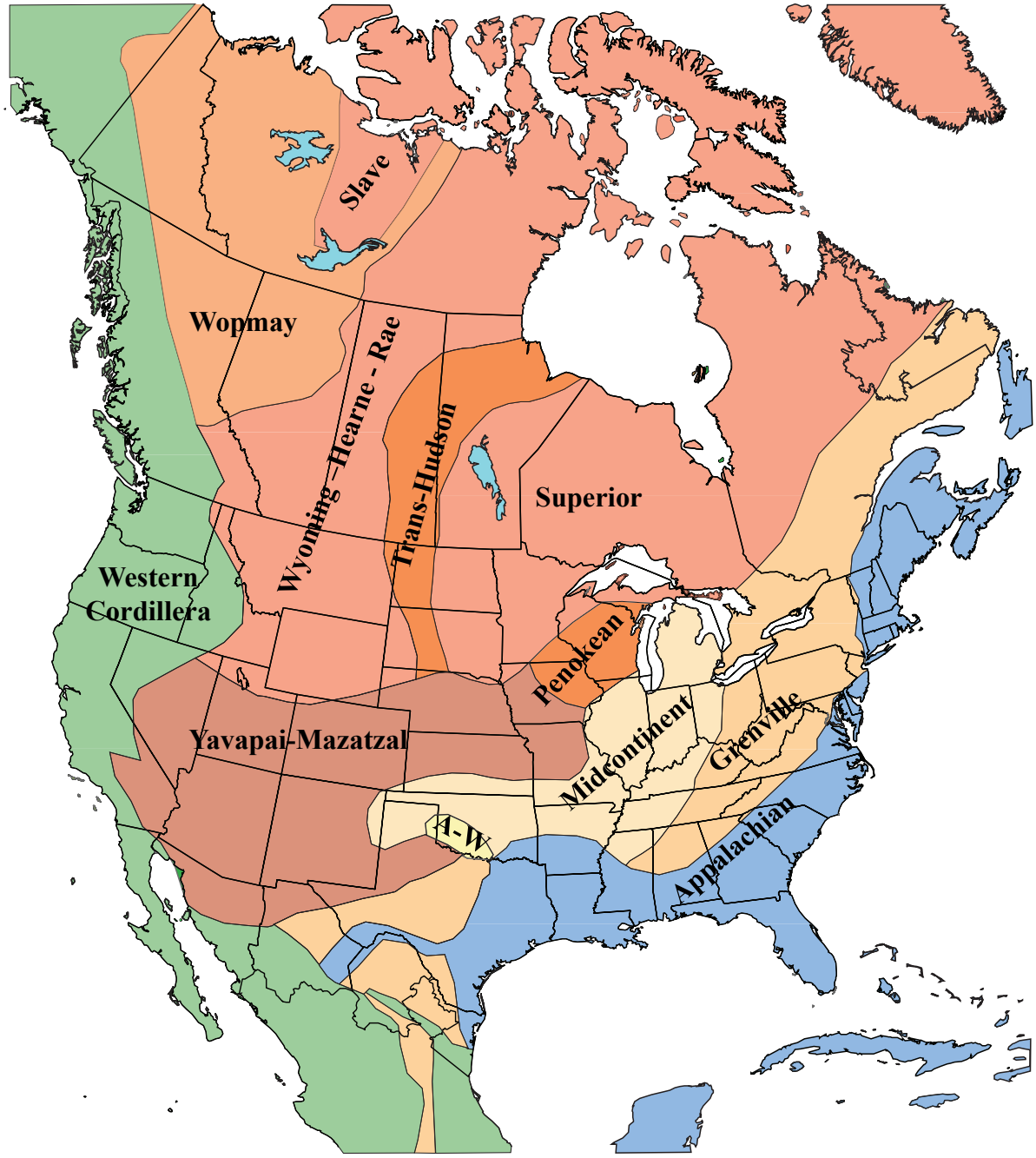

Figure 5: Primary detrital zircon source terranes in North America. For a more thorough explanation, see Table 1. From Blum and Pecha (2014), originally from Dickinson and Gehrels (2009).

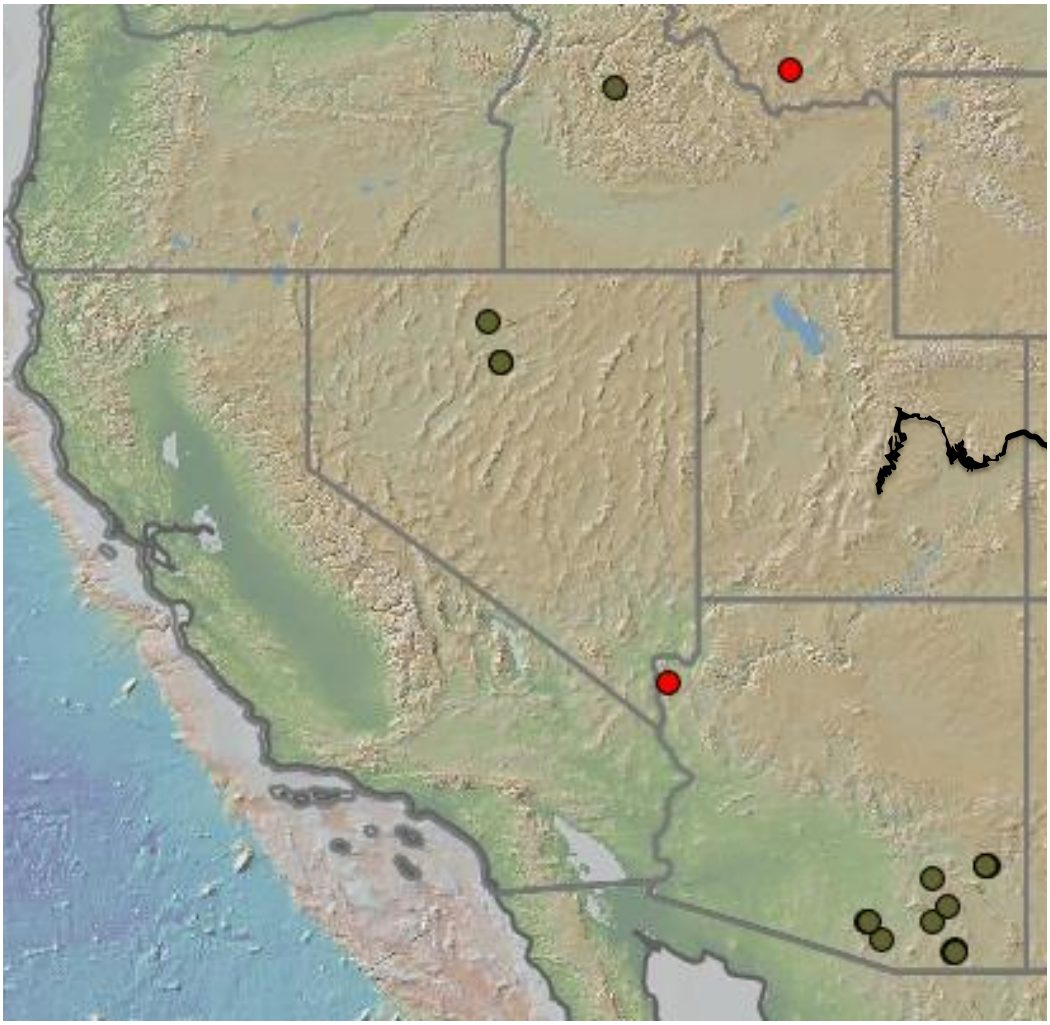

Figure 6: Locations of radiometrically-dated volcanic rocks for ca. 80-72 Ma, showing the potential source locations within the U.S. Western Interior for syndepositional volcanic rocks of intermediate to felsic composition for the young zircon grain populations relative to the Wasatch Plateau and Book Cliffs (black outline). Red dots are from the USGS database, and green dots are from the NAVDAT database. Map generated using the community database <earthchem.org>.

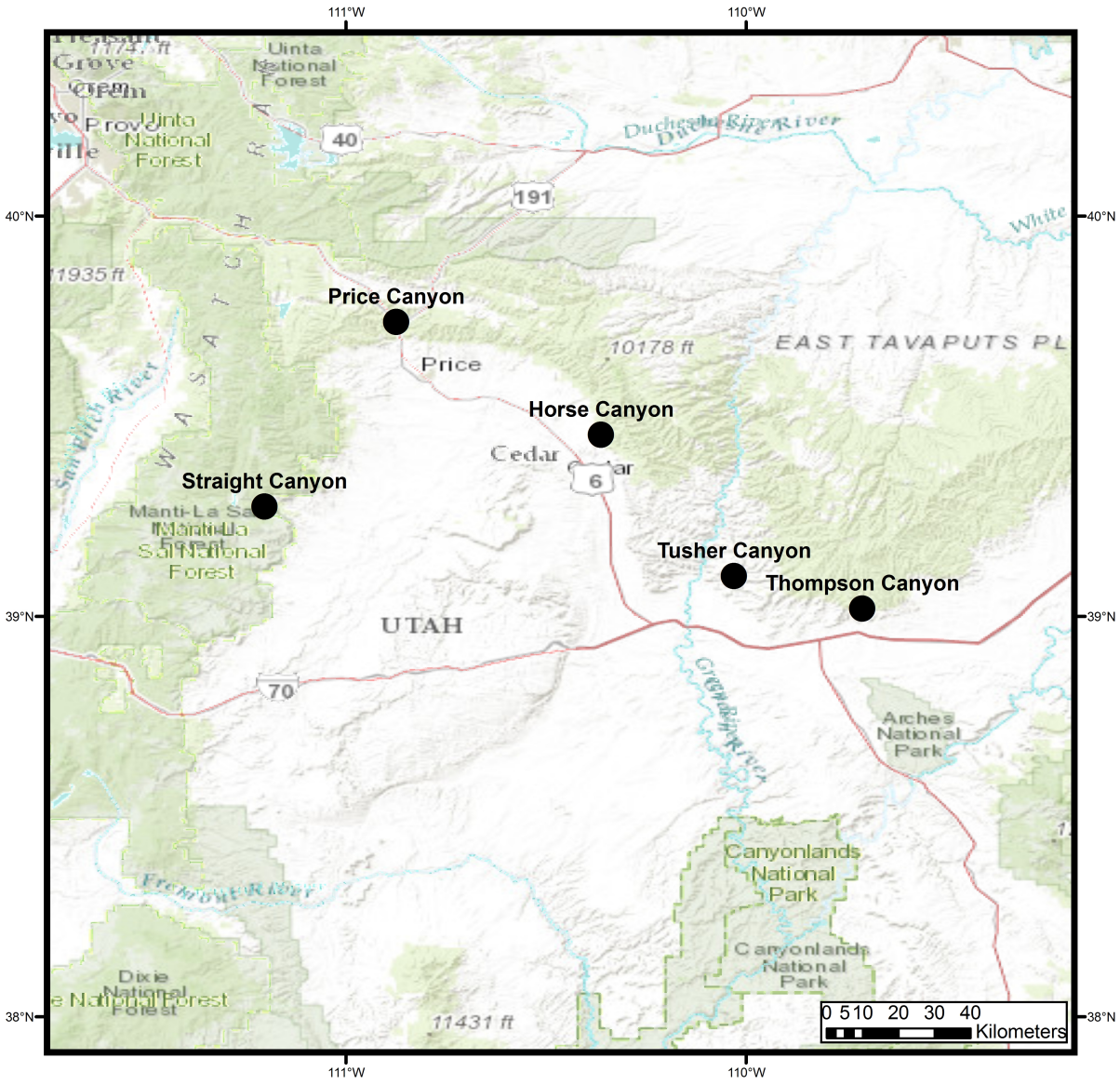

Figure 7: Canyon locations on a topographic map. Coordinates of individual sample locations are included in Table 2.

Figure 8: Stratigraphic correlation showing sample locations through study area. The Straight Canyon section was measured as part of this thesis; Price Canyon section is the "Gentile Wash" section in Gani et al. (2015) up to the base of the Lower Castlegate, then from "The Castlegate" section from Willis (1997); Horse Canyon is from this thesis to the base of the Lower Castlegate, then from the Willis (1997) through the Bluecastle Tongue; Tusher Canyon is from the Van Wagoner (1995) "Tuscher Canyon SWNE Sec. 8" to the top of the Lower Castlegate, then Willis (1997) through the Sego; Thompson Canyon is from the "Sego #2 Well" in Morehouse (2015).

Wasatch Plateau
Book Cliffs
SSW
NNE
60 km
approximate depositional strike
WNW
ESE
80 km
approximate depositional dip
Castlegate Sandstone
Bluecastle Tongue
Upper Castlegate
Lower Castlegate
Blackhawk Formation
Star Point Fm
Castlegate Sandstone
Blue-castle Tongue
Neslen Formation
Sego Sandstone
Buck Tongue
Lower Castle-gate
Blackhawk Formation
Price Canyon
Straight Canyon (aka Joe's Valley)
Horse Canyon
Tusher Canyon
Thompson Canyon
BC-17
BC-16
BC-15
BC-13
BC-14
KBH-19
KBH-01
KBH-12
KBH-15
KBH-02
BC-07
BC-08
BC-09
BC-10
BC-11
KBH-16
KBH-17
KBH-18
KBH-10
KBH-11
MD-03
MD-04
MD-05
MD-06
MD-02
MD-07
MD-01
BC-06
BC-05
KBH-08
BC-03
BC-01
KBH-09
KBH-07
KBH-06
KBH-04
KBH-05
KBH-03
LEGEND
coal
siltstone
mudstone
sandstone
sample for U-Pb analysis
sample for grain size analysis
STUDY AREA
cross section
Utah
study area
Price Canyon
Horse Canyon
Straight Canyon
Tusher Canyon
Thompson Canyon

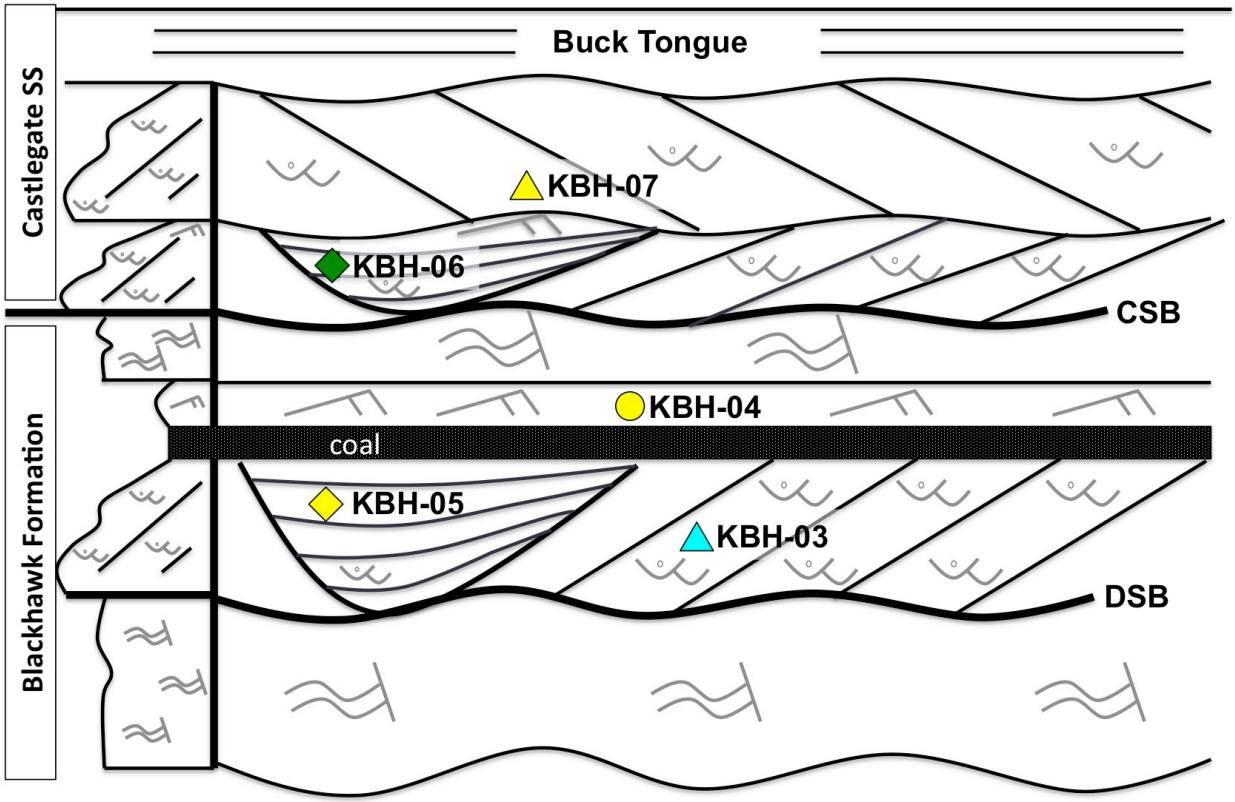

Figure 9: Schematic diagram of sampling strategy in Thompson Canyon. Triangles represent channel-belt facies, diamonds represent abandoned channel-fill facies, and the circle represents crevasse splay facies. The color of each refers to the cluster in which each sample plots.

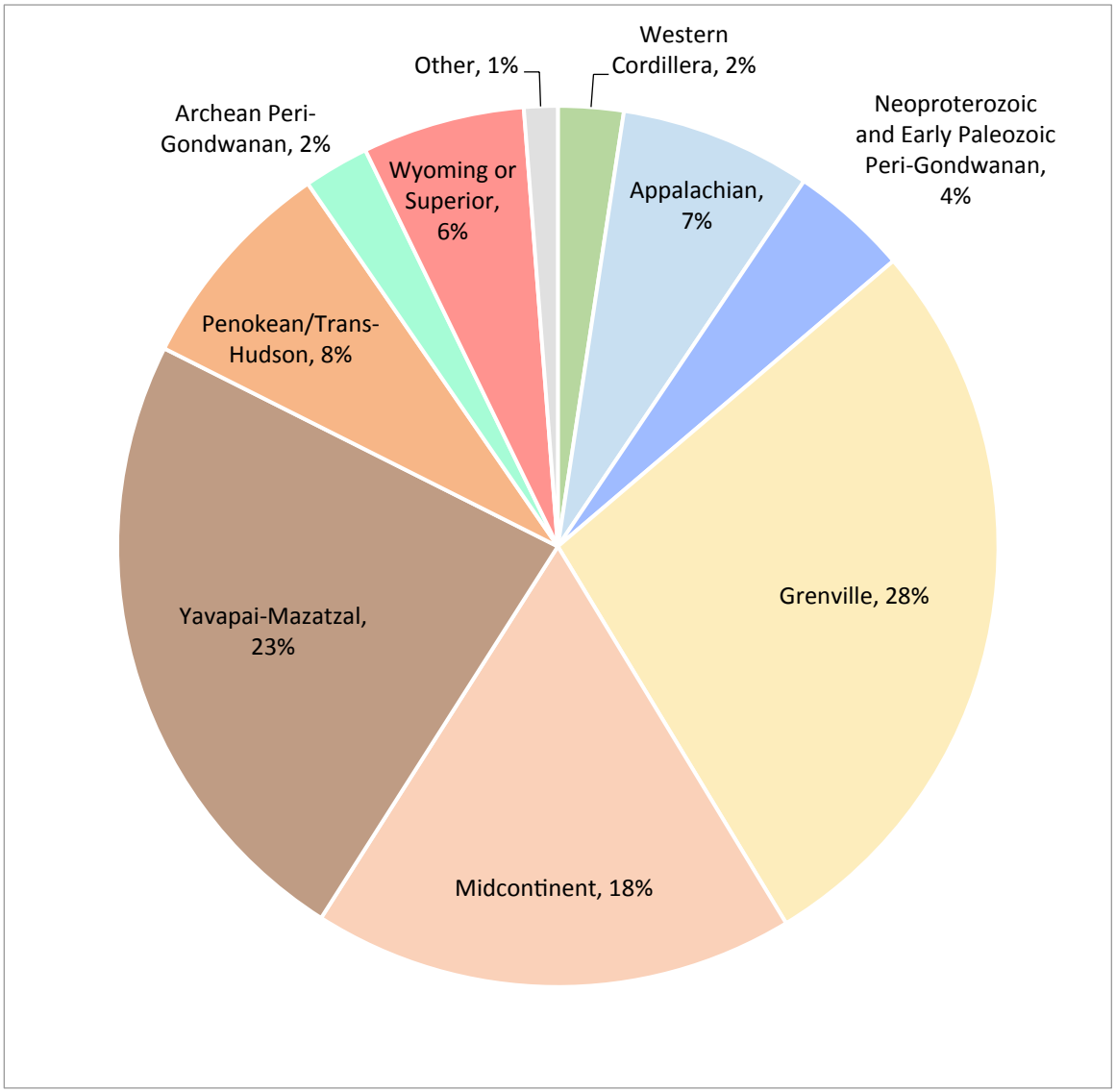

Figure 10: Average percentage of age populations present within each sample.

Figure 11: Normalized KDEs (Bandwidth = 10) in stratigraphic order for samples in A) Straight Canyon, B) Price Canyon, C) Horse Canyon, D) Tusher Canyon, and E) Thompson Canyon.

11A) Straight Canyon

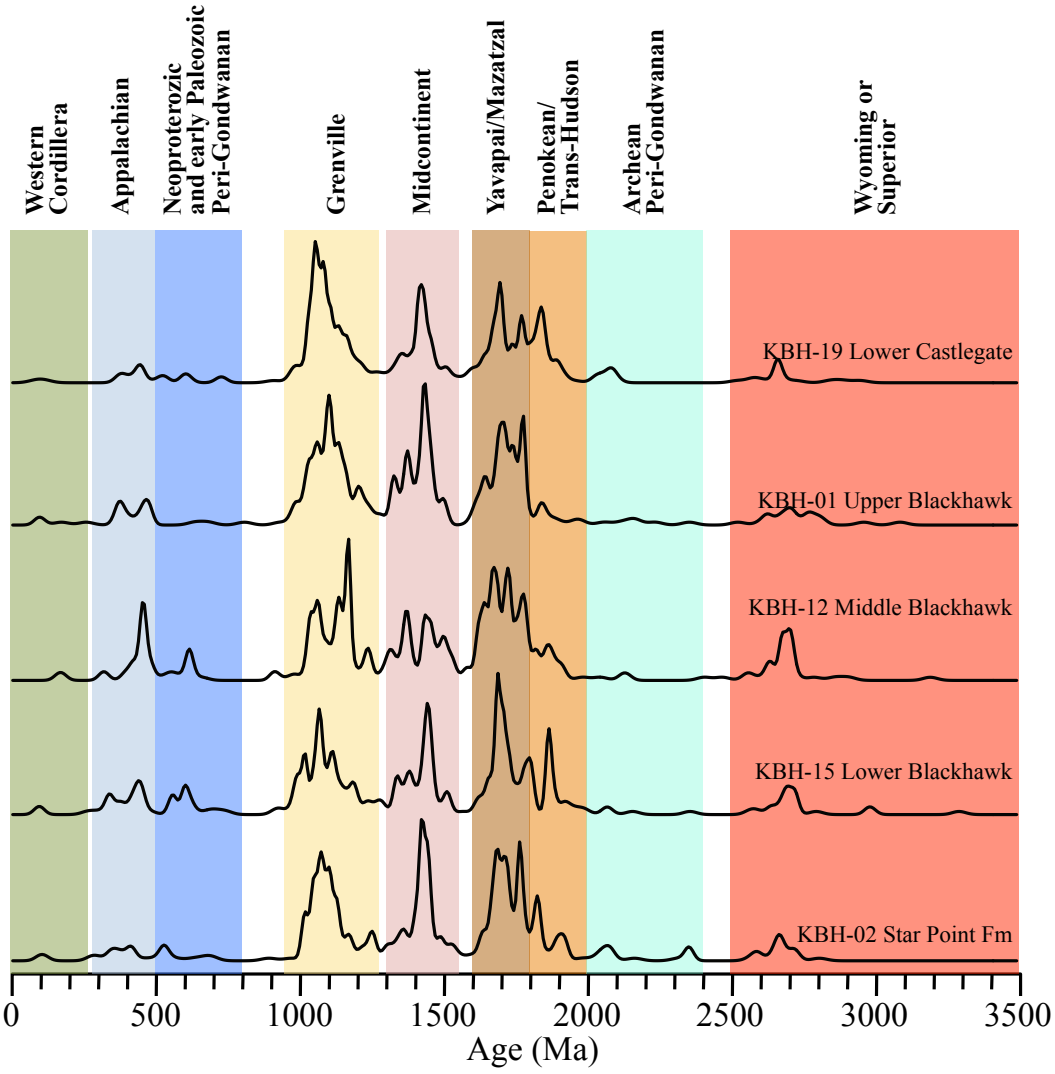

11C) Price Canyon

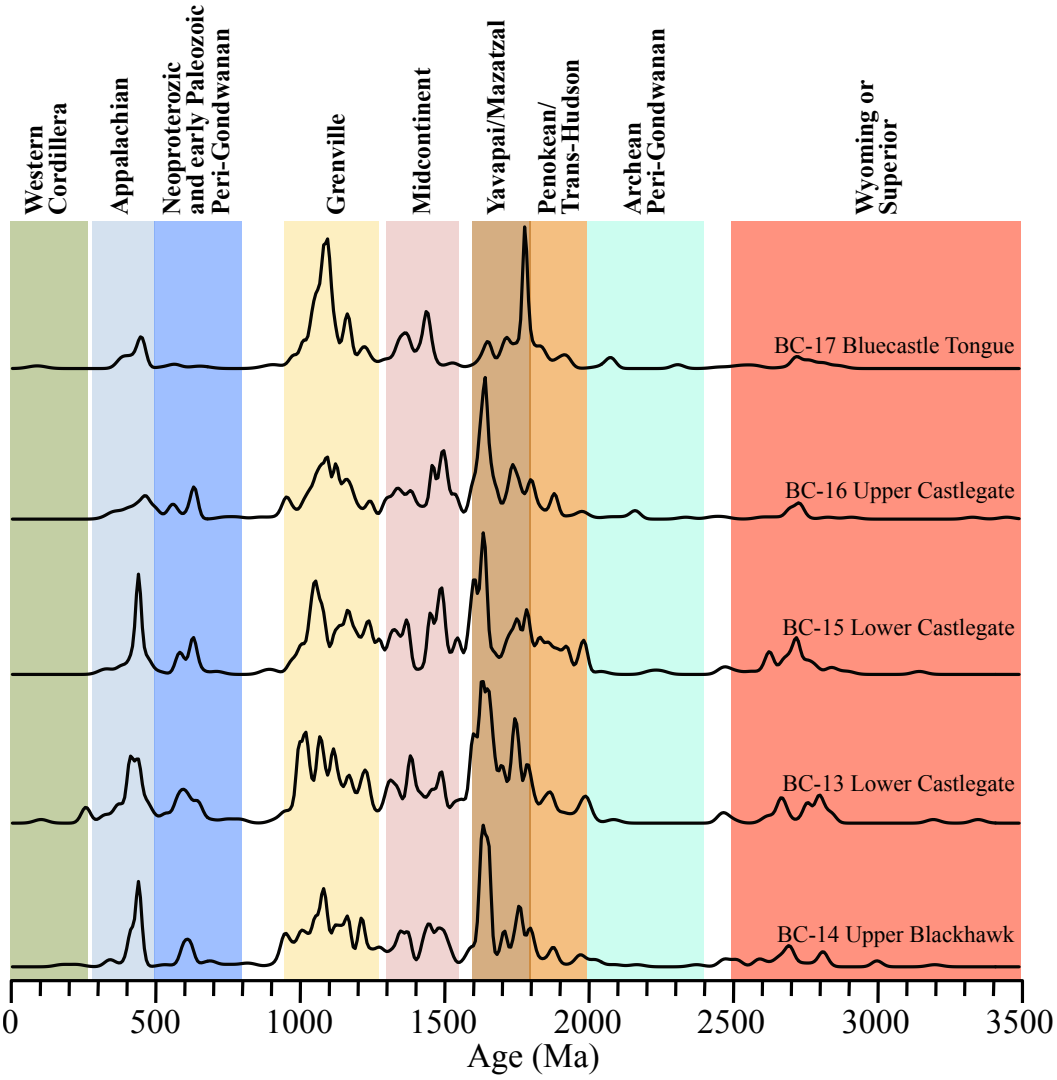

11C) Horse Canyon

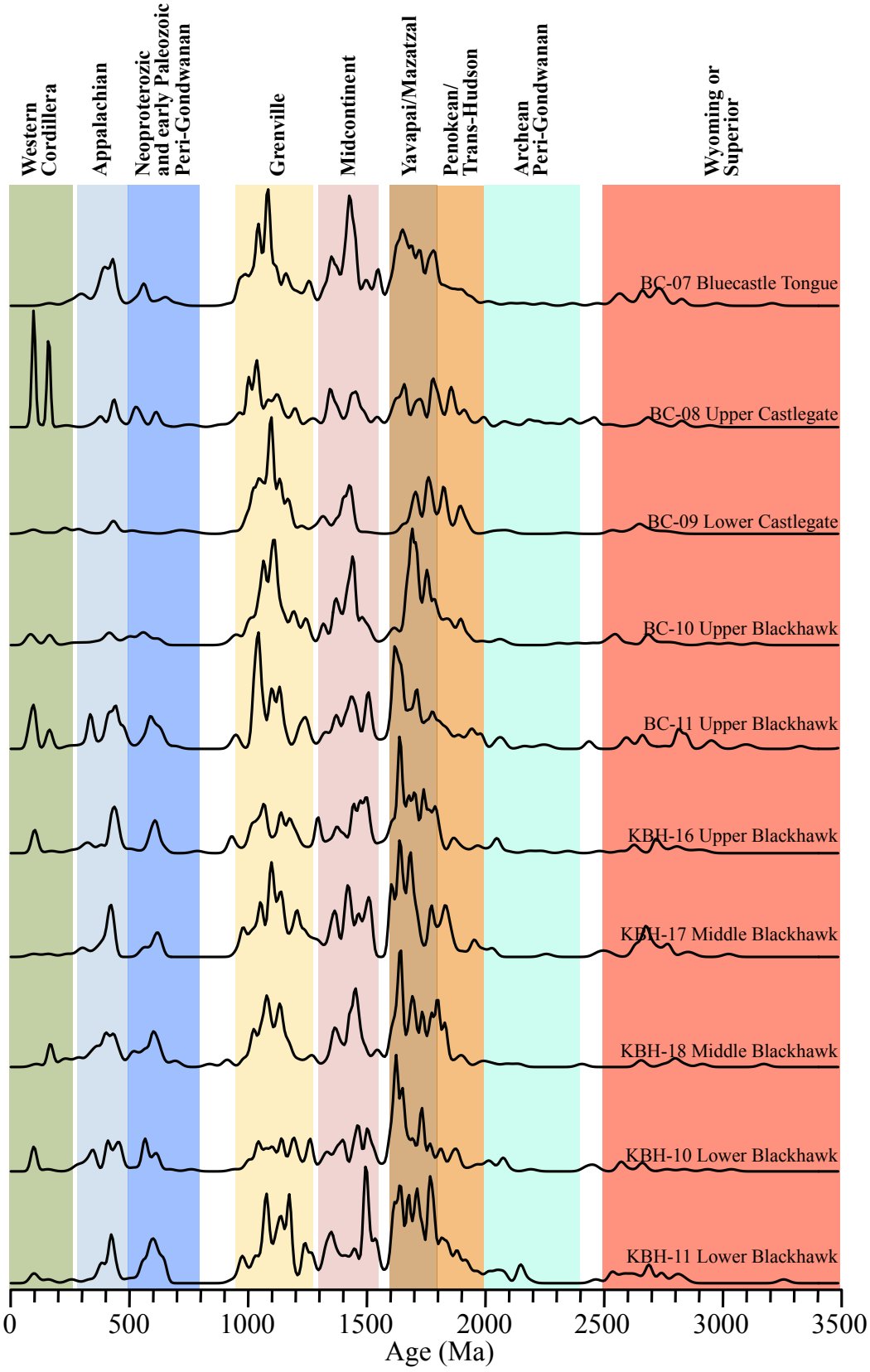

11D) Tusher Canyon

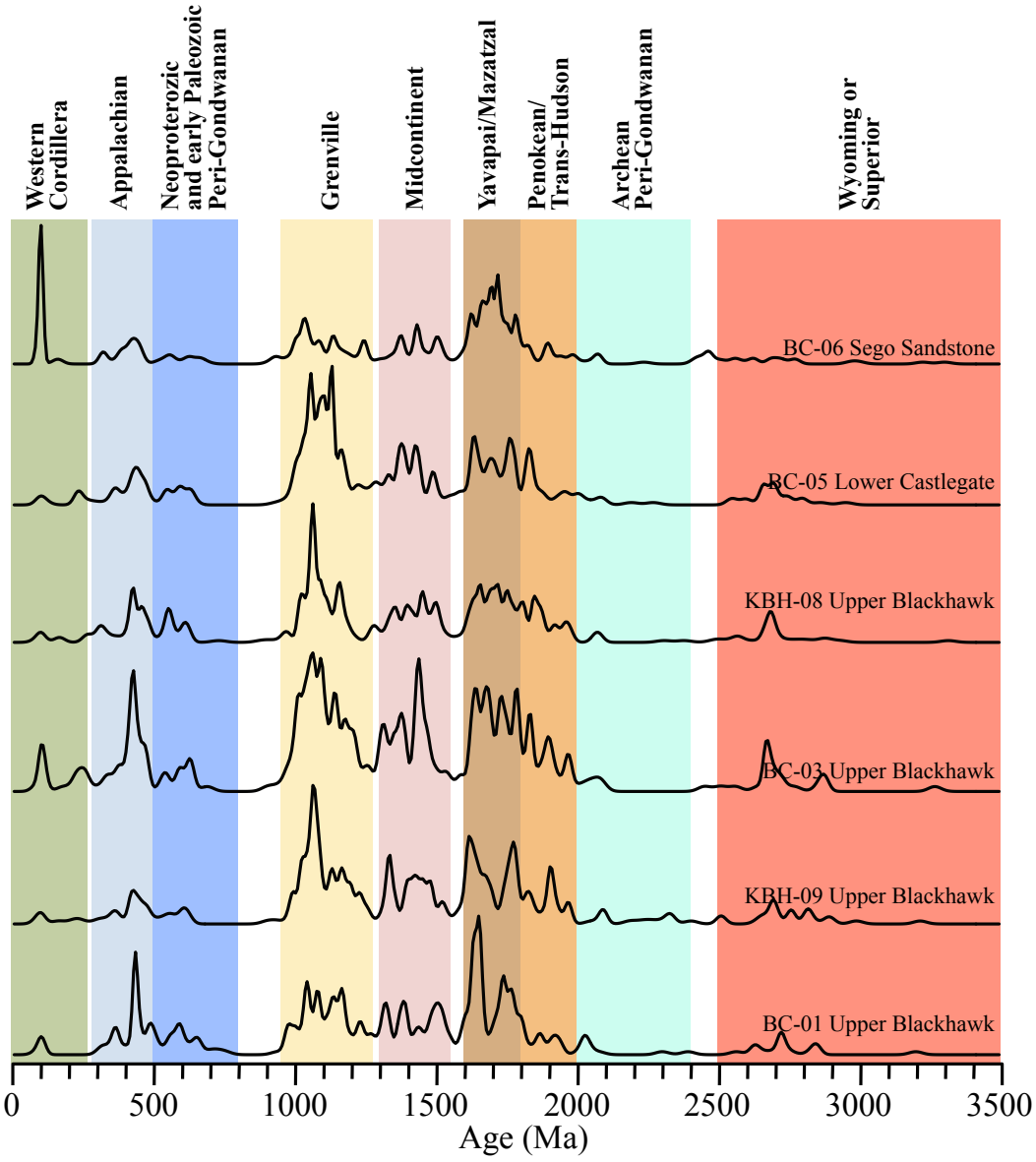

11E) Thompson Canyon

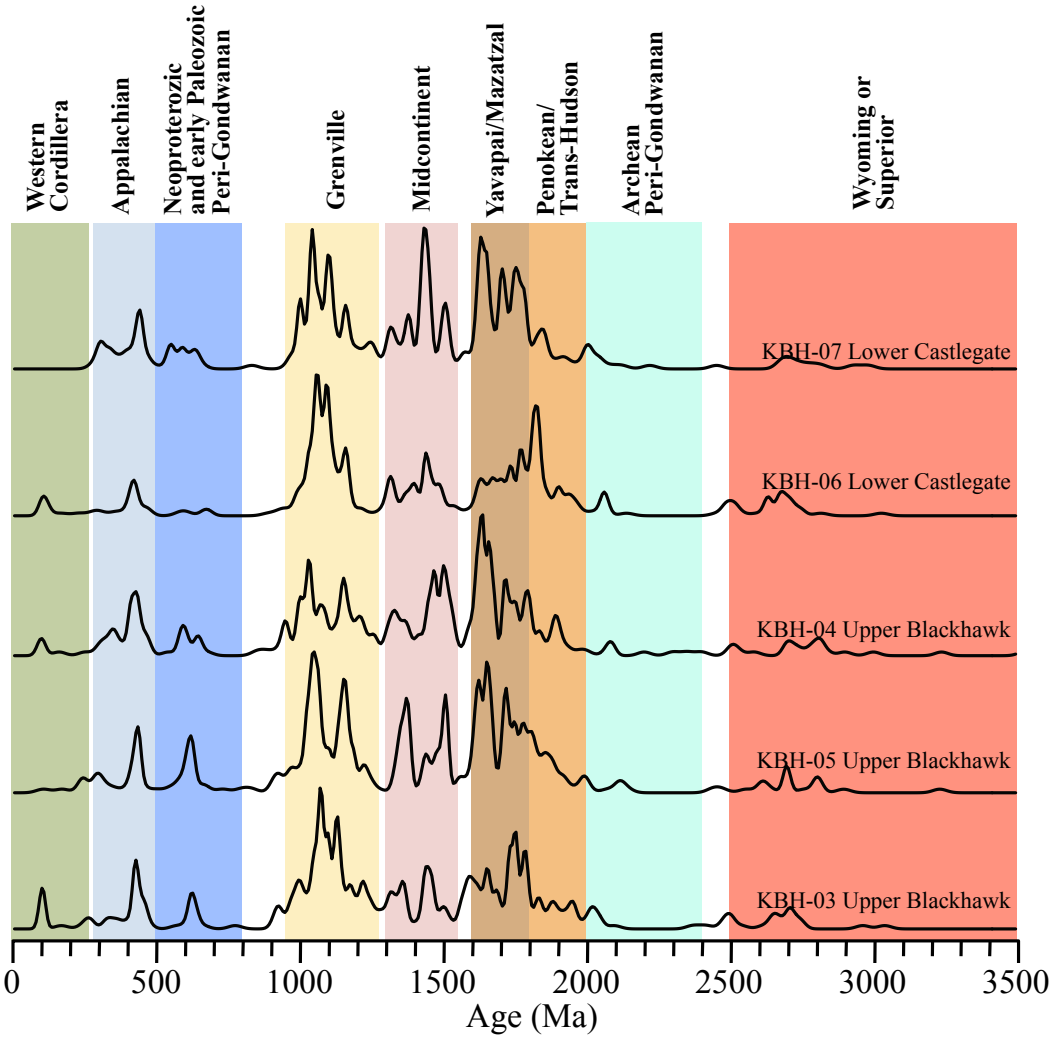

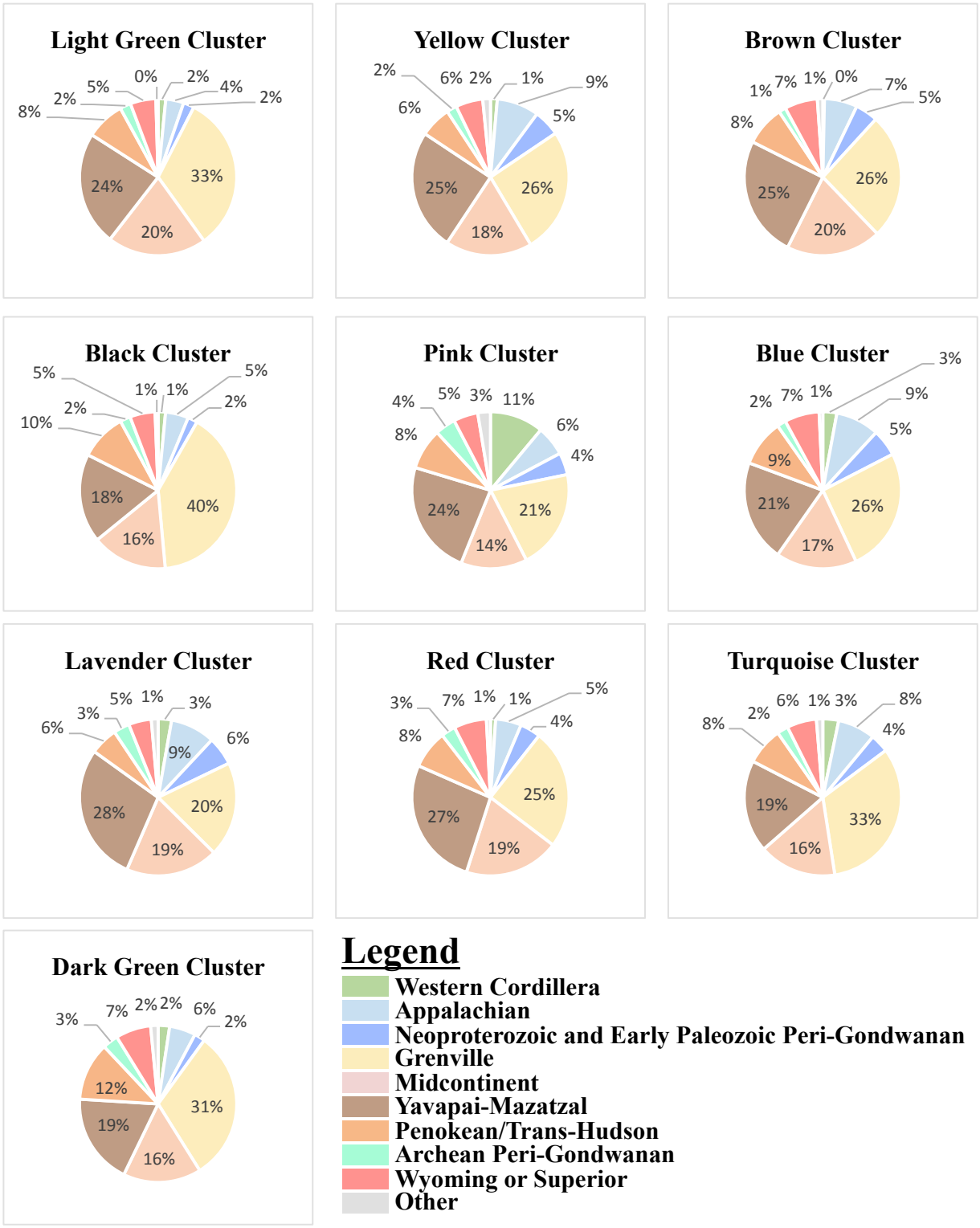

Figure 12: Average percentage of age populations present within each cluster.

A.

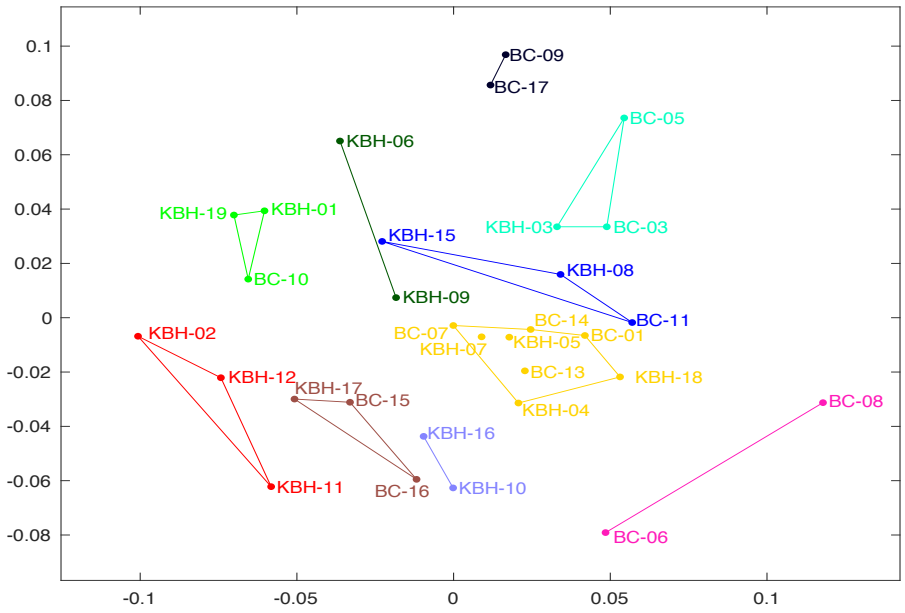

B.

Cluster Name	Sample Name	Canyon Location	Stratigraphic Position
Light Green	KBH-19	Straight	Lower Castlegate
	KBH-01	Straight	Upper Blackhawk
	BC-10	Horse	Upper Blackhawk
Yellow	BC-07	Horse	Upper Castlegate
	BC-13	Price	Lower Castlegate
	KBH-07	Thompson	Lower Castlegate
	KBH-04	Thompson	Upper Blackhawk
	KBH-05	Thompson	Upper Blackhawk
	BC-14	Price	Upper Blackhawk
	BC-01	Tusher	Upper Blackhawk
	KBH-18	Horse	Middle Blackhawk
Brown	BC-16	Price	Upper Castlegate
	BC-15	Price	Lower Castlegate
	KBH-17	Horse	Middle Blackhawk
Black	BC-17	Price	Bluecastle Tongue
	BC-09	Horse	Lower Castlegate
Pink	BC-06	Tusher	Lower Sego
	BC-08	Horse	Upper Castlegate
Blue	KBH-08	Tusher	Upper Blackhawk
	BC-11	Horse	Upper Blackhawk
	KBH-15	Straight	Lower Blackhawk
Lavender	KBH-16	Horse	Upper Blackhawk
	KBH-10	Horse	Lower Blackhawk
Red	KBH-12	Straight	Middle Blackhawk
	KBH-11	Horse	Lower Blackhawk
	KBH-02	Straight	Star Point Fm.
Turquoise	BC-05	Tusher	Lower Castlegate
	BC-03	Tusher	Upper Blackhawk
	KBH-03	Thompson	Upper Blackhawk
Dark Green	KBH-06	Thompson	Lower Castlegate
	KBH-09	Tusher	Upper Blackhawk

Figure 13: (A) Multidimensional scaling plot of 10 aggregate age distributions, projected into two dimensions. (B) Table that describes the samples comprising each cluster.

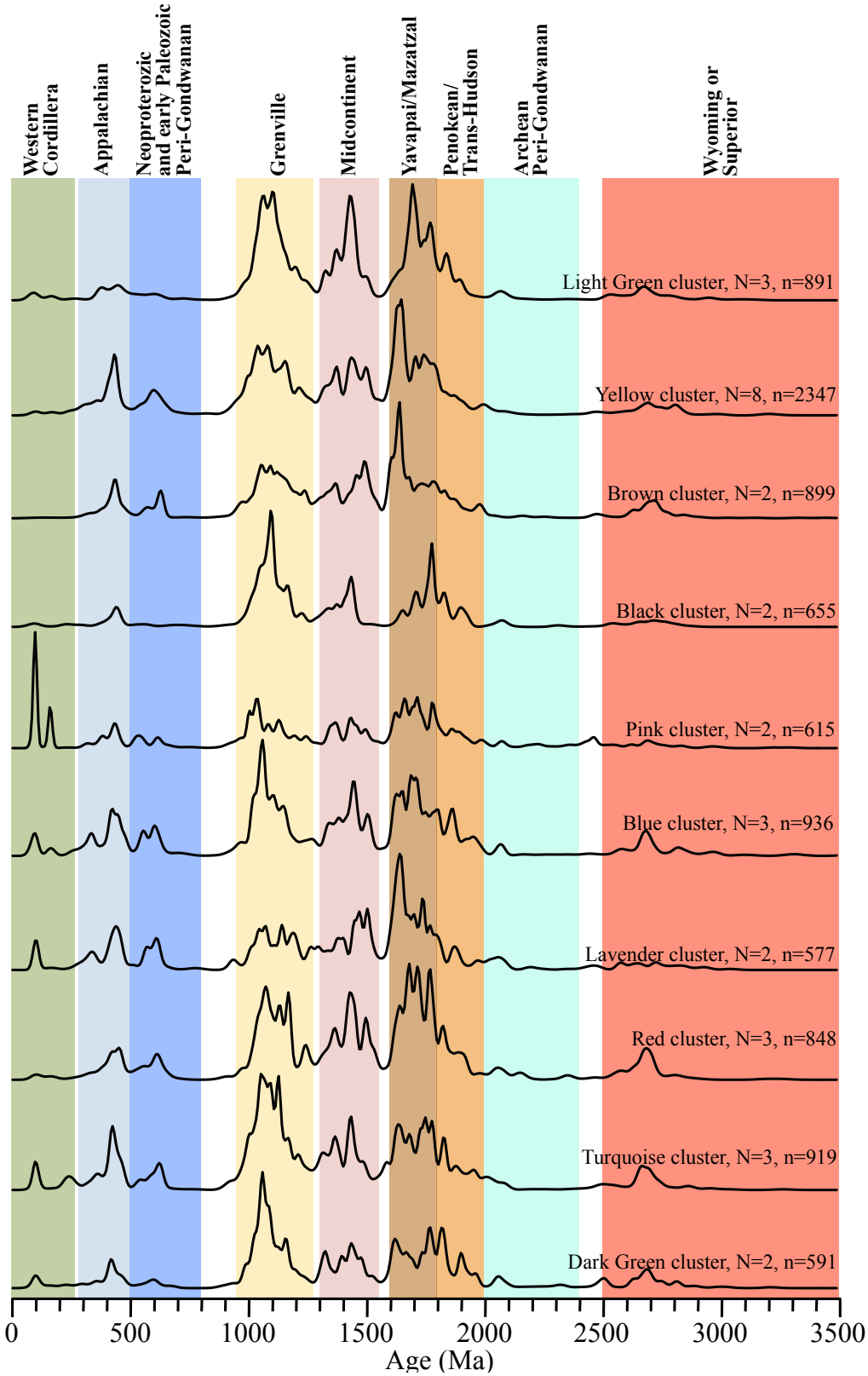

Figure 14: Normalized KDE distributions (bandwidth = 10) of the aggregate clusters identified in Figure 11.

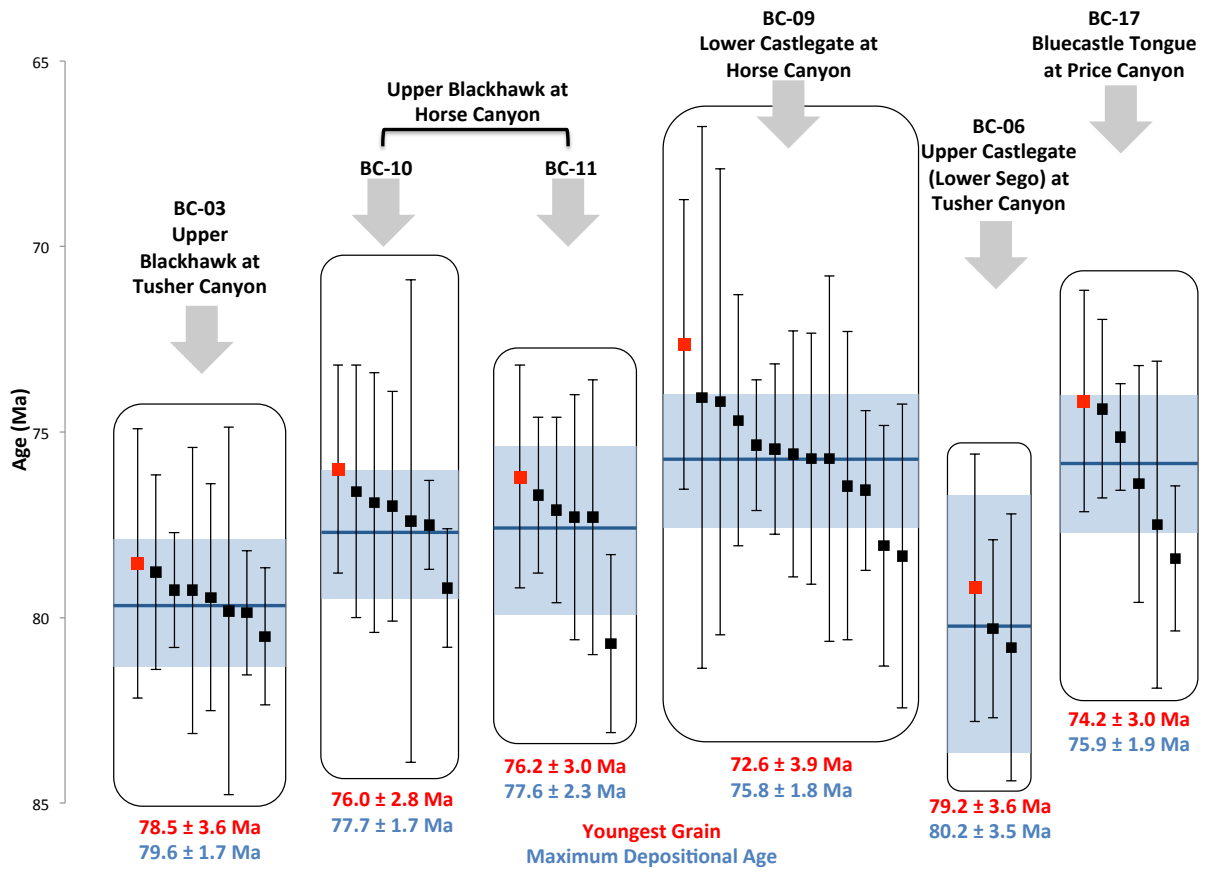

Figure 15: Weighted MDAs of each sample for which there were enough grains (n≥3) to calculate MDA. Youngest grains are shown in red, MDA in blue, and weighted error represented by blue box.

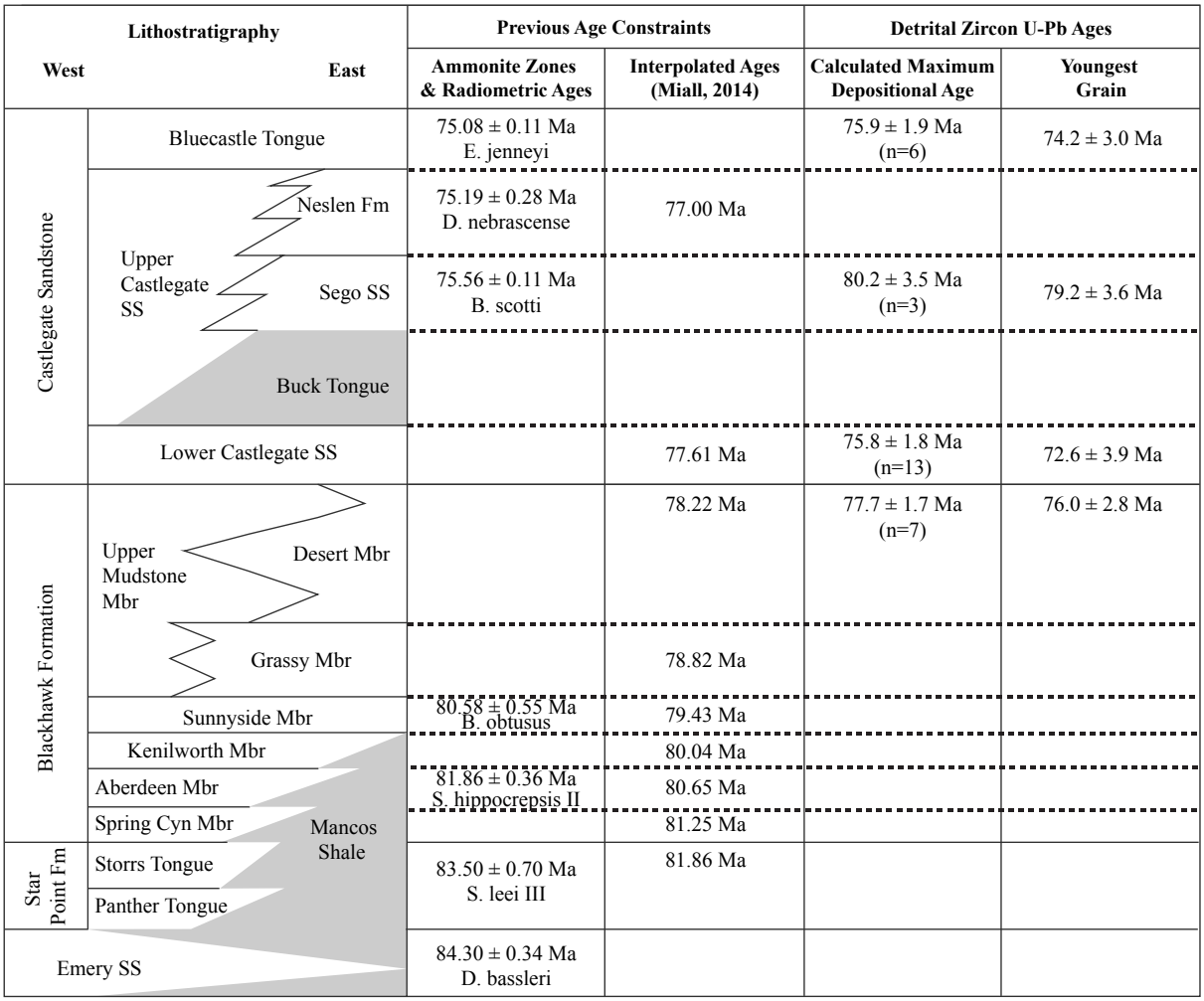

Figure 16: Stratigraphic section by Yoshida (2000) modified to include the previous age constraints and new DZ U-Pb data.

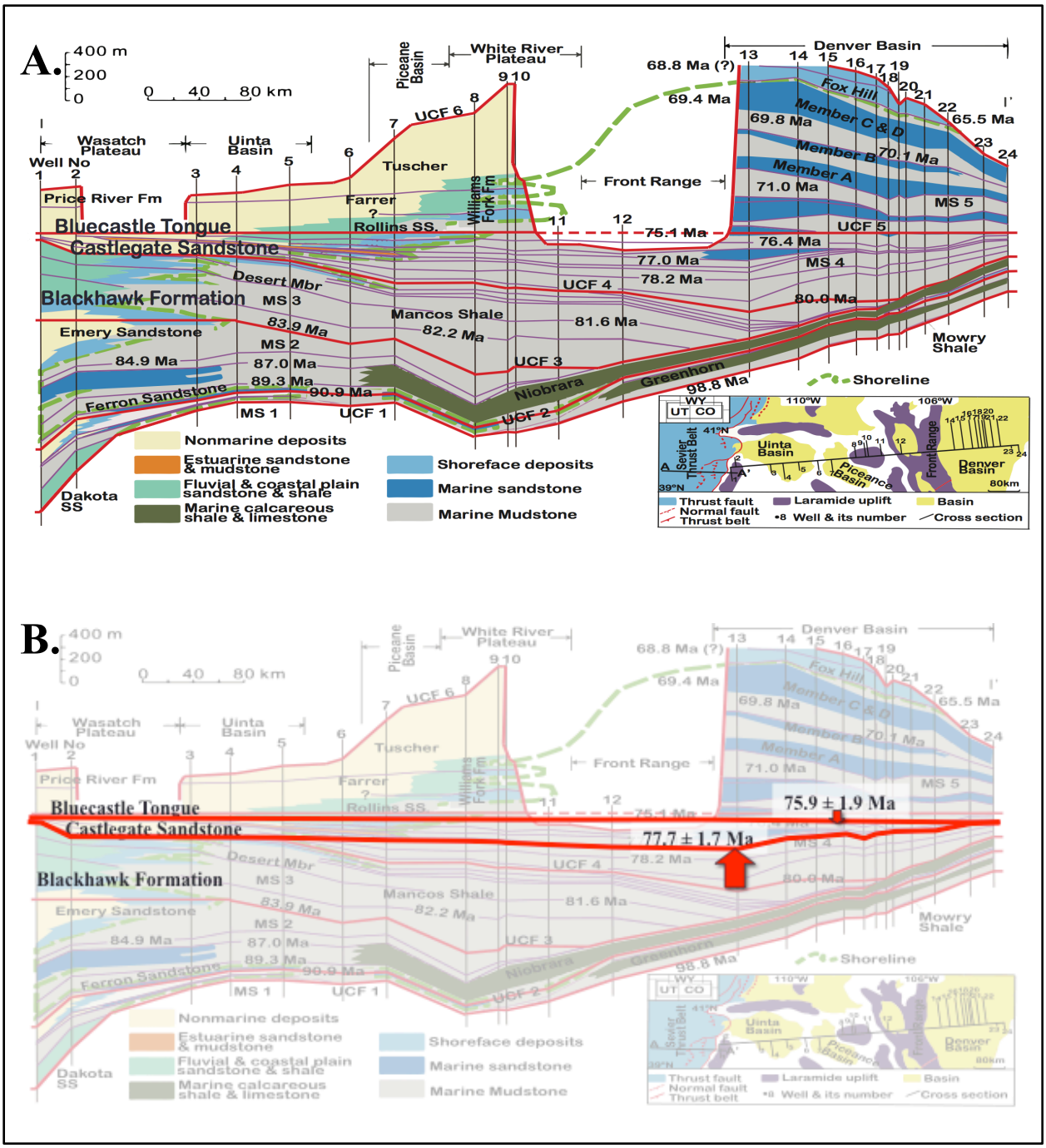

Figure 17: Correlation panels modified from Liu et al. (2014). (A) Stratigraphic correlation through the Upper Cretaceous stratigraphy from Utah to Colorado, based on 24 well logs, ammonite biozonations, and radiometric dates. Major regional unconformities ("UCFs") are red, and correlatable surfaces are purple. (B) Two unconformity surfaces are reinterpreted and correlated to the basinal deposits using the calculated MDAs based on U-Pb ages presented in this paper. UCF 4 forms ~2.3 Myr later, and UCF 6 forms ~0.8 Myr earlier than the original interpretations.

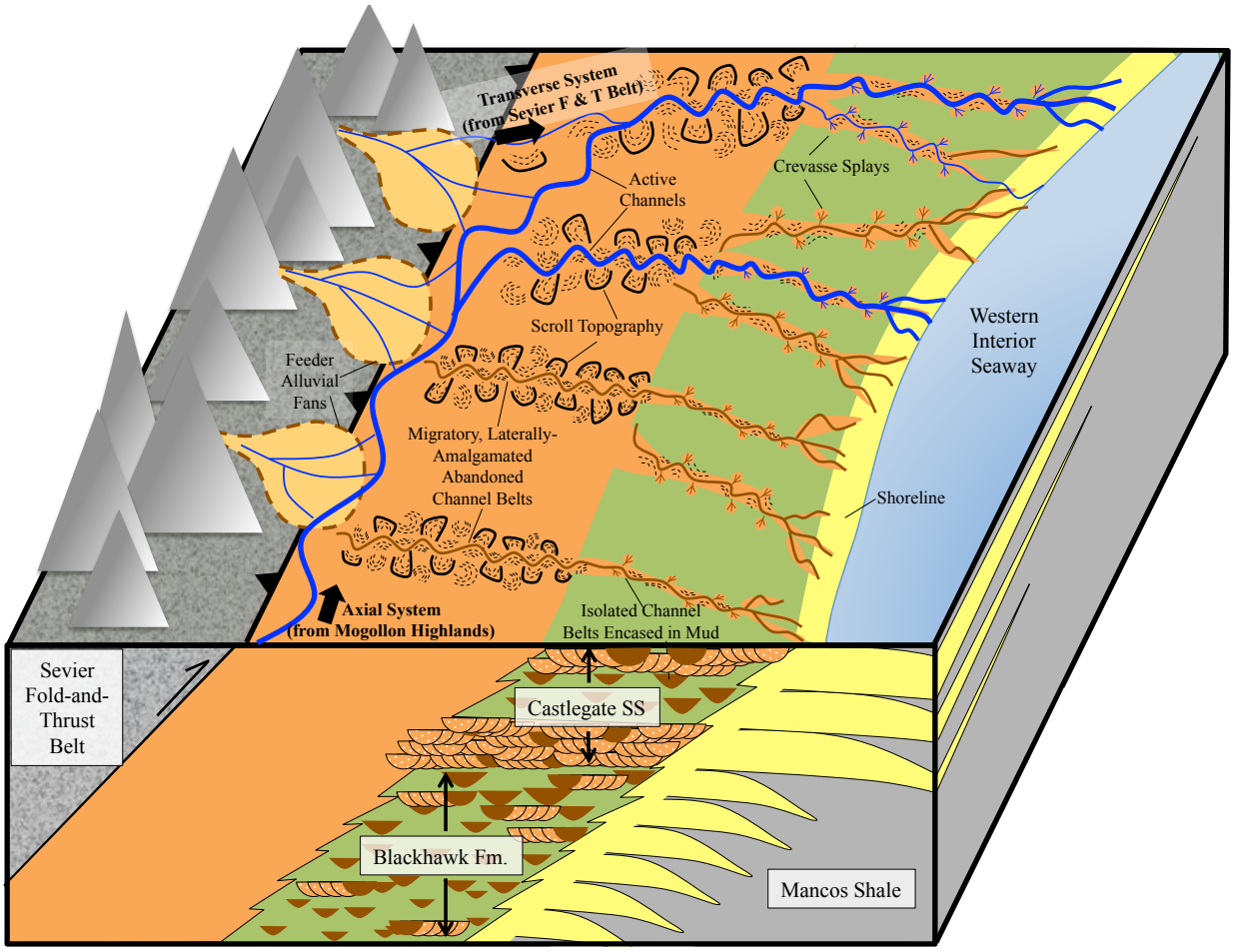

Figure 18: Block diagram illustrating the environments of deposition (top) and progradational stratigraphic architecture (side) for the Blackhawk-Castlegate succession.

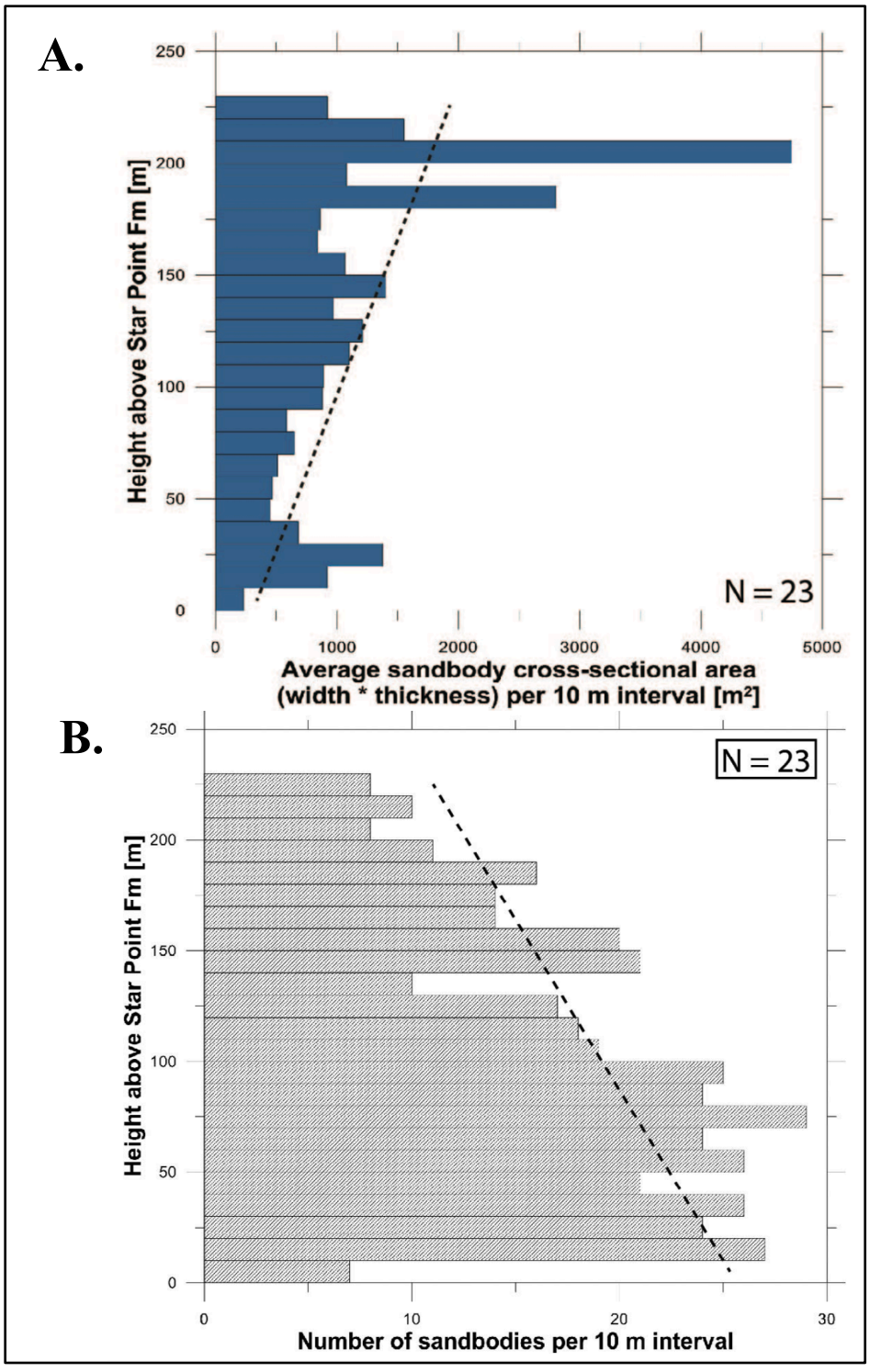

Figure 19: Plots of sandbody measurements through the Blackhawk Formation in Straight Canyon, from Rittersbacher et al. (2014). (A) The cross-sectional area of measured sandbodies averaged over 10 meter intervals and plotted against height above the contact between the Star Point and lower Blackhawk Formations. (B) Number of channels per 10 m interval of the Blackhawk Formation.

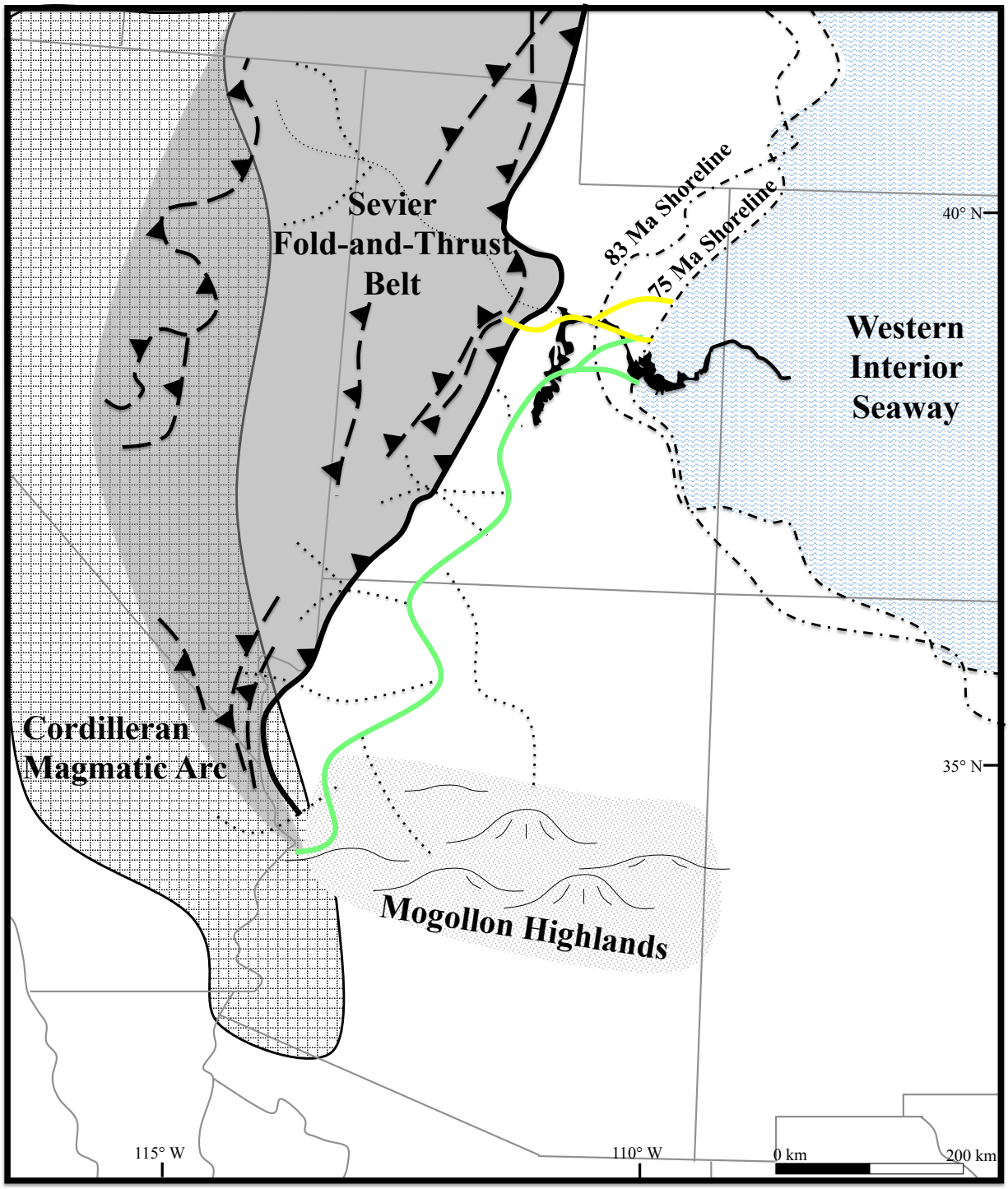

Figure 20: Paleographic reconstruction of the Western Interior during Campanian time (~83.5 Ma-71.3 Ma). Paleodrainage interpretation shown as dotted tributaries to the two parent rivers that feed deposits of the Light Green cluster through Straight Canyon, and the Yellow cluster in Price Canyon. Tectonic elements from Fig. 15 of DeCelles (2004), shoreline positions of Western Interior Seaway from Ron Blakey, and paleodrainage reconstruction adapted from Fig. 13 of Szwarc et al. (2014).

9 Tables

Table 1: Original source and potential recycled locations of U-Pb age populations present in this study. Adapted from Blum et al. (2017), and summarized from Becker et al. (2005), Whitmeyer and Karlstrom (2007), Dickinson and Gehrels (2009), Park et al. (2010), and Laskowski et al. (2013).

Population Name	Age Range	Primary Source	Potential Recycled Location
Western Cordillera	275-0 Ma	Cordilleran Magmatic Arc in Nevada, California, or southwestern Arizona, syndepositional volcanics in southeastern Arizona	Potential reworking of ashfall blankets near volcanic centers, Mesozoic foreland-basin strata of the US Western Interior
Paleozoic Appalachian	500-290 Ma	Appalachian-Ouachita Cordillera	Paleozoic Appalachian-Ouachita foreland-basin strata, Paleozoic passive margin strata of the Western US
Neo-proterozoic and early Paleozoic Peri-Gondwanan	800-500 Ma	Pan-African/Brasiliano terrane, synrift rocks of the Iapetus Rift, Wichita Mountains of Oklahoma	Appalachian-Ouachita foreland-basin strata, Paleozoic passive margin strata of the Western US
Grenville	1250-950 Ma	Shawinigan and Ottawan Orogenies in the Great Lakes region, Llano Province in Texas	Paleozoic sandstones of US midcontinent, Appalachian-Ouachita foreland-basin strata, Paleozoic passive margin strata of the Western US
Midcontinent	1550-1300 Ma	NE-SW trend across the eastern US Midcontinent to area of present day Rocky Mountains, plutonic intrusions into the Yavapai-Mazatzal provinces	Paleozoic sandstones of US midcontinent, Appalachian-Ouachita foreland-basin strata, Paleozoic passive margin strata of the Western US
Yavapai-Mazatzal	1800-1600 Ma	Yavapai and Mazatzal Orogens and associated intrusions exposed in the Mogollon Highlands of central Arizona	Paleozoic foreland-basin strata of the Western US
Penokean/Trans-Hudson	2000-1800 Ma	Paleo-proterozoic Trans-Hudson and Penokean Orogens in southcentral Canada (Manitoba and Saskatchewan) and Great Lakes region of the US, Elves Chasm Gneiss in Arizona	Pervasive in North American strata
Archean Peri-Gondwanan	2400-2000 Ma	The peri-Gondwanan Carolina, Suwannee, and Avalon terranes accreted during Trans-Amazonian events along the eastern margin of North America, miogeoclinal sediments of the Snowy Pass Supergroup in Great Lakes region, Huronian Supergroup of present-day New Mexico	A small portion of Paleozoic passive margin strata of the Western US
Wyoming or Superior	>2500	Northern US midcontinent to present-day northern Rocky Mountains province	Pervasive in North American strata

Table 2: Sample Descriptions for: A) KBH Sample Set (collected in 2016) and B) BC Sample Set (collected in 2012)

A) KBH Sample Set

Sample	Canyon	Unit	Longitude	Latitude	Grain	Description/Notes
KBH-01	Straight	Upper Blackhawk	-111.271235	39.293665	278	Collected from interbedded very fine sands and coarse silts, rich in organic matter. Sample taken from the uppermost Blackhawk, 1 m below Castlegate contact near the road adjacent to the reservoir. Interpreted to be crevasse splay deposits in a coastal plain.
KBH-02	Straight	Star Point Fm.	-111.205291	39.275201	291	Sample collected from fine lower interval within a hummocky fine to medium sandstone, at the location across the road from the mine cart.
KBH-03	Thompson	Upper Blackhawk	-109.709222	39.019727	294	Sample taken from a medium to fine channel-belt sandstone with trough cross beds in the Blackhawk Desert member. Located adjacent to corral and petroglyphs on BLM road.
KBH-04	Thompson	Upper Blackhawk	-109.709063	39.019647	286	Sample collected from a fine sand interceded with carbonaceous mud directly above a coal, interpreted to be crevasse splay facies in the Blackhawk Desert member. Located adjacent to corral and petroglyphs on BLM road.
KBH-05	Thompson	Upper Blackhawk	-109.709057	39.019652	296	Sample collected from a thin bedded, fine to very fine sand in a facies that's interbedded with mud and ripple laminated, interpreted to be channel fill in the Blackhawk Desert member. Located adjacent to corral and petroglyphs on BLM road.
KBH-06	Thompson	Lower Castlegate	-109.707401	39.018753	296	Sample collected from interbedded fine to very fine sands and silts, interpreted to be Castlegate channel fill. There is shell hash in the VF sand beds. Collected over the hill from the corral and petroglyphs on the BLM road.
KBH-07	Thompson	Lower Castlegate	-109.708530	39.019737	283	Sample collected from the fine to lower medium, trough cross bedded sandstone at the base of the Castlegate channel belt directly above KBH-06. Base has organic debris. Collected over the hill from the corral and petroglyphs on the BLM road.
KBH-08	Tusher	Upper Blackhawk	-110.032467	39.099797	380	Collected from the a very-fine lower-grained sandstone in the Blackhawk Desert member non-amalgamated fluvial/coastal plain facies. Note: Collected from same location as BC-04, which was analyzed using LA-ICPMS at Laserchron in 2013. The mount could not be found to upgrade, so KBH-08 was collected and run at n=300, and merged with the existing grains of BC-04.
KBH-09	Tusher	Upper Blackhawk	-110.032060	39.097984	295	Sample collected from organic-rich, silt to fine-grained sandstone interpreted to be channel fill in the Blackhawk Desert member. Outcrop is adjacent to BC-03 location on Tusher Canyon Road.
KBH-10	Horse	Lower Blackhawk	-110.357094	39.460477	281	Collected from a fine lower to VF upper, hummocky cross-stratified sadstone interpreted to be distal lower shoreface. Outcrop is the second Blackhawk shoreface in Horse Canyon, likely the Kenilworth shoreface (according to the correlation in Rittersbacher et al., 2014)
KBH-11	Horse	Lower Blackhawk	-110.360119	39.457899	273	Collected from fine lower to VF upper, hummocky cross-stratified sandstone interpreted to be distal lower shoreface. Outcrop is the first Blackhawk shoreface in Horse Canyon, likely the Aberdeen shoreface (according to the correlation in Rittersbacher et al., 2014)
KBH-12	Straight	Middle Blackhawk	-111.206069	39.278995	284	Collected from fine-grained, coarsening upwards sandstone under a Blackhawk channel body, interpreted to be coarsening upward splay complex.
KBH-15	Straight	Lower Blackhawk	-111.206200	39.276326	258	Collected from well-cemented, ripple-laminated, thin-bedded, very fine sand.
KBH-16	Horse	Upper Blackhawk	-110.345038	39.465529	296	Collected from very-fine 2-3 inch sandstone beds interbedded with silt sones, interpreted to be a crevasse splay complex. Sample collected 80 m below BC-10 and BC-11.
KBH-17	Horse	Middle Blackhawk	-110.351530	39.462553	269	Collected from well-cemented, 7-30 cm fine sandstone beds interbedded with mud. Interpreted to be a Blackhawk channel belt.
KBH-18	Horse	Middle Blackhawk	-110.355675	39.461137	256	Collected from very-fine lower sandstone beds up to 30 cm thick, interpreted to be sheet flood deposits.
KBH-19	Straight	Lower Castlegate	-111.270930	39.300325	303	Collected from a well-cemented, fine-upper sandstone interpreted to be a Castlegate fluvial channel belt. Collected just above the Castlegate unconformity adjacent to Joe's Valley Reservoir.

Table 2 (cont.)
B) BC Sample Set

Sample	Canyon	Unit	Longitude	Latitude	Grain	Description/Notes
BC-01	Tusher	Upper Blackhawk	-110.033730	39.099480	294	Collected from thick-bedded (~2 m) fine-grained sandstone, hummocky cross-bedded facies interpreted to represent the Blackhawk Grassy Lower Shoreface facies. Also interpreted as Grassy HST by Van Wagoner. Located on Tusher Canyon Road.
BC-03	Tusher	Upper Blackhawk	-110.032261	39.098157	294	Collected from the tidally-influenced heterolithic, very-fine lower sandstone, believed to be a channel-fill sandstone within the Blackhawk Desert member. Outcrop adjacent to KBH-09 location on Tusher Canyon Road.
BC-05	Tusher	Lower Castlegate	-110.034049	39.099998	331	Collected from a fine-lower sandstone, a Castlegate fluvial outcrop at Tusher Canyon near the base of section, at the same location as BC-01 on Tusher Canyon Road.
BC-06	Tusher	Lower Sego	-109.998600	39.079200	300	Collected from the meter-thick, very-fine lower sandstone bed in an overall inclined heterolithic strata-dominated section. It was the first major Sego outcrop at road level on Tusher Canyon Road.
BC-07	Horse	Upper Castlegate	-110.328280	39.477350	307	Collected from medium-grained, trough to plane-bedded sandstone interpreted to be a channel-belt sandstone in the moderately amalgamated upper Castlegate, just above contact with purple/gray mudstones interbedded with sands.
BC-08	Horse	Upper Castlegate	-110.335660	39.475960	315	Collected from the medium-grained, well-cemented sand within a channel-belt sand of the non-amalgamated upper Castlegate (described by some authors as "middle Castlegate"), encased in oxidized and reduced mudrocks with thin tabular sands.
BC-09	Horse	Lower Castlegate	-110.342260	39.470750	326	Collected from medium-grained, trough cross-bedded sandstone with large-scale inclined strata. Within the amalgamated multi-story channel-belt sandstones of the lower Castlegate.
BC-10	Horse	Upper Blackhawk	-110.344350	39.471100	310	Collected from the medium- to fine-grained, trough cross bedded quartzarenite interpreted to represent Blackhawk fluvial overlain by non-amalgamated coastal plain. Sample taken from the 1st major channel-belt sandbody below the clear Castlegate.
BC-11	Horse	Upper Blackhawk	-110.345540	39.468210	298	Collected from medium- to fine-grained quartz-rich sandstone that also has chert and other accessory minerals. Facies interpreted to be fluvial channel-belt within a non-amalgamated Blackhawk section.
BC-13	Price	Lower Castlegate	-110.886417	39.751405	300	Collected from trough-cross bedded, fine- to medium-grained sandstone with organic detritus. Sample is from the lower Castlegate near the base of the exposure where it intersects the road.
BC-14	Price	Upper Blackhawk	-110.886769	39.752106	325	Collected from thin-bedded (1-2 m), fine-lower sandstone within coaly and muddy succession. Sample is from just below the Castlegate unconformity, based on correlation with section of Miall and Arush (2001), at the same location as BC-13 but on the other end of the roadside pulloff.
BC-15	Price	Lower Castlegate	-110.889512	39.756948	310	Collected from the heterolithic fine-grained channel-belt sandbody near the estimated top of the Lower Castlegate
BC-16	Price	Upper Castlegate	-110.891128	39.758913	320	Collected from thin, fine-grained, ripple laminated, very-fine lower sandstone with small troughs, 2-3 m maximum thickness in the non-amalgamated portion believed to be the upper Castlegate (middle Castlegate by some authors)
BC-17	Price	Bluecastle Tongue	-110.894117	39.761184	329	Collected from the thick, multi-story, medium-lower grained sandstone interpreted to be channel belt where it cuts across non-amalgamated section, believed to be the Bluecastle Tongue

Table 3: Summary of the MDAs calculated for each interval and U-Pb age data of grains used for calculation.

Sample Description	Calculated MDA	Age (Ma)	2σ Error (Ma)
BC-17: Bluecastle Tongue at Price Canyon	75.9 ± 1.9 Ma (2.6%)	74.2	3.0
		74.4	2.4
		75.1	1.4
		76.4	3.2
		77.5	4.4
		78.4	2.0
BC-06: Upper Castlegate (Lower Sego) at Tusher Canyon	80.2 ± 3.5 Ma (4.4%)	79.2	3.6
		80.3	2.4
		80.8	3.6
BC-09: Lower Castlegate at Horse Canyon	75.8 ± 1.8 Ma (2.4%)	74.1	7.3
		74.2	6.3
		74.7	3.4
		75.4	1.8
		75.5	2.3
		75.6	3.3
		75.7	3.4
		75.7	4.9
		76.4	4.2
		76.6	2.2
		78.1	3.2
		78.3	4.1
BC-11: Upper Blackhawk at Horse Canyon	77.6 ± 2.3 Ma (2.9%)	76.2	3.0
		76.7	2.1
		77.1	2.5
		77.3	3.3
		77.3	3.7
		80.7	2.4
BC-10: Upper Blackhawk at Horse Canyon	77.7 ± 1.7 Ma (2.2%)	76.0	2.8
		76.6	3.4
		76.9	3.5
		77.0	3.1
		77.4	6.5
		77.5	1.2
		79.2	1.6
BC-03: Upper Blackhawk at Tusher Canyon	79.6 ± 1.7 Ma (2.2%)	78.5	3.6
		78.8	2.6
		79.3	1.6
		79.3	3.9
		79.5	3.1
		79.8	4.9
		79.9	1.7
		80.5	1.8

Table 4: Channel height and grain size data of 7 channel belt samples collected in Horse Canyon.

Sample	Channel Height (m)	Grain Size							Folk (1968)	
		Gravel	Very Coarse	Coarse	Medium	Fine	Very Fine	Mud	Φ50	Sorting
MD-03	5.0	0.12%	2.64%	22.67%	17.87%	26.15%	18.80%	11.97%	2.27	poorly sorted
MD-04	4.0	0.38%	2.92%	26.21%	12.20%	20.52%	25.21%	12.59%	2.40	very poorly sorted
MD-05	3.5	0.54%	3.37%	35.02%	11.86%	11.61%	20.39%	17.09%	1.92	poorly sorted
MD-06	1.0	0.39%	1.37%	13.61%	23.02%	52.34%	6.55%	2.63%	2.22	very poorly sorted
MD-02	3.4	0.07%	0.77%	41.61%	45.21%	10.50%	1.49%	0.62%	1.17	very poorly sorted
MD-07	2.8	0.13%	0.81%	12.62%	17.36%	36.57%	27.21%	5.25%	2.52	very poorly sorted
MD-01	4.6	0.33%	6.50%	34.18%	16.50%	19.62%	15.39%	7.49%	1.54	poorly sorted

10 Appendices

Appendix A: Measured Sections

The Straight Canyon section was measured as part of this thesis; Price Canyon section is the "Gentile Wash" section in Gani et al. (2015) up to the base of the Lower Castlegate, then from "The Castlegate" section from Willis (1997); Horse Canyon is from this thesis to the base of the Lower Castlegate, then from the Willis (1997) through the Bluecastle Tongue; Tusher Canyon is from the Van Wagoner (1995) "Tuscher Canyon SWNE Sec. 8" to the top of the Lower Castlegate, then the Willis (1997) through the Sego; Thompson Canyon is from the "Sego #2 Well" in Morehouse (2015).

Straight Canyon A

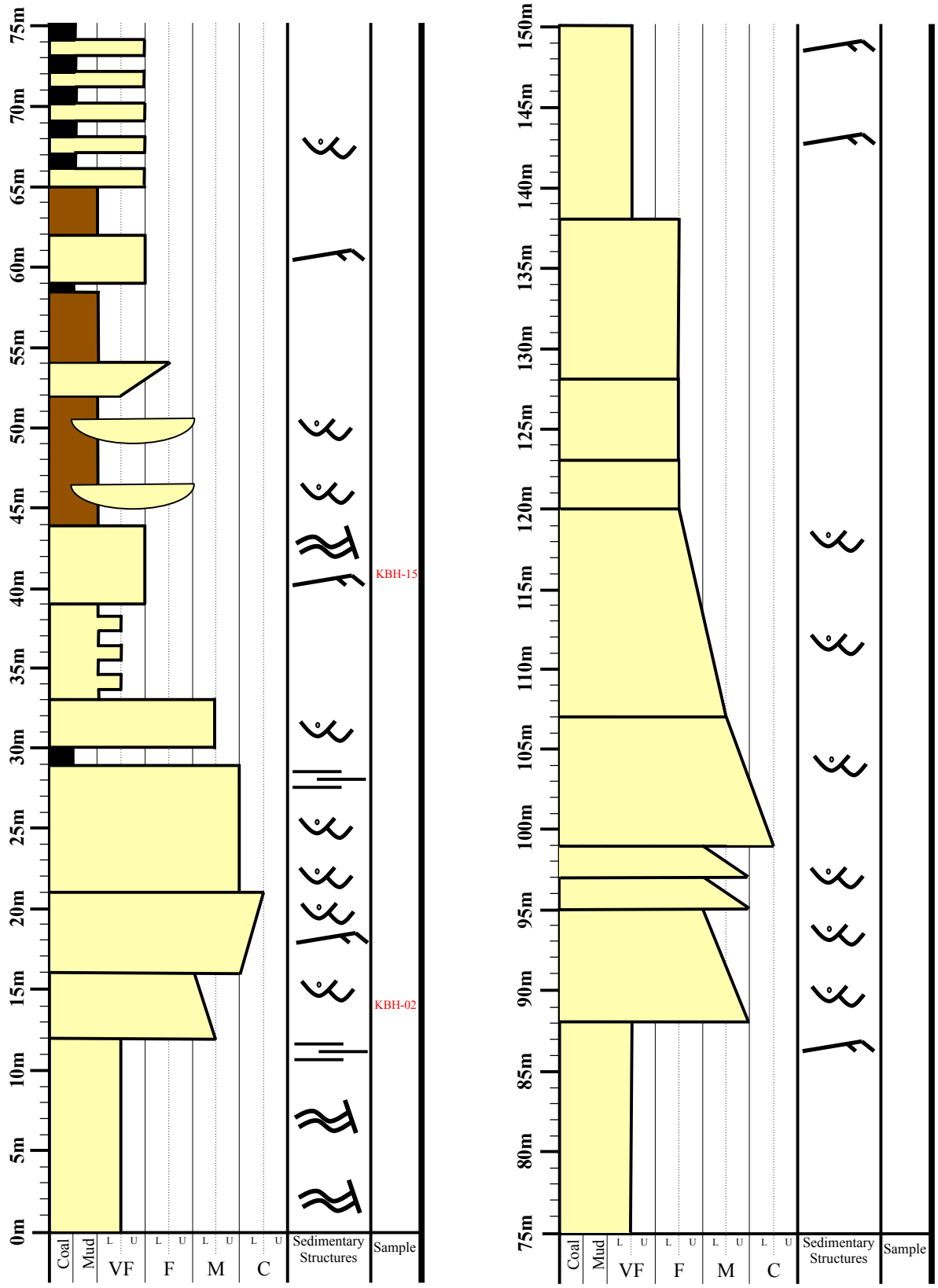

Straight Canyon B

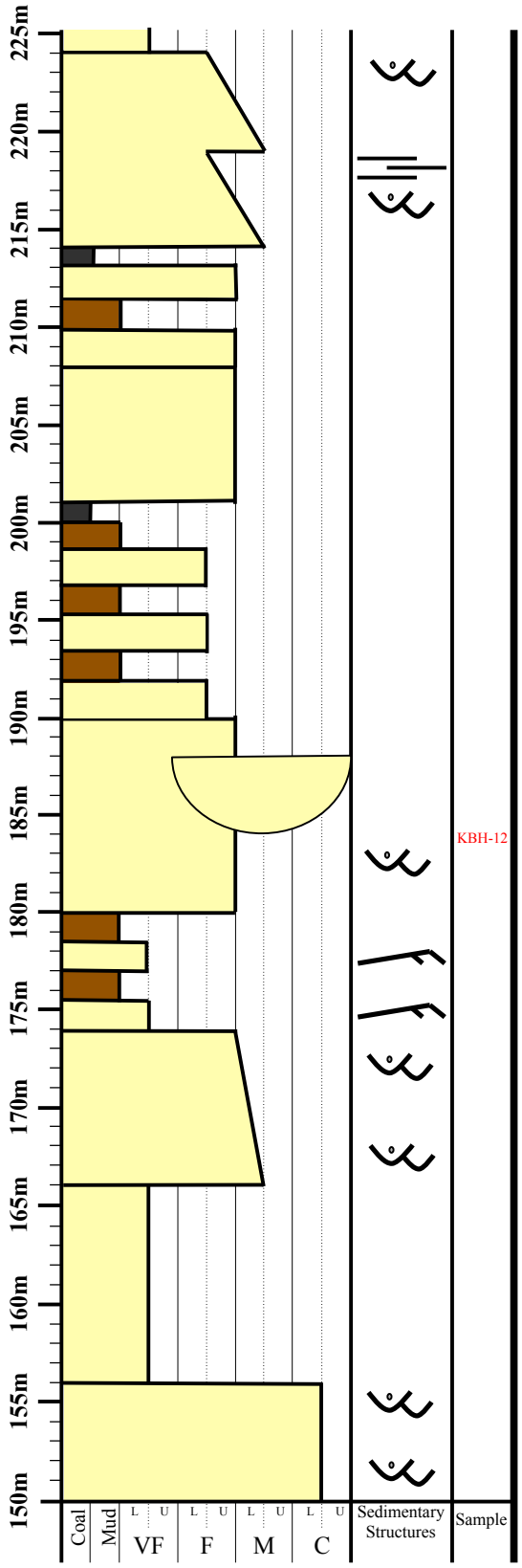

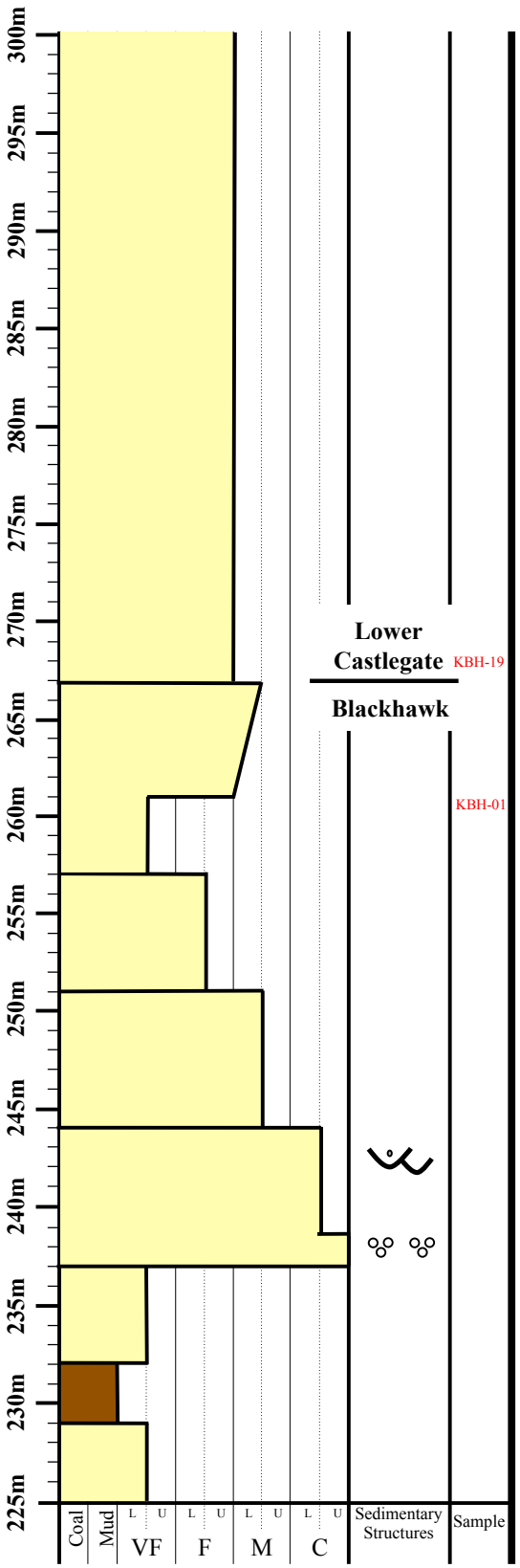

Price Canyon A

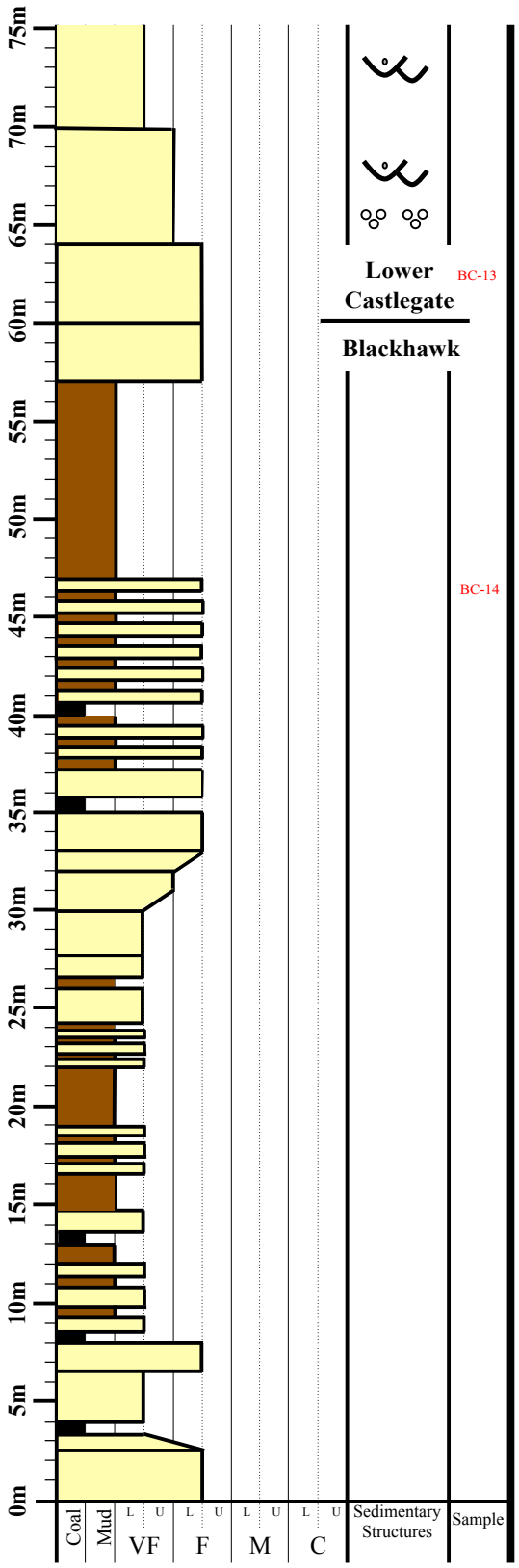

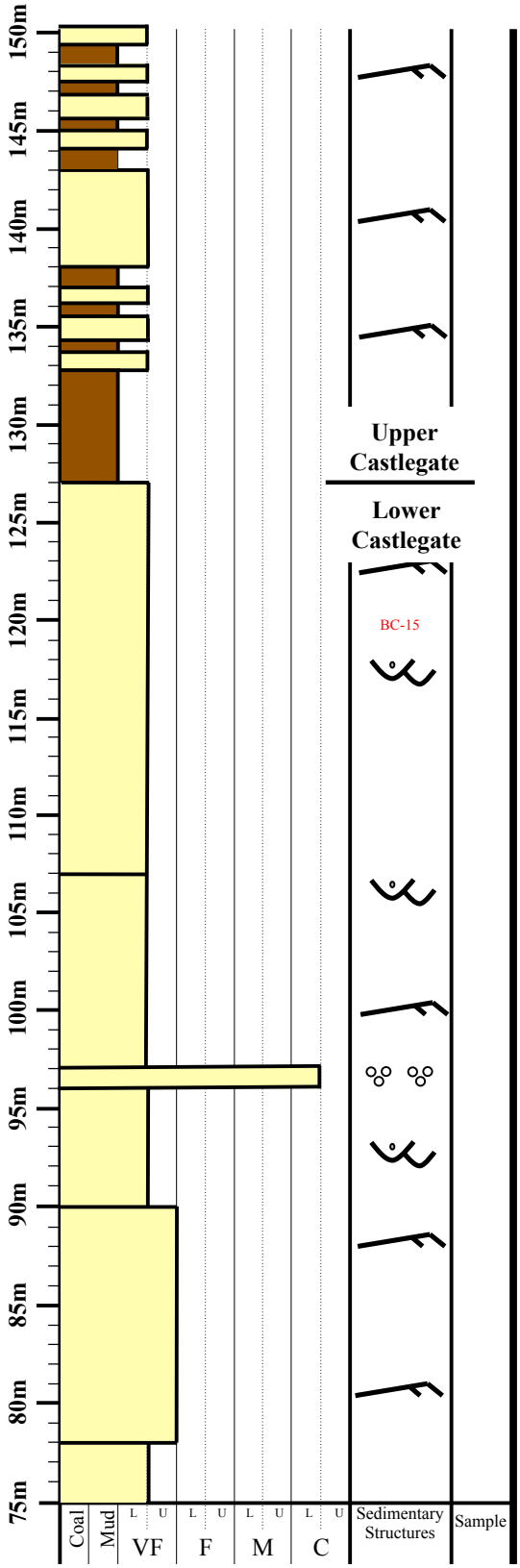

Price Canyon B

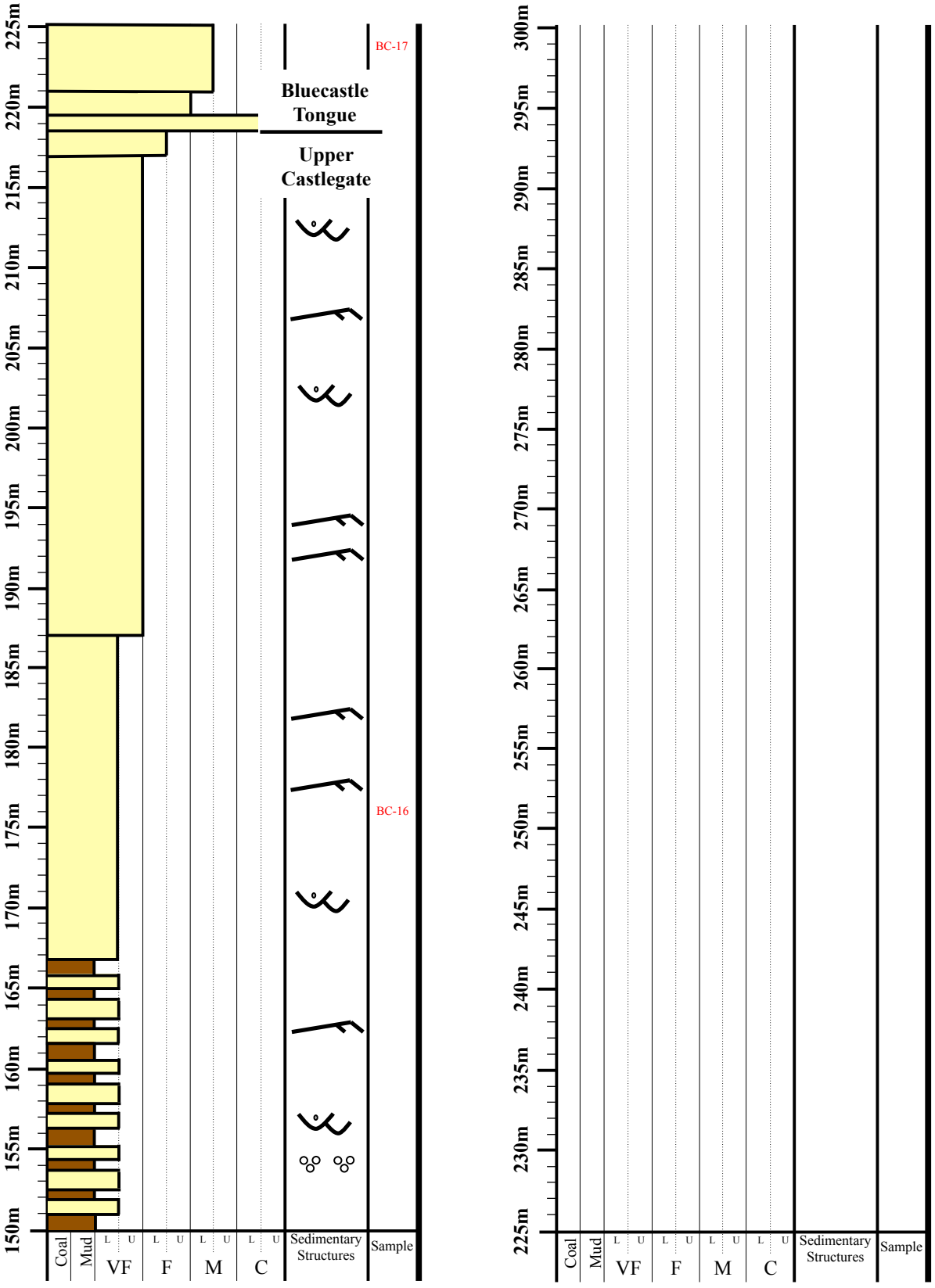

Horse Canyon A

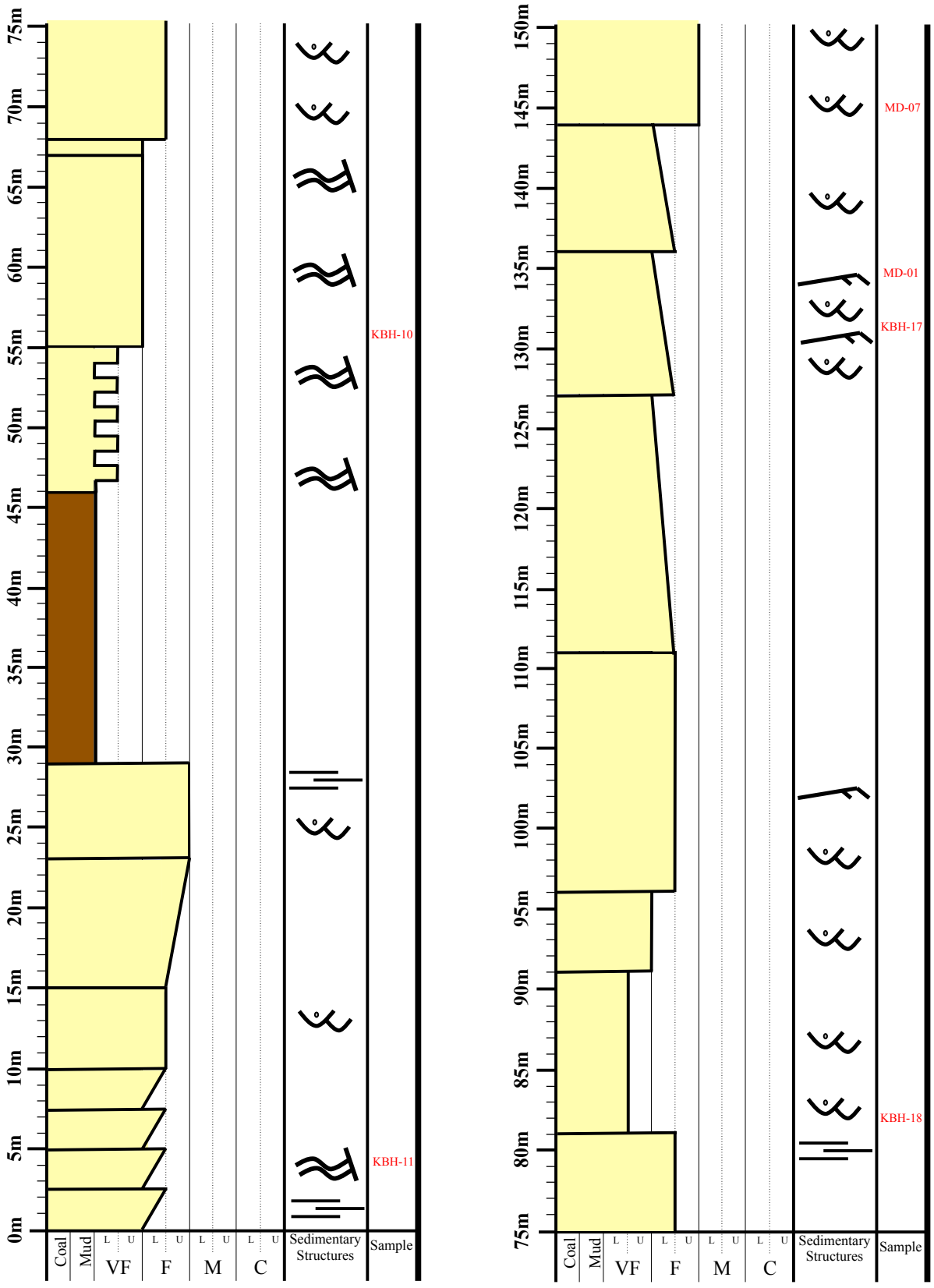

Horse Canyon B

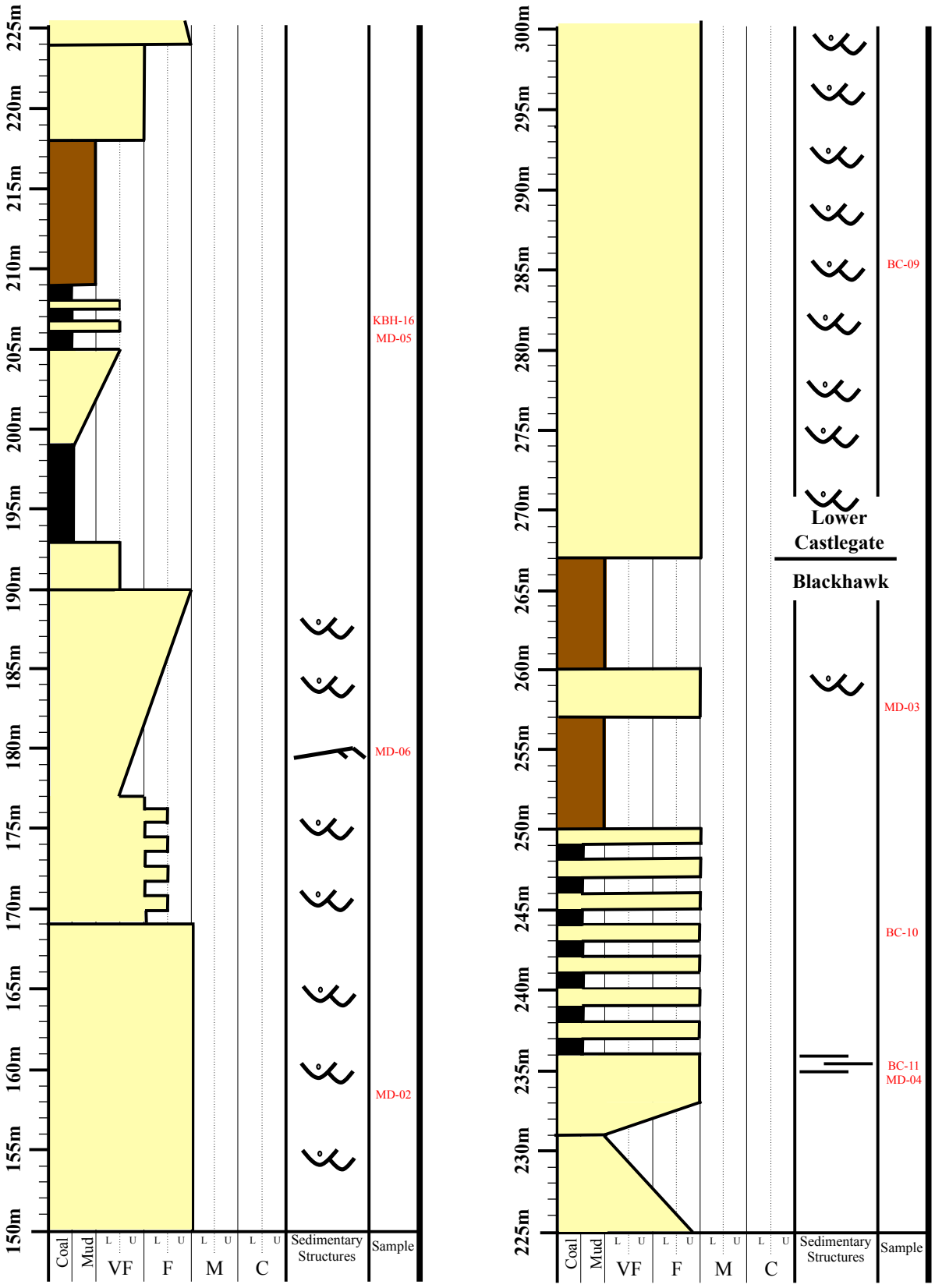

Horse Canyon C

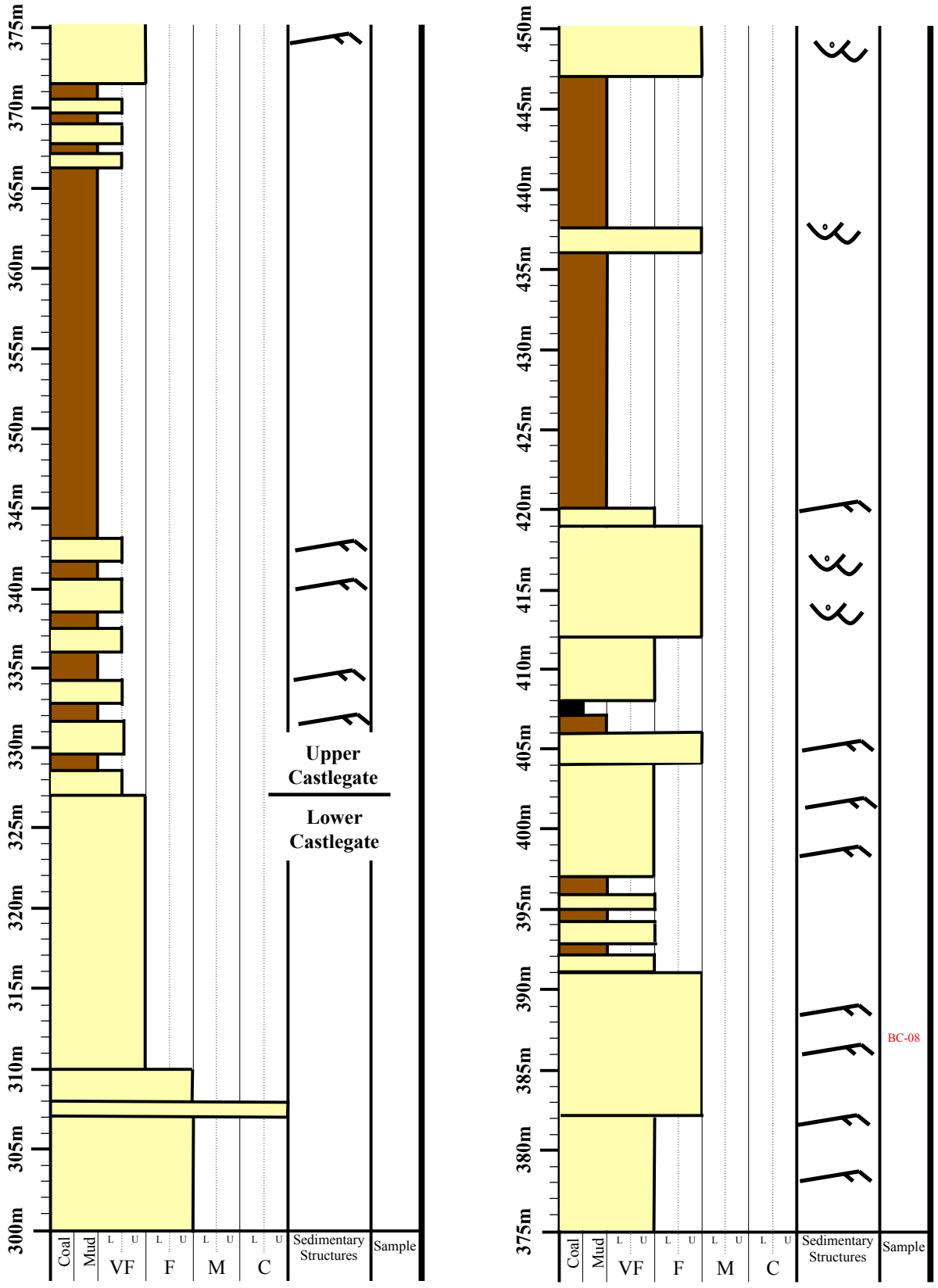

Horse Canyon D

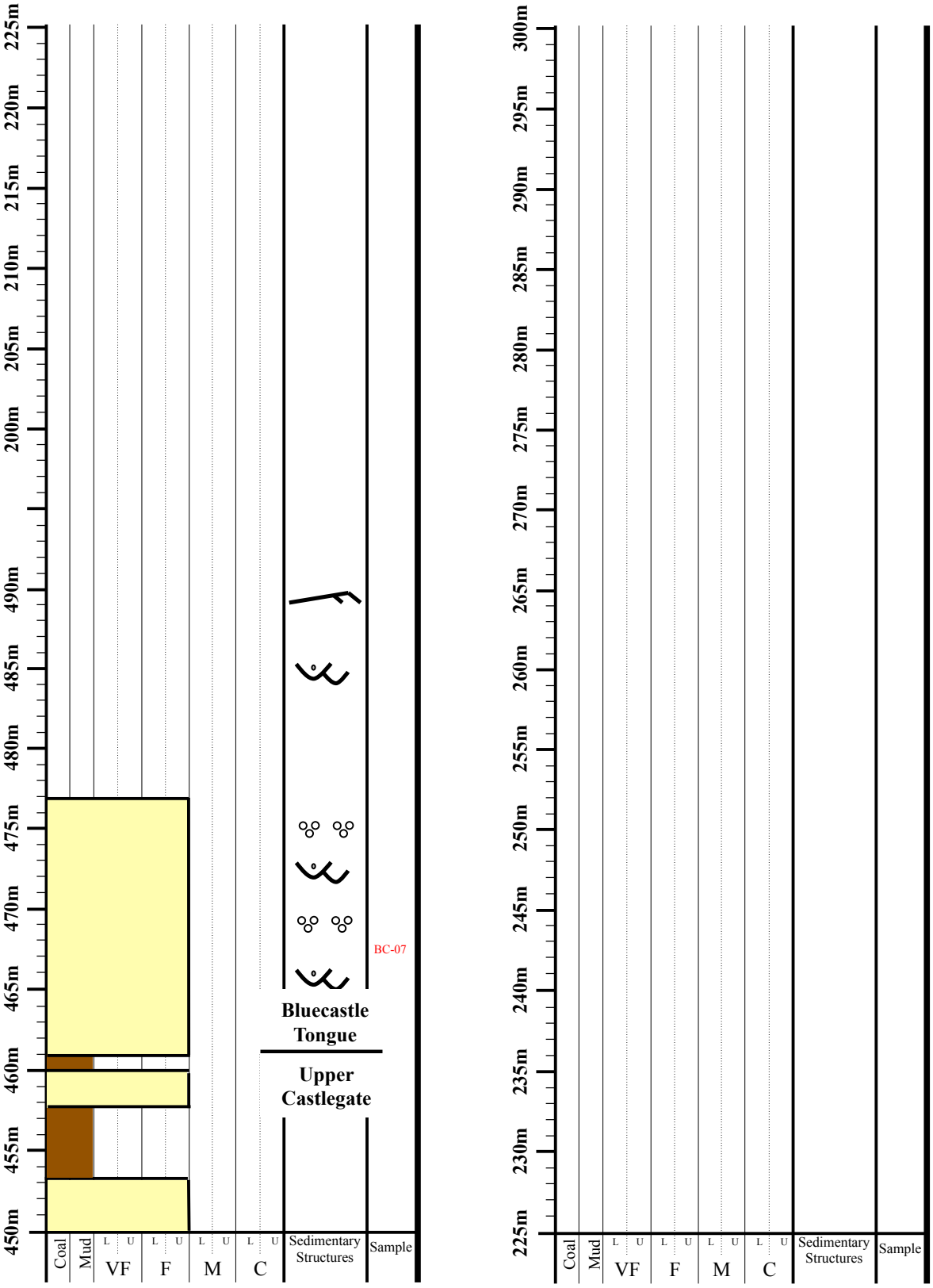

Tusher Canyon

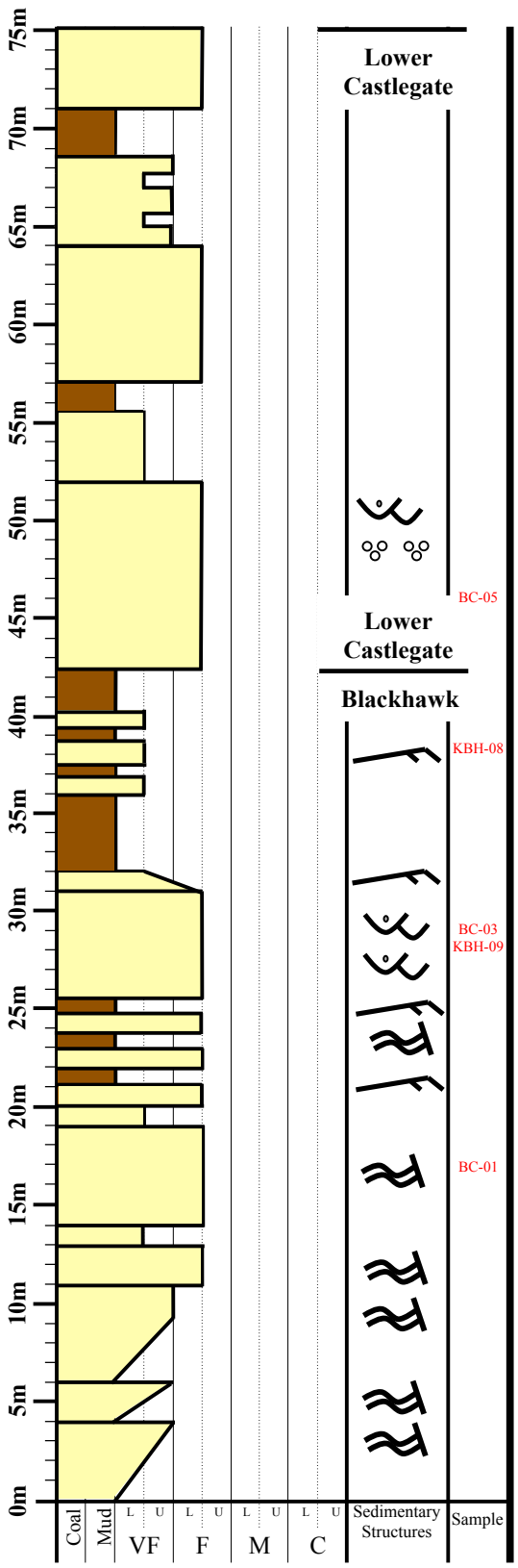

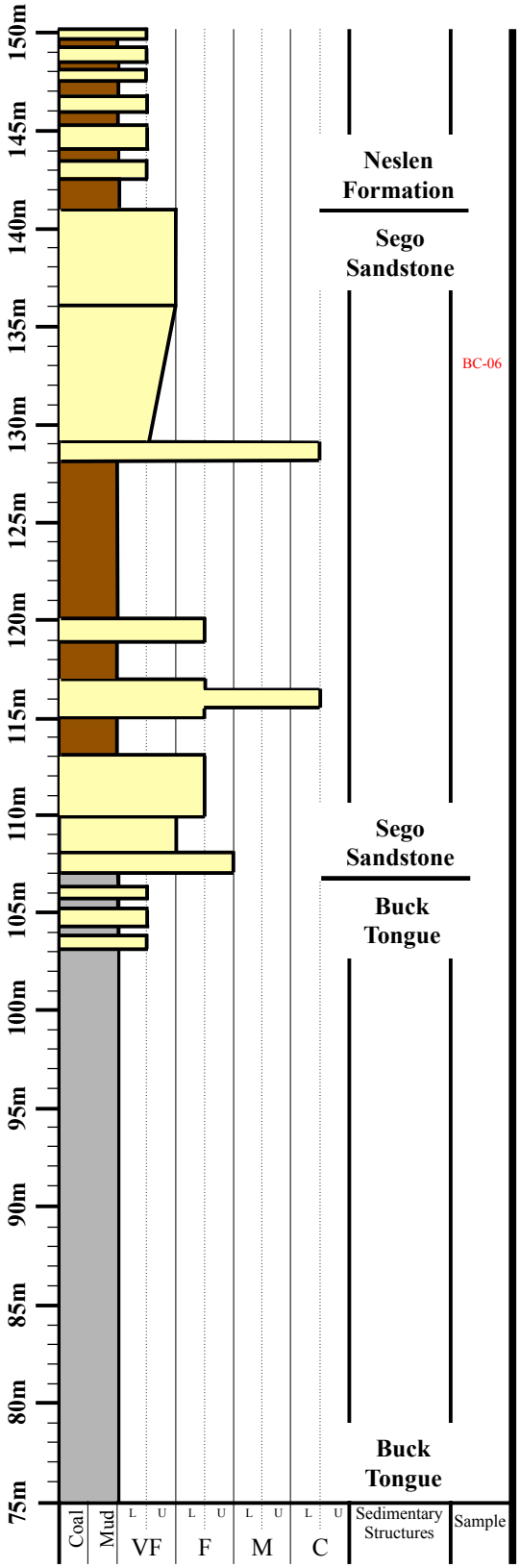

Thompson Canyon

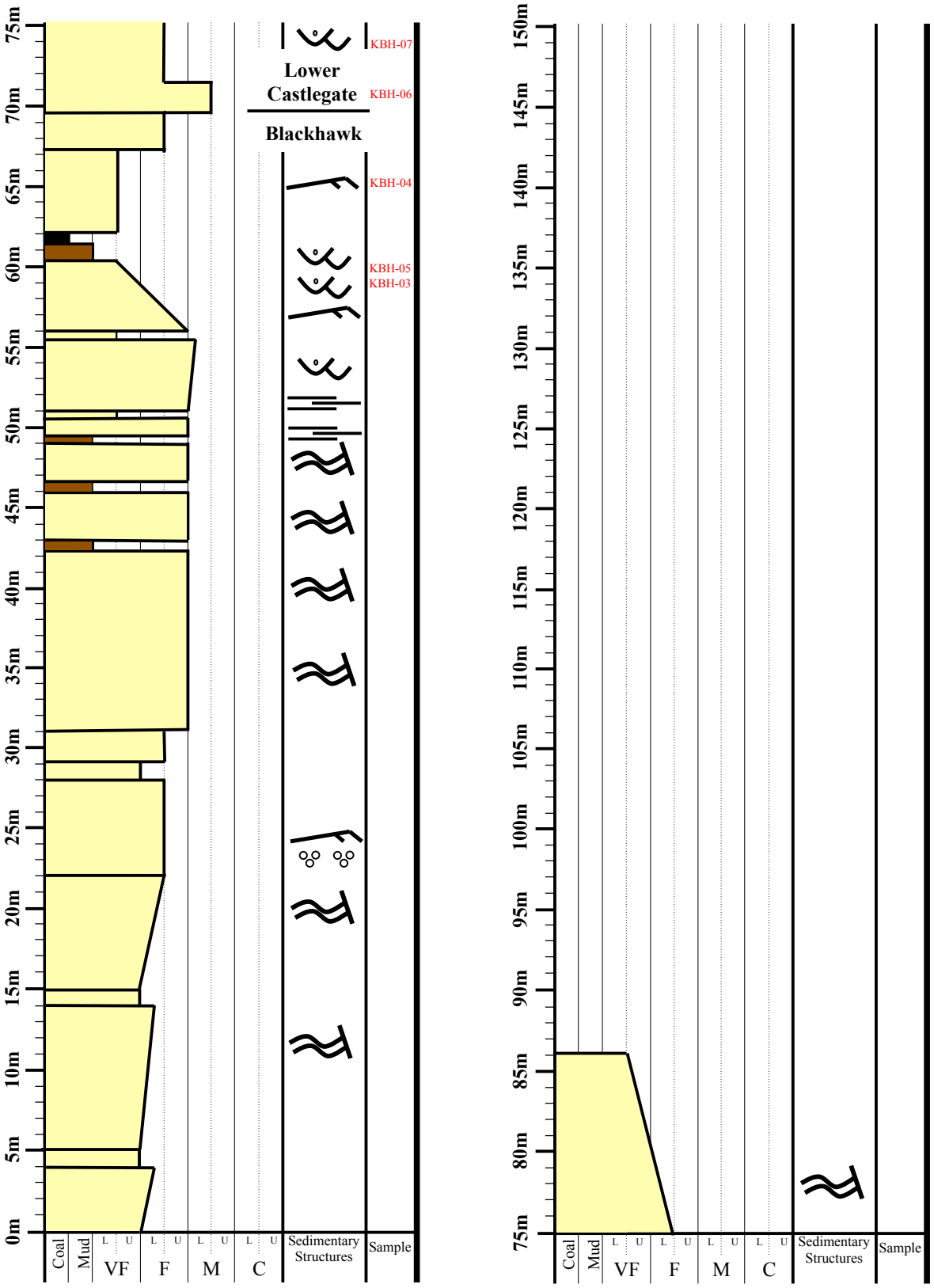

Appendix B: Analytical methods at the Arizona LaserChron Center

Zircon crystals are extracted from samples by traditional methods of crushing and grinding, then separated with a Wilfley table, heavy liquids, and a Frantz magnetic separator. Samples are processed such that all zircons are retained in the final heavy mineral fraction. A large split of these grains (generally thousands of grains) is incorporated into a 1" epoxy mount together with fragments of the LaserChron Center Sri Lanka standard zircon. The mounts are sanded down to a depth of ~20 microns, polished, imaged, and cleaned prior to isotopic analysis.

U-Pb geochronology of zircons is conducted by laser ablation multicollector inductively coupled plasma mass spectrometry (LA-MC-ICPMS) at the Arizona LaserChron Center (Gehrels et al. 2006, 2008). The analyses involve ablation of zircon with a Photon Machines Analyte G2 excimer laser using a spot diameter of 20 microns. The ablated material is carried in helium into the plasma source of a Nu HR ICPMS, which is equipped with a flight tube of sufficient width that U, Th, and Pb isotopes are measured simultaneously. All measurements are made in static mode, using Faraday detectors with $3x10^{11}$ ohm resistors for ^{238}U, ^{232}Th, ^{208}Pb -^{206}Pb, and discrete dynode ion counters for ^{204}Pb and ^{202}Hg. Ion yields are ~0.8 mv per ppm. Each analysis consists of one 15-second integration on peaks with the laser off (for backgrounds), 15 one-second integrations with the laser firing, and a 30 second delay to purge the previous sample and prepare for the next analysis. The ablation pit is ~15 microns in depth.

For each analysis, the errors in determining ^{206}Pb /^{238}U and ^{206}Pb /^{204}Pb result in a measurement error of ~1-2% (at 2-sigma level) in the ^{206}Pb /^{238}U age. The errors in measurement of ^{206}Pb /^{207}Pb and ^{206}Pb /^{204}Pb also result in ~1-2% (at 2-sigma level) uncertainty in age for grains that are >1.0 Ga, but are substantially larger for younger grains due to low intensity of the ^{207}Pb signal. For most analyses, the cross-over in precision of ^{206}Pb /^{238}U and ^{206}Pb /^{207}Pb ages occurs at ~1.0 Ga.

^{204}Hg interference with ^{204}Pb is accounted for by measurement of ^{202}Hg during laser ablation and subtraction of ^{204}Hg according to the natural ^{202}Hg /^{204}Hg of 4.35. Hg correction is not significant for most analyses because our Hg backgrounds are low (~150 cps at mass 204).

Common Pb correction is accomplished by using the Hg-corrected ^{204}Pb and assuming an initial Pb composition from Stacey and Kramers (1975). Uncertainties of 1.5 for ^{206}Pb /^{204}Pb and 0.3 %?? for ^{207}Pb /^{204}Pb are applied to these compositional values based on the variation in Pb isotopic composition in modern crystal rocks.

Inter-element fractionation of Pb/U is generally ~5%, whereas apparent fractionation of Pb isotopes is generally <0.2%. In-run analysis of fragments of a large zircon crystal (generally every fifth measurement) with known age of 563.5 ± 3.2 Ma (2-sigma error) is used to correct for this fractionation. The uncertainty resulting from the calibration correction is generally 1-2% (2-sigma) for both ^{206}Pb /^{207}Pb and ^{206}Pb /^{238}U ages.

Concentrations of U and Th are calibrated relative to the Laserchron Center Sri Lanka zircon, which contains ~518 ppm of U and 68 ppm Th. Uncertainties are shown at the 1-sigma level, and include only measurement errors. Analyses that are >20% discordant (by comparison of ^{206}Pb /^{238}U and ^{206}Pb /^{207}Pb ages) or >5% reverse discordant are not considered further.

Appendix C: Backscattered electron images and example spot locations on KBH sample mounts

KBH-01

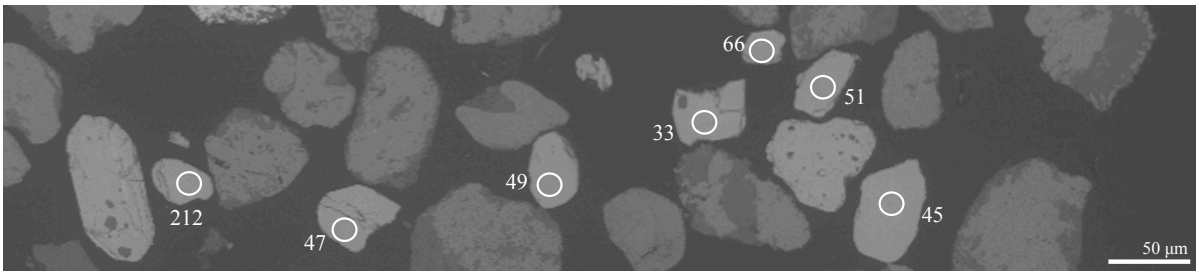

KBH-02

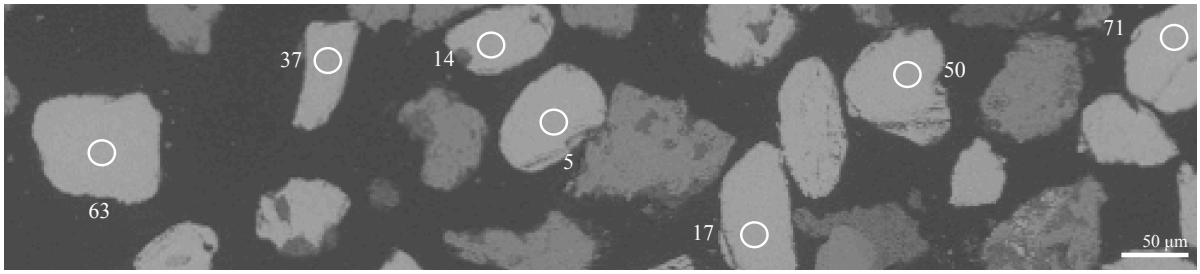

KBH-03

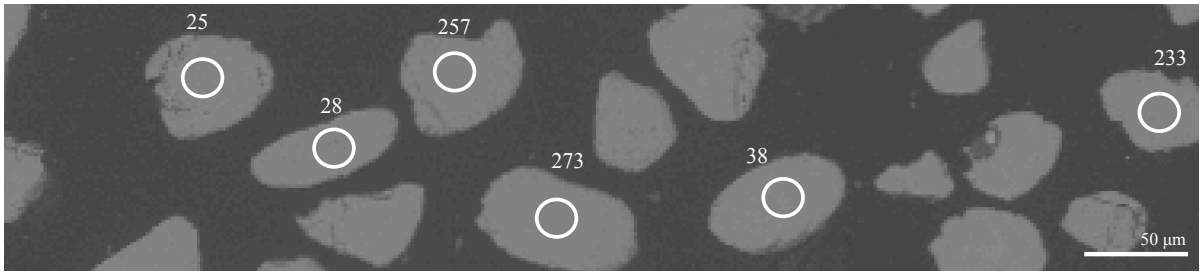

KBH-04

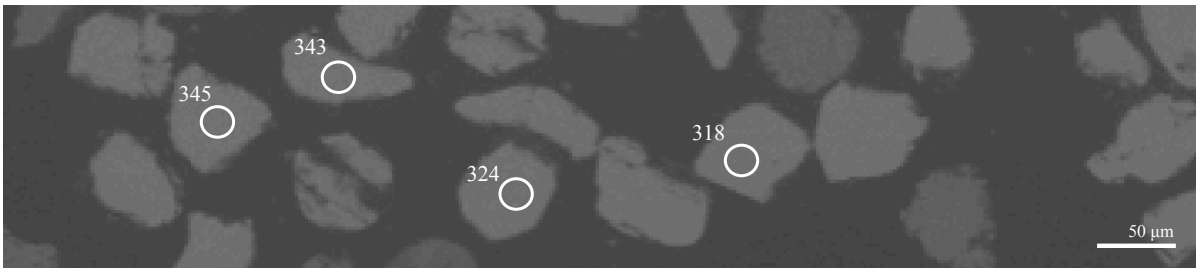

KBH-05

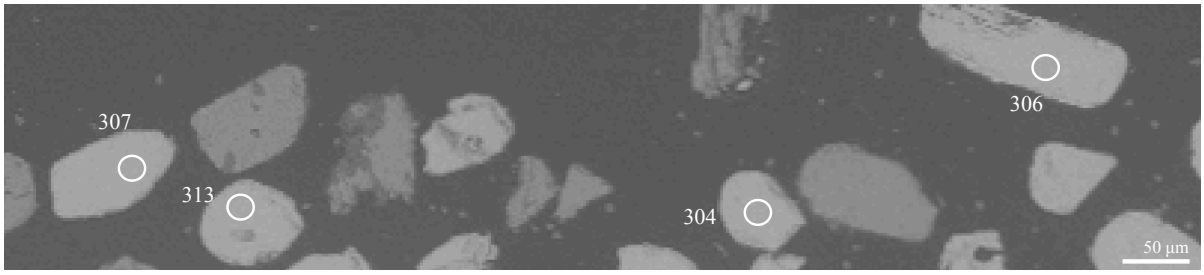

KBH-06

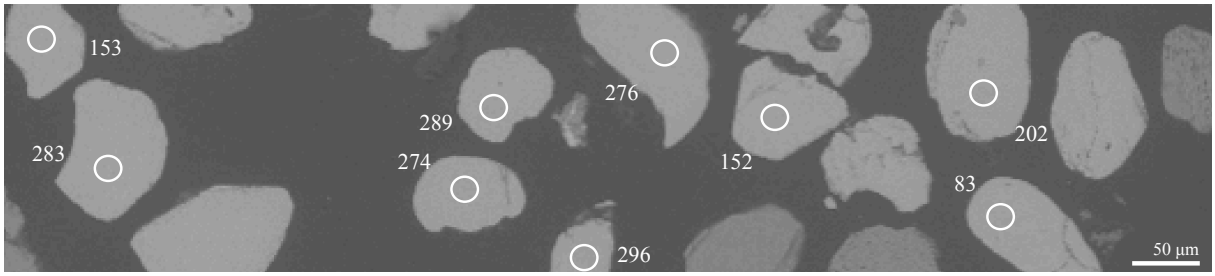

KBH-07

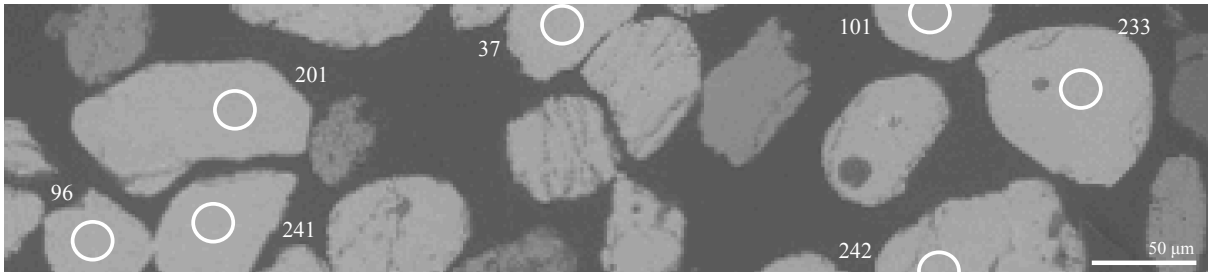

KBH-08

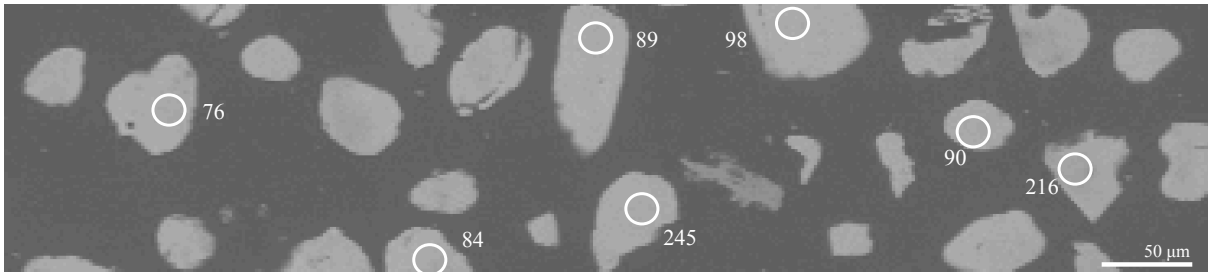

KBH-09

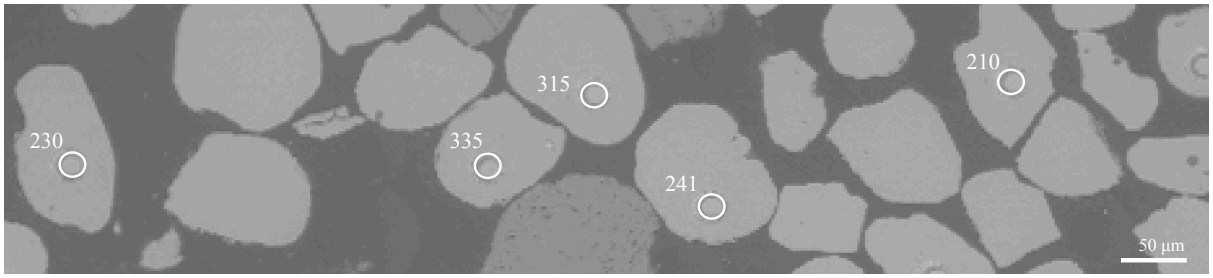

KBH-10

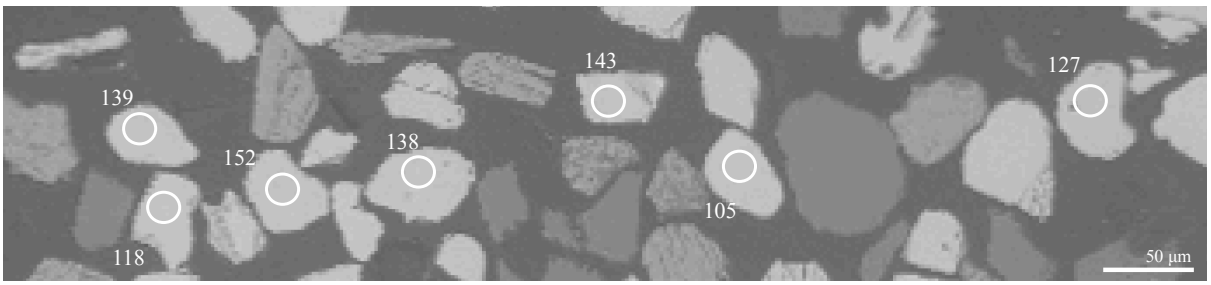

KBH-11

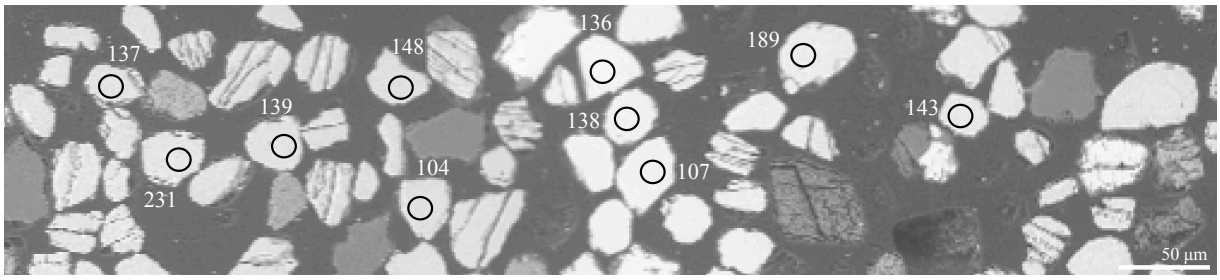

KBH-12

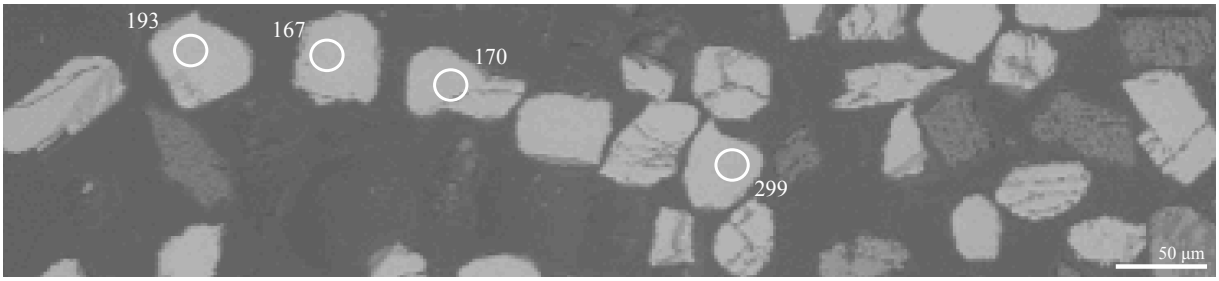

KBH-15

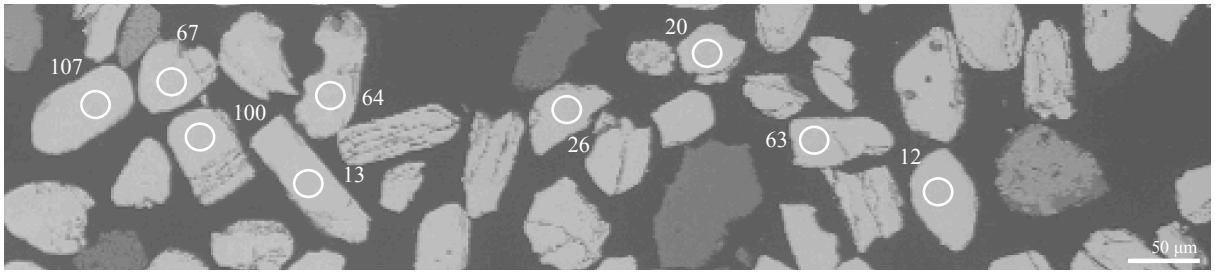

KBH-16

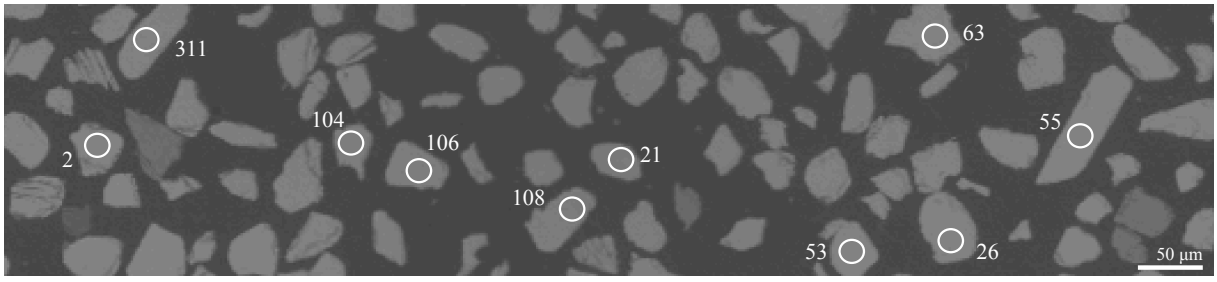

KBH-17

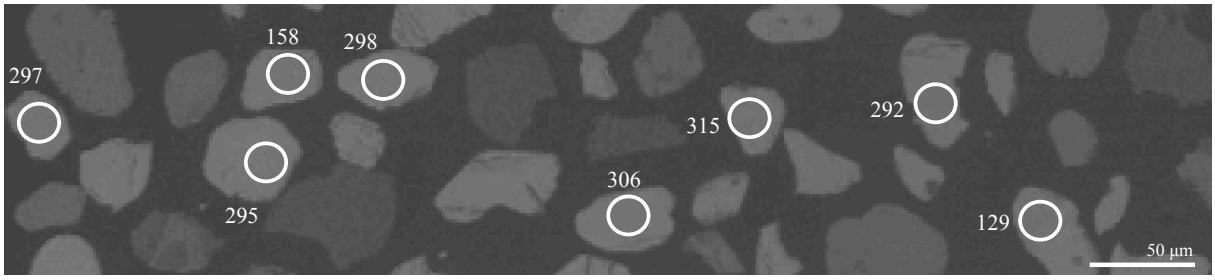

KBH-18

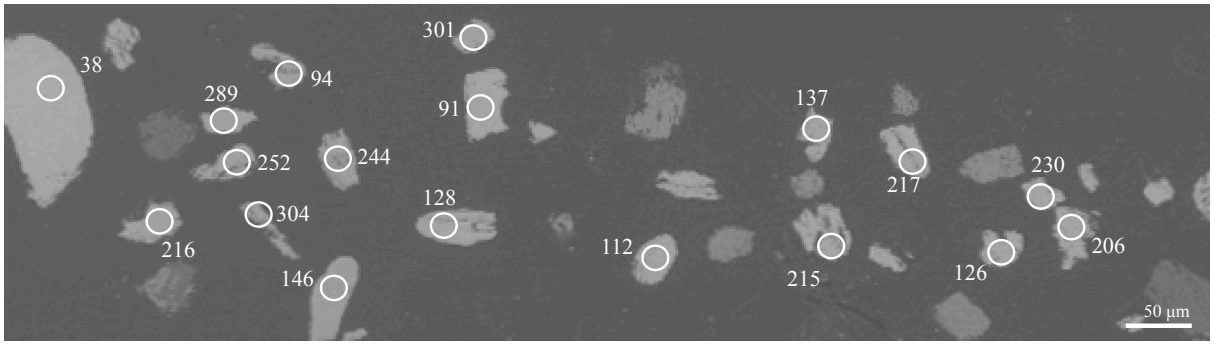
301
38
94
289
91
137
252
244
217
230
128
304
216
112
206
146
215
126
50 µm

KBH-19

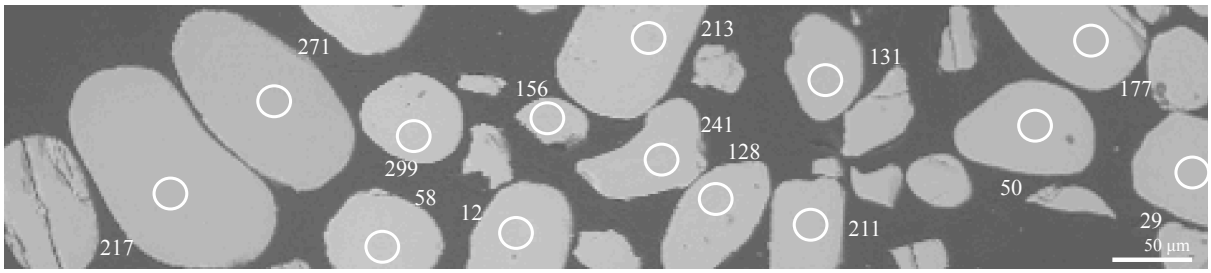
213
271
131
156
177
241
128
299
50
58
12
211
29
217
50 µm